NOISE ANALYSIS IN WDM OPTICAL FIBER COMMUNICATION SYSTEMS

by

Mehmet Akgül

A Thesis Submitted to the
Graduate School of Engineering
in Partial Fulfillment of the Requirements for
the Degree of

Master of Science

in

Electrical & Computer Engineering

Koç University

August, 2009

Koç University

Graduate School of Sciences and Engineering

This is to certify that I have examined this copy of a master's thesis by

Mehmet Akgül

and have found that it is complete and satisfactory in all respects,
and that any and all revisions required by the final
examining committee have been made.

Committee Members:

Assoc. Prof. Alper Demir

Prof. Dr. Alphan Sennaroğlu

Assoc. Prof. Mine Çağlar

Date:

To my family...

ABSTRACT

In this thesis we investigate the noise effect on Wavelength Division Multiplexed (WDM) Optical Fiber Transmission Systems (OFCSs). Optical Amplifiers (OAs), which are used for optical signal amplification in OFCSs, bring in noise, known as Amplified Spontaneous Emission (ASE) noise to system. The noise together with fiber non-linearity degrades the OFCS performance thorough non-linear phase changes of the optical signal, which is known as non-linear phase noise. In the thesis, we present a unifying theory, and a comprehensive methodology and computational techniques for the analysis and characterization of non-linear phase noise and its impact on system performance.

Considering both un-modulated and modulated carriers, in the analysis, we use the stochastic non-linear Schrdinger equation (NLSE) that arises in the analysis of wave propagation phenomena. Starting with the NLSE, we derive new systems of differential equations that characterize noise propagation along the fiber.

We provide both analytical and numerical solution methodologies for the solution of derived noise equation(s). For both un-modulated and modulated carriers we develop a system Bit Error Ratio (BER) evaluation methodology and compute the system BER for Differential Binary Phase Shift Keying (DBPSK) and Differential Quadrature Phase Shift Keying (DQPSK) modulation schemes. We present results which are obtained using different system parameters, to explore the effect of noise on system performance.

ÖZETÇE

Bu tezde dalgaboyu bölmeli coğullamalı (WDM) fiber optik iletişim sistemlerinde (OFCSs) gürültü analizi ele alınmıştır. Fiber optik iletişim sistemlerinde optik sinyali yükselten optik yükselteçler(OAs), sisteme kendiliğinden yükseltilmiş yayılmadan (ASE) kaynaklanan gürültü eklemektedirler. Gürültüyle birlikte fiberden kaynaklanan nonlineer etmenler, optik sinyalde nonlineer faz gürültüsü olarak bilinen nonlineer faz değişikliklerine sebep olarak iletişim sisteminin performansını düşürmektedir. Bu tezde, nonlineer faz gürültüsünün ve sistem üzerindeki etkisinin karakterizasyonu ve analizi için birleştirici teori, geniş kapsamlı metodoloji ve nümerik teknikler sunulmuştur.

Gürültü analizinde kiplenmiş ve kiplenmemiş taşıyıcılar için dalga yayılım analizinden elde edilen stokastik nonlineer Schrödinger (NLSE) eşitliği kullanılmıştır. NLSE eşitliği kullanılarak gürültü yayılımını karekterize eden yeni denklemler elde edilmiştir.

Gürültü denklem(ler)inin çözümü için analitik ve nümerik yöntemler sunulmuştur. Kiplenmiş ve kiplenmemiş taşıyıcılar için sistemin bit hata oranını hesaplama yöntemi sunulmuş ve farksal ikili faz kaydırmalı kipleme (DBPSK) ve farksal dördün faz kaydırmalı kipleme (DQPSK) teknikleri için sistemin bit hata oranları hesaplanmıştır. Ayrıca çeşitli sistem konfigurasyonları kullanılarak elde edilen sonuçlar sunularak , gürültünün sistem performansı üstündeki etkileri araştırılmıştır.

ACKNOWLEDGMENTS

I would like to express my gratitude to Prof. Alper Demir, for his valuable help and patience in the completion of this thesis.

I am also thankful to the committee members Prof. Alphan Sennaroğlu and Prof. Mine Çağlar for a careful evaluation of the work in this thesis, and also for their corrections and suggestions.

I would like to thank and express my deepest gratitude to my family for their great love and invaluable support.

TABLE OF CONTENTS

LIST OF FIGURES

NOMENCLATURE

OA	Optical Amplifier
OFCS	Optical Fiber Communication System
WDM	Wavelength-Division Multiplexing
SPM	Self Phase Modulation
XPM	Cross Phase Modulation
FWM	Four-Wave Mixing
ASE	Amplified Spontaneous Emission
DBPSK	Differential Binary Phase Shift Keying
DQPSK	Differential Quadrature Phase Shift Keying
NLSE	Non-Linear Schrdinger Equation
BER	Bit Error Ratio
CW	Continuous Wave
FFT	Fast Fourier Transform
PSD	Power Spectral Density
SER	Symbol Error Ratio
SNR	Signal to Noise Ratio
PDE	Partial Differential Equation
AB	Adams Bashforth
AM	Adams Moulton

Chapter 1

INTRODUCTION

In recent years it has became apparent that the use of Optical Fibers (OFs) increased significantly. They span the long distances between local phone systems as well as providing the backbone for many network systems. With the invention of new communication techniques their usage increased even further, including medicine, military, automotive, and industrial applications [13]. In principle OFs serve the same purpose as copper wire by moving information from one place to another. However, the transmission medium is light, which propagates in OFs via the principle of total internal reflection [13]. The main advantages of the use of fiber optics are its speed characteristics and high information-carrying capacity, or bandwidth. However the existence of non-linear effects of OFs brings in design challenges. A basic Optical Fiber Communication System (OFCS) consist of a transmitting device, which generates the light signal; an optical fiber, which transmits the light; and a receiver which accepts the transmitted light [13]. Optical fiber itself has no generative properties. The schematic of an OFCS is shown in figure 1.1.

Optical transmitter converts the electrical signal, which is input to the system, to light signal. For this operation generally light emitting diodes (LEDs) are used. Converted light signal propagates in optical fiber through total internal reflection. The last step of transmission is optical receiver which converts the light signal to the form of electrical signal.

Figure 1.1: OFCS Schematic

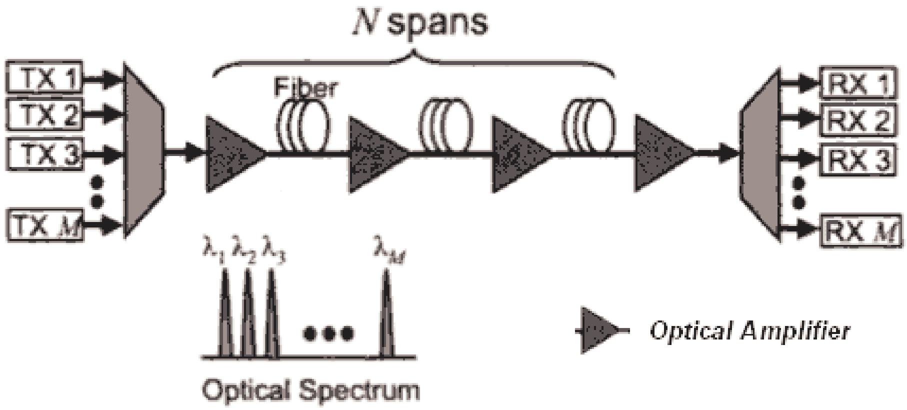

Figure 1.2: Many channels are multiplexed in a single fiber in a WDM System

Generally p-i-n diodes are used in the conversion process. To increase the transmission distance early OFCSs contained repeaters which were essentially a combination of optical receiver and transmitter. They convert the signal from optical domain to electrical domain form, amplify the signal and then convert the electrical signal back to optical form again.

The invention of Optical Amplifiers (OAs) removed the use of electrical amplifiers. They amplify the signal without converting the signal between electrical and optical form thus increased the efficiency of the OFCSs. Another emerged technology was Wavelength-Division Multiplexing (WDM) which increased the bandwidth of the system. The basic principle of WDM system is to convey information through use of light with different wavelengths within single optical fiber. The schematic of a WDM system is shown in figure 1.2 [15].

A WDM system contains a multiplexer at the transmitter that joins the signals with different wavelengths and a de-multiplexer that splits the received signal into their own wavelengths.

Although the invention of OAs and WDM technology increased the system efficiency they also bring in some difficulties in the design of OFCSs. The difficulties arise from the properties of transmission media, which is optical fiber. Optical fibers have linear and non-linear effects on the optical signal [21].

Linear effects include *attenuation* and *dispersion*. Attenuation results in decrease in the power of the signal as shown in figure 1.3. Dispersion on the other hand results in pulse spreading, which limits the information carrying capacity of the fiber [21]. The effect of

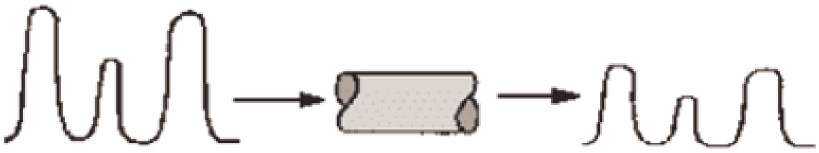

Figure 1.3: Effect of Attenuation On the Signal

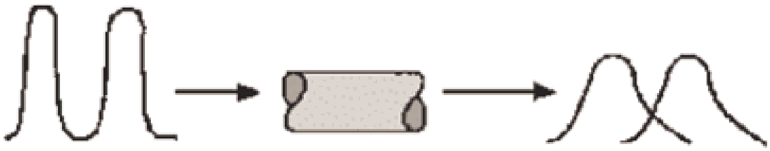

Figure 1.4: Effect of Dispersion On the Signal

dispersion on the signal is shown in figure 1.4.

Non-linear effect of optical fiber is known as Kerr effect. Kerr effect is a result of non-linear change of refractive index of the optical fiber with the power of the optical signal. The refractive index of the optical fiber n depends on optical power as [21]

$$n = n_0 + n_2 \cdot P/A_{eff} \tag{1.1}$$

where n_0 is the refractive index of the fiber at low optical powers, n_2 is the nonlinear refractive index coefficient, P is the power of the optical signal and A_{eff} is the effective area of the fiber. Kerr effect results in Self Phase Modulation (SPM), Cross Phase Modulation(XPM) and Four-Wave Mixing(FWM) [21].

SPM results in non-linear phase change in the optical signal itself [21]. The change of the phase is non-linearly related with the power of the signal. The effect of SPM on the signal is shown in figure 1.5.

XPM appears only in WDM systems as a result of non-linear interaction of signals with different wavelengths [21]. XPM like SPM results in phase change of the signal. However the phase changes not only include the effect of power of the signal itself but also effects of the powers of the other signals coming from different channels (wavelengths).

FMW is another non-linear effect that emerges only in WDM systems. The result of FWM is the emergence of artificial frequencies in the optical signal as shown in figure 1.6 [21].

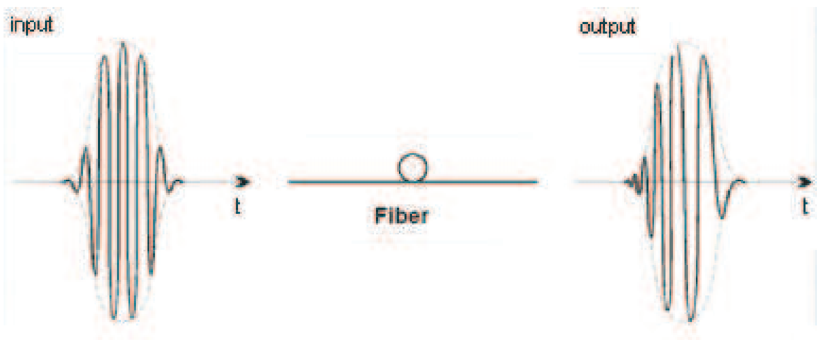

Figure 1.5: Effect of SPM On the Signal

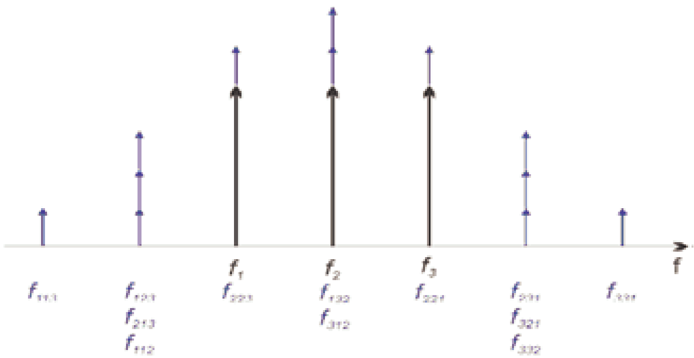

Figure 1.6: FWM Phenomena

In figure 1.6 the frequencies $f1$,$f2$ and $f3$ are the original frequencies that makes up the optical signal. All other frequencies are the frequencies emerged as a result of FWM. The emerged frequencies are at $f1 \mp f2 \mp f3$.

Although the invention of OAs eliminated the side-effects of electrical amplifiers they bring in noise, known as Amplified Spontaneous Emission (ASE) noise to the system [21]. ASE noise causes fluctuations on the intensity of the optical signal. The fluctuations of the optical intensity together with non-linearity degrade the OFCSs performance through non-linear phase changes of the optical signal, which is known as Non-Linear Phase Noise.

During the development phase of OAs and WDM technology there was an interest in the use of phase/frequency modulation scheme of the optical carrier as opposed to the On-Off Keying (OOK) which is simpler to implement [1]. The reason behind the use of phase/frequency modulation was greater receiver sensitivity and increased spectral efficiency.

It was Gordon & Mollenauer that first pointed out the effects of ASE noise on the system performance that uses phase modulation schemes. In their seminal paper published in 1990 they showed that non-linear phase noise due to interaction of ASE noise and Kerr effect degrades the OFCSs performance which use phase modulation [14]. They argued that systems that use phase modulation in fact suffered more from non-linear phase noise as opposed to the systems that uses intensity modulation or OOK. The invention of OAs and the use of WDM systems with OOK scheme increased the system capacity and made it possible to achieve higher receiver sensitivity which in turn eliminated the use of more complex schemes such as phase/frequency modulation during 90s. However the need for more bandwidth required more spectral efficiency which resulted in special interest in the use of phase modulation schemes in OFCSs.

In this thesis, we first analyze the effect of non-linear phase noise that uses DBPSK and DQPSK modulation schemes through BER evaluation of the system as done by Demir in [9]. However Demir's analysis in [9] is done only for un-modulated, continuous-wave [1] , optical carrier case. Although Demir made an analysis for modulated [2] carrier case in [8], by approaching the problem as a stochastic differential system, he did not make analysis

[1]An unmodulated signal is expressed as $\exp(jwt)$ in time domain

[2]A modulated signal is expressed as $m(t)\exp(jwt)$ in time domain

through BER evaluation. In this thesis we first generate the results as Demir did in [9] and [8] for a WDM OFCS. Main contribution of the thesis is the BER analysis methodology for modulated carrier case.

The outline of the thesis is as follows:

In **Chapter 2** we give the general methodology to analyze the non-linear phase noise on the system performance for both modulated and un-modulated carrier case. We will also compare the analysis methods between modulated and un-modulated carrier case.

In **Chapter 3** and **Chapter 4** we consider un-modulated and modulated optical carrier case, respectively, where analytical and numerical methods developed for the noise analysis of a WDM system.

Chapter 5 is the main contribution of the thesis where we give methodology for computing BER performance of a WDM system where carriers are modulated.

We conclude the thesis with **Chapter 6** where a summary of the thesis is discussed.

Chapter 2

OVERVIEW OF THESIS

The equation that governs the complex electric field of the optical signal in a single mode optical fiber is

$$\frac{\partial U(z,t)}{\partial z} = -\alpha U(z,t) - j\frac{1}{2}\beta_2\frac{\partial^2 U(z,t)}{\partial t^2} + \frac{1}{6}\beta_3\frac{\partial^3 U(z,t)}{\partial t^3} + j\gamma|U(z,t)|^2 U(z,t) \qquad (2.1)$$

where t is time, z is the distance along the fiber, α models the loss of the fiber, β_2 and β_3 model second and third order dispersion, γ models the non-linearity of the fiber and $j = \sqrt{-1}$ [1].

Equation 2.1 is known as Non-Linear Schrdinger Equation (NLSE) and can be written as

$$\frac{\partial U(z,t)}{\partial z} = L[U] + NL[U] \qquad (2.2)$$

where

$$\begin{aligned} L[U] &= -\alpha U(z,t) - j\frac{1}{2}\beta_2\frac{\partial^2 U(z,t)}{\partial t^2} + \frac{1}{6}\beta_3\frac{\partial^3 U(z,t)}{\partial t^3} \\ NL[U] &= j\gamma|U(z,t)|^2 U(z,t) \end{aligned} \qquad (2.3)$$

$L[U]$ being the linear part and $NL[U]$ being the non-linear part of the equation 2.1.

Although analytical solution of 2.2 exists if either $L[U] = 0$ or $NL[U] = 0$, in general there is no analytical solution of equation 2.2 except for a subset of physical systems [22]. In these cases solution of 2.2 requires the use of numerical methods.

The exact behavior of the noise in a non-linear system such as in 2.1 can be extracted by the use of Monte Carlo simulations. However, the computational cost of Monte Carlo simulations is very high, making them impractical to apply. Another technique known as *perturbation methods* has been applied successfully in the solution of non-linear stochastic dynamical systems [12, 7]. By using perturbation methods, an approximate solution to a problem which cannot be solved can be found exactly. However, the use of perturbation methods requires that the solution of the problem can be formulated by the addition of small terms to the solvable problem in an exact way [4]. Coincidentally, in most practical engineering problems the noise and undesired disturbances are very small with respect to the original signals which they mix; in which case application of perturbation methods becomes possible. Especially the use of first order perturbation methods is very practical because they actually correspond to the linearization of nonlinear systems around an expansion point.

By use of perturbation methods, one can analyze the noise behavior of non-linear dynamical system such as in 2.1 as follows:

1. First, solve the non-linear equation by only considering the large desired signals. In case of 2.1, generally only numerical solution can be found.

2. Second, express the solution found in Step 1 as a sum of desired large signal and a small term representing any disturbances to the system

3. Third, perform a linearization to the equations obtained in Step 2. This operation is actually corresponds to a Taylor series expansion by using the solution of Step 1 as an expansion point.

4. Last, solve the equation obtained in Step 3 to obtain the behavior of the noise in the system. Because noise has not a well-defined waveform, the solution in this step should be understood that computing stochastic properties of the noise such as mean or spectral density of the noise

In this thesis we will analyze the noise behavior in WDM OFCSs with un-modulated and modulated carriers. The noise will be represented as a small disturbance to the large desired signal U as

$$U(z,t) = U_0(z,t) + a(z,t)$$

where $U_0(z,t)$ is the solution of equation 2.1 by disregarding the noise effects and $a(z,t)$ is the noise term. We will represent the noise term $a(z,t)$ as

$$a(z,t) = a_r(z,t) + ja_i(z,t)$$

where $a_r(z,t)$ is the in-phase component of the noise and $a_i(z,t)$ is the quadrature component of the noise. We will consider the noise term $a(z=0,t)$ as a zero-mean Gaussian stochastic process with in-phase and quadrature components being uncorrelated. Thus, we want to characterize the in-phase and quadrature components of the noise at the end of the fiber that is $a(z=L,t)$, L being the fiber length. Because for a linear system Gaussian process stays Gaussian [17] the noise at the optical receiver can be modeled as Gaussian, the in-phase and quadrature components of the noise are no longer uncorrelated due to non-linearity imposed by optical fiber.

2.1 Unmodulated Carrier Case

For a WDM OFCS with continuous wave carries, the equation that characterizes the noise obtained in Step 3 explained above is not a single equation, but rather a system of differential equations with time-invariant but z varying coefficients, z being the space coordinate of the optical fiber where the optical carrier propagates through.

The system of differential equations with time-invariant coefficients can be solved in frequency domain via the calculation of transfer function. The same methodology will be used here: first, the transfer function from $z=0$ to $z=L$ will be computed, and then the spectral density of the noise will be calculated at the end of the fiber so that we can extract the behavior of the noise. Although noise entered to the system is white, at the end of the fiber link it becomes colored due to noise signal interaction via non-linearity.

The computational cost of the calculation of transfer function depends on the numerical scheme being used and the bandwidth of the optical carrier. In our treatment we use the trapezoidal rule so that we do not deal with stability issues imposed by the numerical integration scheme. Transfer function matrix should be calculated for each w in the bandwidth of the optical carrier. However, the calculation of the transfer function can only be done for discrete values of w. For a specific w, the computational cost of the calculation of transfer function is $O(NN_z)$, N being the number of channels and N_z being the number of discrete z points between $z=0$ to $z=L$, resulting in a total cost of $O(NN_zN_w)$, where N_w is the number of frequency points taken in the range of the bandwidth of the optical carrier.

By using the transfer functions , we will compute the spectral density of the noise at the end of the fiber. Note that because there is more than one unknown, we will actually compute spectral density matrix which gives second-order stochastic properties of the noise. To find the actual effect of noise on the system performance, we have to calculate the Bit Error Ratio (BER) of the system. We will use Monte Carlo simulations for BER calculation.

2.2 Modulated Carrier Case

For a WDM OFCS with modulated carriers, the equation that characterizes the noise behavior obtained in Step 3 above is not trivial as in the case of un-modulated carrier case. In this case, we do not get a system of differential equations, but rather a linear partial differential equation. This is a result of the noise characteristic:

- in case of CW carriers, noise components around each carrier are stationary so that we are able to deal with the noise for all channels separately.
- in case of modulated carriers, the noise around each carrier is not stationary because of modulation. Modulation does not only affect the optical carrier but also the noise around it.

The non-linear partial differential equation obtained in this case has both time and z varying coefficients. Thus we cannot use transfer function methodology easily. In this case, we will propagate the covariance matrix through the fiber so that we can obtain the noise behavior at the end of the fiber.

Another difficulty emerged in the modulated carrier case is the noise dependence on the input signal. Contrary to CW case where noise characteristics do not depend on the input signal, for modulated carrier case noise characteristics depend on input spectrum which requires the computation of signal spectrum through the fiber.

In summary, for noise analysis in modulated carrier case we will do the following:

- Compute the signal spectrum along the fiber.
- Propagate the covariance matrix through the fiber.
- Compute the BER of the system via Monte Carlo simulation.

Like all other numerical simulations, computational cost of the analysis of noise in case of modulated carriers depends on the numerical scheme being used. We will use the method described at [11] for the solution of signal spectrum and covariance matrix propagation. Because of non-linearity, we cannot solve the resulting non-linear differential equation in frequency domain. However, we will propagate the linear part of the equation in frequency domain and non-linear part in time domain. This operation requires the use of Fast Fourier Transform (FFT)s going back and forward between time and frequency domain. Although we will give the details of the computation of noise characteristic for modulated carrier case in chapter four, we will give the computational complexities of the operations done for the solution of signal spectrum and covariance matrix.

Because noise is not stationary, the covariance of the noise samples depends on the sampling time. For simulation, because we cannot simulate for infinite time interval, we will limit the signal time to T, and assume that it is periodic so that we can use FFTs. For a N channel WDM system with T being the bit period of the optical signal, computation of signal spectrum along the optical fiber requires $O(N_z N_t \log N_t)$ operation and covariance matrix propagation costs $O(N_z^2 N_t \log N_t)$ operation where N_z is the number of z points between $z = 0$ and $z = L$ and N_t is the number of discrete time points between t, time, $t = 0$ to $t = T$. Note that unlike un-modulated carrier case, the computational complexity in modulated carrier case does not depend on the number of channels, N.

BER computation for modulated carrier case is the same as un-modulated carrier case except we get the covariance matrix between time samples of the noise at the end of the fiber directly, while in un-modulated case we first compute spectral density matrix and then get the covariance matrix. By Monte Carlo simulation, we will compute the system BER performance.

Although we need the noise characteristic at the end of the fiber to analyze its effect on the system performance, the methodology for obtaining noise characteristic differs for modulated and un-modulated carrier case. Main differences are:

- While the equation that characterizes the noise in the optical fiber consists of system of linear differential equations in un-modulated carrier case, it is a single partial differential equation in modulated carrier case.

- Because for un-modulated carrier case system of differential equations has time invariant coefficients which enable the use of transfer function concept, numerical computation of noise propagation is simpler in un-modulated carrier case compared to the modulated carrier case.

- While noise does not depend on input signal in un-modulated carrier case, it depends on input signal in modulated carrier case which requires the numerical solution of equation 2.1 along the fiber.

We will give the details of the noise analysis for un-modulated carrier case in chapter 3 and modulated carrier case in in chapter 4.

Chapter 3

UNMODULATED CARRIER CASE

In this chapter we will analyze the noise effect on WDM system performance by assuming that channel carriers are un-modulated. In the noise analysis we will follow the procedure given in section 2.1.We will first find the equation that characterize the noise and use the noise characteristic equation to find transfer functions between channels. Next, we will apply transfer function methodology to compute noise spectral density at the end of the fiber. Finally, we will generate noise samples by using noise spectral density and make Monte Carlo simulation to compute system's Bit Error Ratio(BER).

In the first step, we have to solve the equation 2.1 by considering only desired large signals. If we ignore FWM products and take only SPM and XPM into consideration imposed by Kerr nonlinearity, we can express the signal envelope U for an N channel WDM system as

$$U(z,t) = \sum_{k=1}^{N} U_k(z,t)e^{-jw_k t} \tag{3.1}$$

where U_k is the envelope of the signal in the k^{th} channel and w_k is the relative frequency of the k^{th} channel carrier with respect to w_c, carrier frequency of U. Here, it is assumed that all signal envelopes, U_k, are band limited and they do not overlap in frequency domain.

Using 3.1 in 2.1 and ignoring all terms that result in FWM products, we get following set of differential equation

$$\begin{aligned}
\frac{\partial U_k(z,t)}{\partial z} &= -\alpha U_k(z,t) \\
&- j\frac{1}{2}\beta_2(\frac{\partial^2}{\partial t^2} - j2w_k\frac{\partial}{\partial t} - w_k^2)U_k(z,t) \\
&+ \frac{1}{6}\beta_3(\frac{\partial^3}{\partial t^3} - j3w_k\frac{\partial^2}{\partial t^2} - 3w_k^2\frac{\partial}{\partial t} + jw_k^3)U_k(z,t) \\
&+ j\gamma\left[\sum_{i=1}^{N} c_i|U(z,t)|^2\right]U_k(z,t)
\end{aligned} \tag{3.2}$$

where $c_i = 1$ for i=k and $c_i = 2$ in the other cases. In equation 3.2, it is assumed that γ is the same for all channels. However, it should be noted that γ is frequency dependent. But, frequency dependency of γ can be neglected due to $w_c \gg w_k$.

Initial condition for equations 3.2 is:

$$U_k(z=0,t) = (\sqrt{P_k} + a_k(z=0,t))\exp(j\phi_k) \tag{3.3}$$

where P_k is the power of the unmodulated noise-free signal, $a_k(z,t)$ is the noise around k^{th} channel, and ϕ_k is the random phase.

Solution of 3.2 with initial condition given by 3.3 is :

$$U_k(z,t) = [\sqrt{P_k} + a_k(z,t)]\exp(-\alpha z + j(\phi_k + \varphi_k^L(z) + \varphi_k^{NL}(z))) \tag{3.4}$$

where

$$\begin{aligned} \varphi_k^L(z) &= (\frac{1}{2}\beta_2 w_k^2 + \frac{1}{6}\beta_3 w_k^3)z & (3.5)\\ \varphi_k^{NL}(z) &= \gamma\left[\sum_{k=1}^{N} c_i P_i\right]\int_0^z \exp(-2\alpha\eta)d\eta & (3.6)\end{aligned}$$

In the second and third step, we have to put the solution found in step 1, equation 3.4, into the original equation 3.2 and ignore all terms that are not linear with respect to $a_k(z,t)$. If we do mathematical calculations, the following set of coupled differential equations are obtained [9]

$$\begin{aligned} \frac{\partial a_k(z,t)}{\partial z} &= -(\beta_2 w_k + \frac{1}{2}\beta_3 w_k^3)\frac{\partial a_k(z,t)}{\partial t} \\ &- j\frac{1}{2}(\beta_2 + \beta_3 w_k)\frac{\partial^2 a_k(z,t)}{\partial t^2} + \frac{1}{6}\beta_3\frac{\partial^3 a_k(z,t)}{\partial t^3} \\ &+ j\gamma\exp(-2\alpha z)\left[\sum_{k=1}^{N} c_i\sqrt{P_k P_i}[a_i(z,t) + a_i^*(z,t)]\right] \end{aligned} \tag{3.7}$$

where * denotes complex conjugate operation.

Noise term $a_k(z,t)$ can be expressed as:

$$a_k(z,t) = a_{kR}(z,t) + ja_{kI}(z,t) \tag{3.8}$$

where $a_{kR}(z,t)$ is the in-phase component and $a_{kI}(z,t)$ is the quadrature component of noise,$a_k(z,t)$.

Using 5.27 in 3.7, we get following set of coupled differential equations

$$\begin{aligned}\frac{\partial a_{kR}(z,t)}{\partial z} =& -(\beta_2 w_k + \frac{1}{2}\beta_3 w_k^2)\frac{\partial a_{kr}(z,t)}{\partial t}\\ &+\frac{1}{6}\beta_3\frac{\partial^3 a_{kr}(z,t)}{\partial t^3}+\frac{1}{2}(\beta_2+\beta_3 w_k)\frac{\partial^2 a_{ki}(z,t)}{\partial t^2}\\ \frac{\partial a_{kI}(z,t)}{\partial z} =& -(\beta_2 w_k + \frac{1}{2}\beta_3 w_k^3)\frac{\partial a_{ki}(z,t)}{\partial t}\\ &+\frac{1}{6}\beta_3\frac{\partial^3 a_{ki}(z,t)}{\partial t^3}-\frac{1}{2}(\beta_2+\beta_3 w_k)\frac{\partial^2 a_{kr}(z,t)}{\partial t^2}\\ &2\gamma\exp(-2\alpha z)\left[\sum_{k=1}^{N} c_i\sqrt{P_kP_i}a_{iR}(z,t)\right]\end{aligned} \tag{3.9}$$

Equation 3.9 represents a system of differential equations with $2N$ unknowns for an N channel WDM system. Note that the coefficients in equation 3.9 are time independent, but z dependent. This property will enable us to solve equations in frequency domain rather than in time domain.

3.1 Transfer Function Calculation

The solution given by 3.9 consists of system of linear differential equations. This is a result of linearization made in the solution of equation 3.7. We will use transfer function methodology in the solution of 3.9. Let's now define 2×2 transfer function matrix in frequency domain $T_{ki}(L,w)$ such that

$$\begin{bmatrix}A_{kR}(z=L,w)\\ A_{kI}(z=L,w)\end{bmatrix} = \underbrace{\begin{bmatrix}T_{ki}^{RR}(z=L,w) & T_{ki}^{IR}(z=L,w)\\ T_{ki}^{RI}(z=L,w) & T_{ki}^{II}(z=L,w)\end{bmatrix}}_{T_{ki}(L,w)}\begin{bmatrix}A_{iR}(z=0,w)\\ A_{iI}(z=0,w)\end{bmatrix} \tag{3.10}$$

where $A_{kR}(z,w)$ and $A_{kI}(z,w)$ are the Fourier Transforms of $a_{kR}(z,t)$ and $a_{kI}(z,t)$ respectively. In equation 3.10 $\mathcal{T}_{ki}(L,w)$ transfers the input which is k^{th}*channel* in-phase $A_{kR}(z=0,w)$ and quadrature $A_{kI}(z=0,w)$ noise component; to the output which is i^{th} channel in-phase $A_{iR}(z=L,w)$ and quadrature $A_{iI}(z=L,w)$ noise component. The elements of $\mathcal{T}_{ki}(L,w)$ are as follows : T_{ki}^{RR} is the transfer function from k^{th}*channel* in-phase noise component to $i^{th} channel$ in-phase noise component, T_{ki}^{IR} is the transfer function from $k^{th} channel$ quadrature noise component to $i^{th} channel$ in-phase noise component, T_{ki}^{RI} is the transfer function from $k^{th} channel$ in-phase noise component to $i^{th} channel$ quadrature noise component and finally T_{ki}^{II} is the transfer function from $k^{th} channel$ quadrature noise component to $i^{th} channel$ quadrature noise component. We define T_{mn} as intra-transfer function if $m = n$ and inter-transfer function if $m \neq n$.

Converting equation 3.9 from time domain to frequency domain by using Fourier Transform, we get

$$\begin{aligned}
\frac{\partial A_{kR}(z,w)}{\partial z} =& -jw(\beta_2 w_k + \frac{1}{2}\beta_3 w_k^2 + \frac{1}{6}\beta_3 w^2)A_{kR}(z,w) \\
& - \frac{1}{2}w^2(\beta_2 + \beta_3 w_k)A_{kI}(z,w) \\
\frac{\partial A_{kI}(z,w)}{\partial z} =& -jw(\beta_2 w_k + \frac{1}{2}\beta_3 w_k^2 + \frac{1}{6}\beta_3 w^2)A_{kI}(z,w) \\
& + \frac{1}{2}w^2(\beta_2 + \beta_3 w_k)A_{kR}(z,w) \\
& + \gamma \exp(-2\alpha z)\left[\sum_{i=1}^{N} c_i \sqrt{P_k P_i} A_{iR}(z,w)\right]
\end{aligned} \tag{3.11}$$

where w comes from Fourier Transform representing the frequency contents of the envelope U_k centered around w_k.

3.1.1 Analytical Computation Of Transfer Functions

The computation of the transfer functions from the equation 3.11 requires the use of numerical methods. However for two specific cases analytical solution of transfer functions can be found : no-nonlinearity and no-dispersion case. In this section, we will give the analytical solution of transfer functions for these two cases.

No-Nonlinearity Case

In this case, $\gamma = 0$. Then equation 3.11 becomes

$$
\begin{aligned}
\frac{\partial A_{kR}(z,w)}{\partial z} =& - jw(\beta_2 w_k + \frac{1}{2}\beta_3 w_k^2 + \frac{1}{6}\beta_3 w^2)A_{kR}(z,w) \\
& - \frac{1}{2}w^2(\beta_2 + \beta_3 w_k)A_{kI}(z,w) \\
\frac{\partial A_{kI}(z,w)}{\partial z} =& - jw(\beta_2 w_k + \frac{1}{2}\beta_3 w_k^2 + \frac{1}{6}\beta_3 w^2)A_{kI}(z,w) \\
& + \frac{1}{2}w^2(\beta_2 + \beta_3 w_k)A_{kR}(z,w)
\end{aligned}
\tag{3.12}
$$

which is a system of decoupled differential equations. Note that inter-transfer functions, $T_{ki}(z,w)$, $k \neq i$, are zero. This is because there is no interaction between the k^{th} and the i^{th} channel. Only intra-transfer functions, $T_{kk}(z,w)$, exist.

Equation 3.12 can be written in vector form as

$$
\frac{\partial}{\partial z}\begin{bmatrix} A_{kR}(z,w) \\ A_{kI}(z,w) \end{bmatrix} = \begin{bmatrix} -jw(\beta_2 w_k + \frac{1}{2}\beta_3 w_k^2 + \frac{1}{6}\beta_3 w^2) & -\frac{1}{2}w^2(\beta_2 + \beta_3 w_k) \\ \frac{1}{2}w^2(\beta_2 + \beta_3 w_k) & -jw(\beta_2 w_k + \frac{1}{2}\beta_3 w_k^2 + \frac{1}{6}\beta_3 w^2) \end{bmatrix} \begin{bmatrix} A_{kR}(z,w) \\ A_{kI}(z,w) \end{bmatrix}
\tag{3.13}
$$

Equation 3.13 is in the form

$$
\frac{\partial}{\partial z}X(z,w) = G(w)X(w,z) \tag{3.14}
$$

where

$$
X(z,w) = \begin{bmatrix} A_{kR}(z,w) \\ A_{kI}(z,w) \end{bmatrix} \tag{3.15}
$$

and

$$
G(w) = \begin{bmatrix} -jw(\beta_2 w_k + \frac{1}{2}\beta_3 w_k^2 + \frac{1}{6}\beta_3 w^2) & -\frac{1}{2}w^2(\beta_2 + \beta_3 w_k) \\ \frac{1}{2}w^2(\beta_2 + \beta_3 w_k) & -jw(\beta_2 w_k + \frac{1}{2}\beta_3 w_k^2 + \frac{1}{6}\beta_3 w^2) \end{bmatrix} \tag{3.16}
$$

Solution of 3.14 is

$$
X(z,w) = \exp(G(w)z)X(z=0,w) \tag{3.17}
$$

Thus intra-transfer function matrix $T_{kk}(z,w)$ is equal to $\exp(G(w)z)$. Expression $\exp(G(w)z)$ can be calculated as follows.

Let's define

$$\begin{aligned} \xi &= -jw(\beta_2 w_k + \frac{1}{2}\beta_3 w_k^2 + \frac{1}{6}\beta_3 w^2) \\ \kappa &= \frac{1}{2}w^2(\beta_2 + \beta_3 w_k) \end{aligned} \tag{3.18}$$

after which $G(w)z$ becomes

$$G(w)z = \begin{bmatrix} \xi & -\kappa \\ \kappa & \xi \end{bmatrix} \cdot z = \begin{bmatrix} \xi z & -\kappa z \\ \kappa z & \xi z \end{bmatrix} \tag{3.19}$$

Further, we can decompose $G(w)z$ into two matrices such that

$$G(w)z = A(w)z + B(w)z \tag{3.20}$$

where

$$A(w) = \begin{bmatrix} \xi & 0 \\ 0 & \xi \end{bmatrix} \textit{ and } B(w) = \begin{bmatrix} 0 & -\kappa \\ \kappa & 0 \end{bmatrix}$$

Exponential of summation of two matrices can be calculated as

$$\exp(A + B) = \exp(A) \cdot \exp(B) \tag{3.21}$$

if and only if $AB = BA$ [16]. For the matrices $A(w)z$ and $B(w)z$ we get

$$[A(w)z] \cdot [B(w)z] = [B(w)z] \cdot [A(w)z] \tag{3.22}$$

which enables the computation of $\exp(G(w)z)$ by first computing $\exp(A(w)z)$ and $\exp(B(w)z)$, and then multiplying the two results.

Exponential of a $n \times n$ diagonal matrix is given by [16]

$$\exp\left(\begin{bmatrix} \lambda_1 & 0 & \cdots & 0 \\ 0 & \lambda_2 & \cdots & 0 \\ \vdots & \vdots & \ddots & \vdots \\ 0 & 0 & \cdots & \lambda_n \end{bmatrix}\right) = \begin{bmatrix} \exp(\lambda_1) & 0 & \cdots & 0 \\ 0 & \exp(\lambda_2) & \cdots & 0 \\ \vdots & \vdots & \ddots & \vdots \\ 0 & 0 & \cdots & \exp(\lambda_n) \end{bmatrix} \tag{3.23}$$

Thus, $\exp(A(w)z)$ is equal to

$$\exp(A(w)z) = \exp\left(\begin{bmatrix}\xi z & 0\\ 0 & \xi z\end{bmatrix}\right) = \begin{bmatrix}\exp(\xi z) & 0\\ 0 & \exp(\xi z)\end{bmatrix} \tag{3.24}$$

The computation of $\exp(B(w)z)$ can be done from the definition of matrix exponential. For an $n \times n$ square matrix, M matrix exponential $\exp(M)$ is defined as [16]

$$\exp(M) = I + M + \frac{M^2}{2!} + \frac{M^3}{3!} + \ldots + \frac{M^k}{k!} + \ldots \tag{3.25}$$

where I is the identity matrix with an equal size of M. By using the matrix exponential definition $\exp(B(w)z)$ is calculated as

$$\begin{aligned}\exp(B(w)z) = {} & \begin{bmatrix}1 & 0\\ 0 & 1\end{bmatrix} + \begin{bmatrix}0 & -\kappa z\\ \kappa z & 0\end{bmatrix} + \frac{1}{2!}\begin{bmatrix}-(\kappa z)^2 & 0\\ 0 & -(\kappa z)^2\end{bmatrix}\\ & + \frac{1}{3!}\begin{bmatrix}0 & (\kappa z)^3\\ -(\kappa z)^3 & 0\end{bmatrix} + \frac{1}{4!}\begin{bmatrix}(\kappa z)^4 & 0\\ 0 & (\kappa z)^4\end{bmatrix} + \ldots\\ = {} & \begin{bmatrix}1 - \frac{(\kappa z)^2}{2!} + \frac{(\kappa z)^4}{4!} - \ldots & -(\kappa z) + \frac{(\kappa z)^3}{3!} - \ldots\\ (\kappa z) - \frac{(\kappa z)^3}{3!} + \ldots & 1 - \frac{(\kappa z)^2}{2!} + \frac{(\kappa z)^4}{4!} - \ldots\end{bmatrix}\end{aligned} \tag{3.26}$$

The Maclaurin series for $sin(x)$ and $cos(x)$ are [19]

$$\begin{aligned} sin(x) &= x - \frac{x^3}{3!} + \frac{x^5}{5!} - \ldots\\ cos(x) &= 1 - \frac{x^2}{2!} + \frac{x^4}{4!} - \ldots \end{aligned} \tag{3.27}$$

From formulae 3.27, we can infer that $\exp(B(w)z)$ is

$$\exp(B(w)z) = \begin{bmatrix}\cos\kappa z & -\sin\kappa z\\ \sin\kappa z & \cos\kappa z\end{bmatrix} \tag{3.28}$$

Thus transfer function matrix $T_{kk}(z, w)$, $\exp(G(w)z)$, is equal to

$$
\begin{aligned}
T_{kk}(z,w) = \exp(G(w)z) &= \exp(A(w)z)\exp(B(w)z) \\
&= \begin{bmatrix} \exp(\xi z) & 0 \\ 0 & \exp(\xi z) \end{bmatrix} \begin{bmatrix} \cos\kappa z & -\sin\kappa z \\ \sin\kappa z & \cos\kappa z \end{bmatrix} \\
&= \exp(\xi z) \begin{bmatrix} \cos\kappa z & -\sin\kappa z \\ \sin\kappa z & \cos\kappa z \end{bmatrix}
\end{aligned}
\tag{3.29}
$$

Note that transfer function matrix $T_{kk}(z,w)$ is unitary. That is,

$$
\begin{aligned}
T^*_{kk}(z,w) &= \exp(-\xi z) \begin{bmatrix} \cos\kappa z & \sin\kappa z \\ -\sin\kappa z & \cos\kappa z \end{bmatrix} \\
&\Rightarrow T_{kk}(z,w)T^*_{kk}(z,w) = \exp(\xi z) \begin{bmatrix} \cos\kappa z & -\sin\kappa z \\ \sin\kappa z & \cos\kappa z \end{bmatrix} \exp(-\xi z) \begin{bmatrix} \cos\kappa z & \sin\kappa z \\ -\sin\kappa z & \cos\kappa z \end{bmatrix} \\
&= \exp(\xi z)\exp(-\xi z) \begin{bmatrix} \cos^2\kappa z + \sin^2\kappa z & \cos\kappa z\sin\kappa z - \sin\kappa z\cos\kappa z \\ \sin\kappa z\cos\kappa z - \cos\kappa z\sin\kappa z & \sin^2\kappa z + \cos^2\kappa z \end{bmatrix} \\
&= \begin{bmatrix} 1 & 0 \\ 0 & 1 \end{bmatrix}
\end{aligned}
\tag{3.30}
$$

where * denotes complex conjugate transpose operation. We will use this property later in the chapter.

No Dispersion Case

Setting dispersion parameters, β_2 and β_3, to zero in the equation 3.11, we get following set of equations

$$
\begin{aligned}
\frac{\partial A_{kR}(z,w)}{\partial z} &= 0 \\
\frac{\partial A_{kI}(z,w)}{\partial z} &= 2\gamma\exp(-2\alpha z)\left[\textstyle\sum_{k=1}^{N} c_i\sqrt{P_k P_i}A_{iR}(z,w)\right]
\end{aligned}
\tag{3.31}
$$

Solution of equation 3.31 can be found as follows

$$
\frac{\partial A_{kR}(z,w)}{\partial z} = 0 \Rightarrow A_{kR}(z=L,w) = A_{kR}(z=0,w) \tag{3.32}
$$

$$
\begin{aligned}
\frac{\partial A_{kI}(z,w)}{\partial z} &= \gamma \exp(-2\alpha z)\left[\sum_{k=1}^{N} c_i\sqrt{P_kP_i}A_{iR}(z,w)\right] \\
&\Rightarrow \int_0^L A_{kI}(z,w)dz = \int_0^L \gamma \exp(-2\alpha z)\left[\sum_{k=1}^{N} c_i\sqrt{P_kP_i}A_{iR}(z,w)\right]dz \\
&\Rightarrow A_{ki}(z=L,w) - A_{kI}(z=0,w) = \left[2\gamma\left[\sum_{k=1}^{N} c_i\sqrt{P_kP_i}A_{iR}(z,w)\right]\frac{\exp(-2\alpha z)}{-2\alpha}\right]_0^L \\
&\Rightarrow A_{kI}(z=L,w) = A_{kI}(z=0,w) + (1-\exp(-2\alpha L))\left[\sum_{k=1}^{N} c_i\sqrt{P_kP_i}A_{iR}(z,w)\right]
\end{aligned} \tag{3.33}
$$

from equation 3.32 and 3.33, we can write the transfer function matrix as

$$
T_{ki}(z=L,w) = \begin{bmatrix} \zeta & 0 \\ \eta\gamma\frac{1}{2\alpha}[1-\exp(1-2\alpha L)]\sqrt{P_kP_i} & \zeta \end{bmatrix} \tag{3.34}
$$

where $\eta = 2, \zeta = 1$ for $k = i$ and $\eta = 4, \zeta = 0$ for $k \neq i$. Note that transfer functions for no-dispersion case are independent of frequency w. But unlike *No-Nonlinearity* case, inter channel transfer functions are not zero.

3.2 Numerical Computation of Transfer Functions

Analytical solution of transfer functions is possible if we ignore either non-linearity or dispersion. However, in case where both non-linearity and dispersion exist solution of transfer functions requires numerical methods. In this section, we present the methodology for numerical solution of transfer functions.

For an N channel WDM system there exist N^2 transfer function matrices. Let's gather all inter and intra transfer functions in matrix form as

$$\begin{bmatrix} A_{1R}(z=L,w) \\ A_{1I}(z=L,w) \\ A_{2R}(z=L,w) \\ A_{2I}(z=L,w) \\ \vdots \\ A_{Nr}(z=L,w) \\ A_{NI}(z=L,w) \end{bmatrix} = \underbrace{\begin{bmatrix} T_{11}(z=L,w) & T_{12}(z=L,w) & \dots & T_{1N}(z=L,w) \\ T_{21}(z=L,w) & T_{22}(z=L,w) & \dots & T_{2N}(z=L,w) \\ \vdots & \vdots & \ddots & \vdots \\ T_{N1}(z=L,w) & T_{N2}(z=L,w) & \dots & T_{NN}(z=L,w) \end{bmatrix}}_{\mathbb{T}(z=L,w)} \begin{bmatrix} A_{1R}(z=0,w) \\ A_{1I}(z=0,w) \\ A_{2R}(z=L,w) \\ A_{2I}(z=L,w) \\ \vdots \\ A_{NR}(z=0,w) \\ A_{NI}(z=0,w) \end{bmatrix} \tag{3.35}$$

where $T_{ki}(z = L, w)$ represents the transfer function matrix from i^{th} channel to the k^{th} channel. Because each transfer function matrix $T_{ki}(z = L, w)$ is 2×2, size of the transfer function matrix, $\mathbb{T}(z = L, w)$, is $2N \times 2N$. We will call $\mathbb{T}(z = L, w)$, as block transfer function matrix.

Equation 3.11 can be written in matrix notation like equation 3.35. Let's define

$$\begin{aligned} \xi_k &= -jw(\beta_2 w_k + \frac{1}{2}\beta_3 w_k^2 + \frac{1}{6}\beta_3 w^2) \\ \kappa_k &= \frac{1}{2}w^2(\beta_2 + \beta_3 w_k) \end{aligned} \tag{3.36}$$

and

$$f_{ki}^z = 2\gamma \exp(-2\alpha z) c_i \sqrt{P_k P_i} \tag{3.37}$$

where $c_i = 1$ if $i = k$ and $c_i = 2$ if $i \neq k$. Then, matrix form of equation 3.11 becomes

$$\frac{\partial}{\partial z}\begin{bmatrix} A_{1R}(z,w) \\ A_{1I}(z,w) \\ A_{2R}(z,w) \\ A_{2I}(z,w) \\ \vdots \\ A_{NR}(z,w) \\ A_{NI}(z,w) \end{bmatrix} = \begin{bmatrix} \begin{pmatrix} \xi_1 & -\kappa_1 \\ \kappa_1 + f_{11}^z & \xi_1 \end{pmatrix} & \begin{bmatrix} 0 & 0 \\ f_{12}^z & 0 \end{bmatrix} & \dots & \begin{bmatrix} 0 & 0 \\ f_{1N}^z & 0 \end{bmatrix} \\ \begin{bmatrix} 0 & 0 \\ f_{21}^z & 0 \end{bmatrix} & \begin{pmatrix} \xi_2 & -\kappa_2 \\ \kappa_2 + f_{22}^z & \xi_1 \end{pmatrix} & \dots & \begin{bmatrix} 0 & 0 \\ f_{2N}^z & 0 \end{bmatrix} \\ \vdots & \vdots & \ddots & \vdots \\ \begin{bmatrix} 0 & 0 \\ f_{N1}^z & 0 \end{bmatrix} & \begin{bmatrix} 0 & 0 \\ f_{N2}^z & 0 \end{bmatrix} & \dots & \begin{pmatrix} \xi_N & -\kappa_N \\ \kappa_N + f_{NN}^z & \xi_N \end{pmatrix} \end{bmatrix} \begin{bmatrix} A_{1R}(z,w) \\ A_{1I}(z,w) \\ A_{2R}(z,w) \\ A_{2I}(z,w) \\ \vdots \\ A_{NR}(z,w) \\ A_{NI}(z,w) \end{bmatrix} \tag{3.38}$$

Equation 3.38 is in the form

$$\frac{\partial \mathbf{A}(z,w)}{\partial z} = \mathbb{D}(w)\mathbf{A}(z,w) + \mathbb{N}(z)\mathbf{A}(z,w) \tag{3.39}$$

where $\mathbf{A}(z,w)$ is

$$\mathbf{A}(z,w) = [A_{1r}(z,w)\ A_{1i}(z,w)\ A_{2r}(z,w)\ A_{2i}(z,w)\ldots A_{Nr}(z,w)\ A_{Ni}(z,w)]^{\dagger 1} \tag{3.40}$$

and $\mathbb{D}(w)$ is z independent, but w dependent block diagonal coefficient matrix

$$\begin{bmatrix} \begin{pmatrix} \xi_1 & -\kappa_1 \\ \kappa_1 & \xi_1 \end{pmatrix} & \begin{pmatrix} 0 & 0 \\ 0 & 0 \end{pmatrix} & \cdots & \begin{pmatrix} 0 & 0 \\ 0 & 0 \end{pmatrix} \\ \begin{pmatrix} 0 & 0 \\ 0 & 0 \end{pmatrix} & \begin{pmatrix} \xi_2 & -\kappa_2 \\ \kappa_2 & \xi_1 \end{pmatrix} & \cdots & \begin{pmatrix} 0 & 0 \\ 0 & 0 \end{pmatrix} \\ \vdots & \vdots & \ddots & \vdots \\ \begin{pmatrix} 0 & 0 \\ 0 & 0 \end{pmatrix} & \begin{pmatrix} 0 & 0 \\ 0 & 0 \end{pmatrix} & \cdots & \begin{pmatrix} \xi_N & -\kappa_N \\ \kappa_N & \xi_N \end{pmatrix} \end{bmatrix} \tag{3.41}$$

and $\mathbb{N}(z)$ is w independent, but z dependent coefficient matrix which contains non-linear terms

$$\begin{bmatrix} \begin{pmatrix} 0 & 0 \\ f^z_{11} & 0 \end{pmatrix} & \begin{pmatrix} 0 & 0 \\ f^z_{12} & 0 \end{pmatrix} & \cdots & \begin{pmatrix} 0 & 0 \\ f^z_{1N} & 0 \end{pmatrix} \\ \begin{pmatrix} 0 & 0 \\ f^z_{21} & 0 \end{pmatrix} & \begin{pmatrix} 0 & 0 \\ f^z_{22} & 0 \end{pmatrix} & \cdots & \begin{pmatrix} 0 & 0 \\ f^z_{2N} & 0 \end{pmatrix} \\ \vdots & \vdots & \ddots & \vdots \\ \begin{pmatrix} 0 & 0 \\ f^z_{N1} & 0 \end{pmatrix} & \begin{pmatrix} 0 & 0 \\ f^z_{N2} & 0 \end{pmatrix} & \cdots & \begin{pmatrix} 0 & 0 \\ f^z_{NN} & 0 \end{pmatrix} \end{bmatrix} \tag{3.42}$$

Equation 3.39 can be solved analytically if $\mathbb{N}(z) = 0$. In that case, solution of 3.39 is

$$\mathbf{A}(z,w) = \exp(\mathbb{D}(w)z)\mathbf{A}(z=0,w) \tag{3.43}$$

Let's define

$$\mathbf{B}(z,w) = \exp(-\mathbb{D}(w)z)\mathbf{A}(z,w) \tag{3.44}$$

[1] $\dagger$ denotes matrix transpose operation.

and compute $\frac{\partial \mathbf{B}(z,w)}{\partial z}$ as

$$\begin{aligned}
\frac{\partial \mathbf{B}(z,w)}{\partial z} &= -\mathbb{D}(w)\exp(-\mathbb{D}(w)z)\mathbf{A}(z,w) + \exp(-\mathbb{D}(w)z)\frac{\partial \mathbf{A}(z,w)}{\partial z} \\
&= -\mathbb{D}(w)\exp(-\mathbb{D}(w)z)\mathbf{A}(z,w) + \exp(-\mathbb{D}(w)z)[\mathbb{D}(w)\mathbf{A}(z,w) + \mathbb{N}(z)\mathbf{A}(z,w)] \\
&= \exp(-\mathbb{D}(w)z)\mathbb{N}(z)\mathbf{A}(z,w) \\
&= \exp(-\mathbb{D}(w)z)\mathbb{N}(z)\exp(\mathbb{D}(w)z)\mathbf{B}(z,w)
\end{aligned} \tag{3.45}$$

In the derivation of $\frac{\partial \mathbf{B}(z,w)}{\partial z}$ we used the equality

$$\mathbb{D}(w)\exp(-\mathbb{D}(w)z) = \exp(-\mathbb{D}(w)z)\mathbb{D}(w) \tag{3.46}$$

because $\mathbb{D}(w)$ and $\exp(-\mathbb{D}(w)z)$ are block diagonal in step 2, and the equation 3.39 in step 3.

The methodology in the solution 3.39 is to first solve 3.45 and then use 3.44 to find $A(z,w)$. The idea behind the solution of 3.45 is to calculate the effect of dispersion exactly. The dispersion terms contained in $\mathbf{D}(w)$ are stiff, i.e. $\mathbf{D}(w)$ has largely varying values due to dispersion. This forces one to use a low-order numerical integration scheme in the solution of 3.39. However, we eliminate the stiffness issue imposed by $\mathbf{D}(w)$ via solving 3.45. That is we can use higher order numerical schemes in the solution of 3.45. We will use Trapezoid Rule in the solution of 3.45. The initial condition for 3.45 is $2N \times 2N$ identity matrix, N being the number of channels. We will first compute $B(z=L,w)$ and then $A(z=L,w)$ by using 3.44.

3.3 Transfer functions for one fiber span in a WDM system

In this section, we give the result of numerical computation of transfer function for one fiber span in a WDM system. We used the same fiber parameters for all of the simulations. The fiber parameters we used are : $\alpha = 0.25$ dB/km , $\beta_2 =$ -21.6 ps^2/km, $\beta_3 = 0.128$ ps^3/km, $\gamma = 2.0$ 1/(W·km), and finally the fiber length for one span is $L = 80$ km. For some cases, we assume that there exist a dispersion compensator at the end of the fiber. Frequency range of the graphs are 0 to 12.5 GHz since frequency spacing of the channels is 25 GHz.

Because transfer function is complex valued, we plot the magnitude of transfer function in the graphs.

Figure 3.1 shows the four intra-channel transfer functions of the middle channel in the system. Each subplot of figure 3.1 shows three curves: one is obtained by ignoring dispersion, the other is obtained by ignoring Kerr-nonlinearity and last one is obtained by ignoring neither dispersion and nor Kerr-nonlinearity, i.e. we obtain the last one by taking into account both dispersion and Kerr-nonlinearity. Figure 3.2, on the other hand, shows the four inter-channel transfer functions from the channel that sits in the middle of the WDM spectrum to the other channels in the system. To observe the actual effect of Kerr-nonlinearity, we also give the figures that show the transfer functions obtained by fully compensating dispersion along the fiber. Figure 3.3 and 3.4 show the intra and inter channel transfer functions considering the dispersion compensation. The dispersion compensation is done by multiplying normal block transfer function matrix, $\mathbb{T}(z = L, w)$, by the matrix T^*_{disp} from left. T^*_{disp} is the complex conjugate transpose of the block transfer function matrix T_{disp} which is obtained by only considering dispersion on the system.

If we compare figure 3.1 and 3.3, we observe that the dips and peaks in the intra transfer functions disappeared in figure 3.3. This means that the dips and peaks shown in figure 3.1 are a consequence of dispersion of the system. This observation is also true for inter channel transfer functions as shown by figures 3.2 and 3.4.

Moreover if we look closer to the graphs 3.3 and 3.4, we observe that transfer functions, both intra and inter, depend on the frequency. This is the result of dispersion despite the fact that we fully compensate the dispersion after the span. Without dispersion, the transfer functions become frequency independent as denoted by the equation 3.34 and shown by figures 3.3 and 3.4.

Another observation from inter channel transfer functions shown by figures 3.2 and 3.4 is the low pass filter behavior of the transfer function from in-phase to quadrature noise components. Also, it can be observed from the graphs 3.2 and 3.4 that the amplitude of noise amplification decreases as the victim channel moves further away from the middle channel.

The graphs 3.1, 3.2, 3.3 and 3.4 show transfer function for only one channel power. To investigate the effect of channel power on transfer functions, we give the figures of transfer

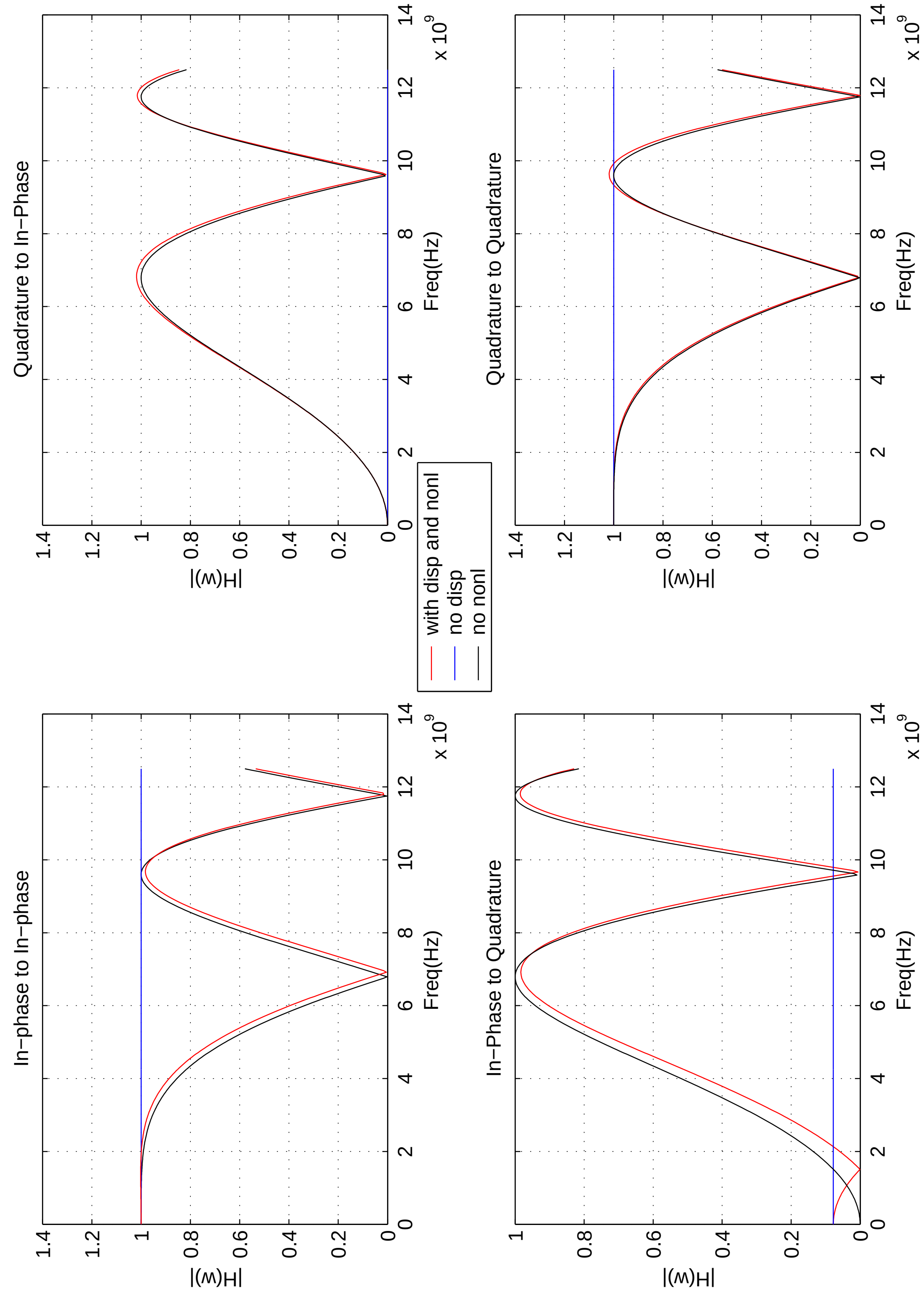

Figure 3.1: Intra-channel transfer functions - no dispersion compensation
System parameters: # of channels: 49, Channel spacing: 25 GHz,
Launch Power: 1.13 mW, α = *0.25 dB/km ,* β_2 = *-21.6* ps^2/km, β_3 = *0.128* ps^3/km, γ = *2.0 1/(W·km), L: 80 km*

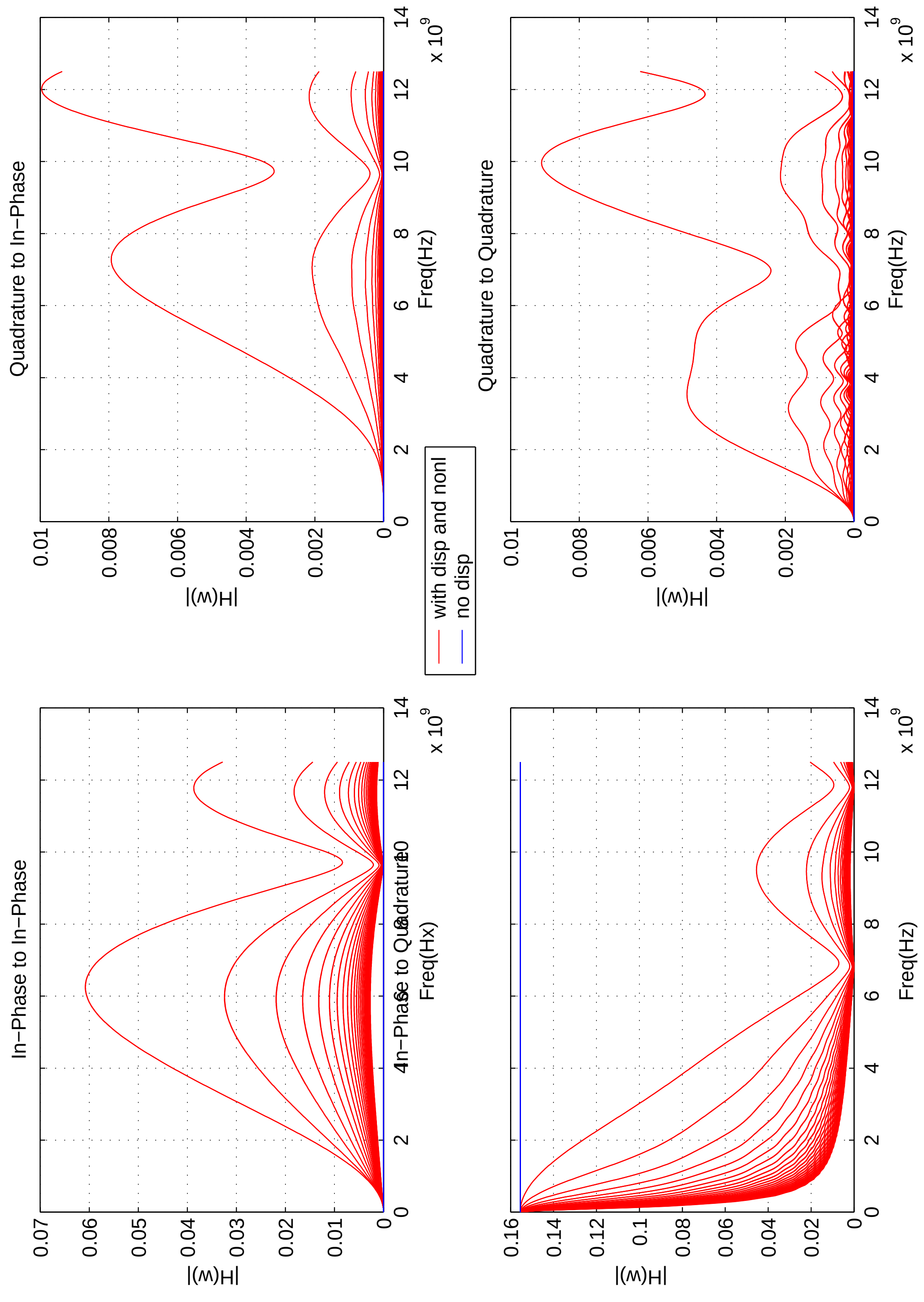

Figure 3.2: Inter-channel transfer functions - no dispersion compensation
System parameters: # of channels: 49, Channel spacing: 25 GHz,
Launch Power: 1.13 mW, α = *0.25 dB/km ,* β_2 = *-21.6* ps^2/km*,* β_3 = *0.128* ps^3/km*,* γ =
2.0 1/(W·km), L: 80 km

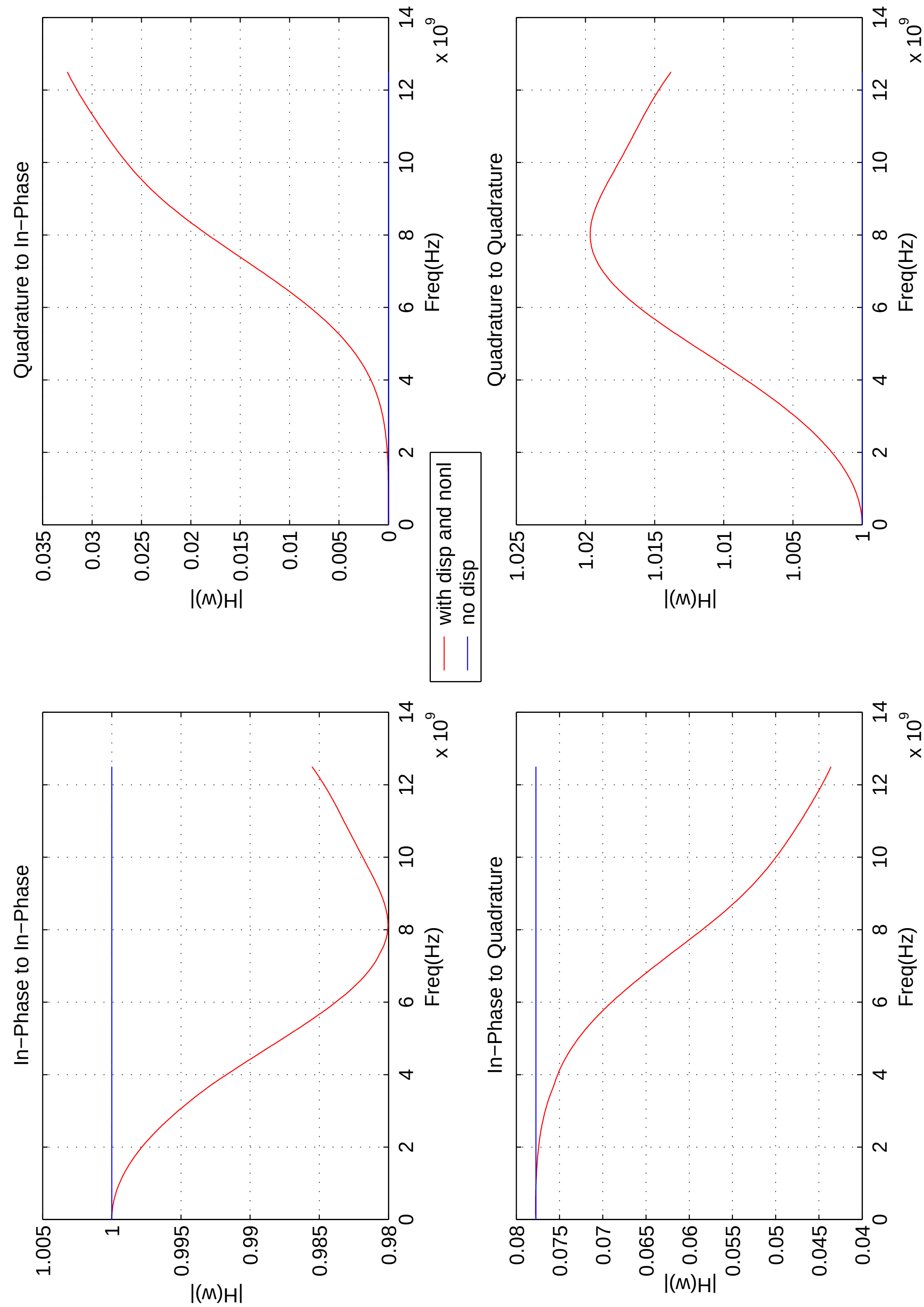

Figure 3.3: Intra-channel transfer functions - with full dispersion compensation
System parameters: # of channels: 49, Channel spacing: 25 GHz,
Launch Power: 1.13 mW, α = *0.25 dB/km ,* β_2 = *-21.6 ps*^{2}*/km,* β_3 = *0.128 ps*^{3}*/km,* γ = *2.0 1/(W·km), L: 80 km*

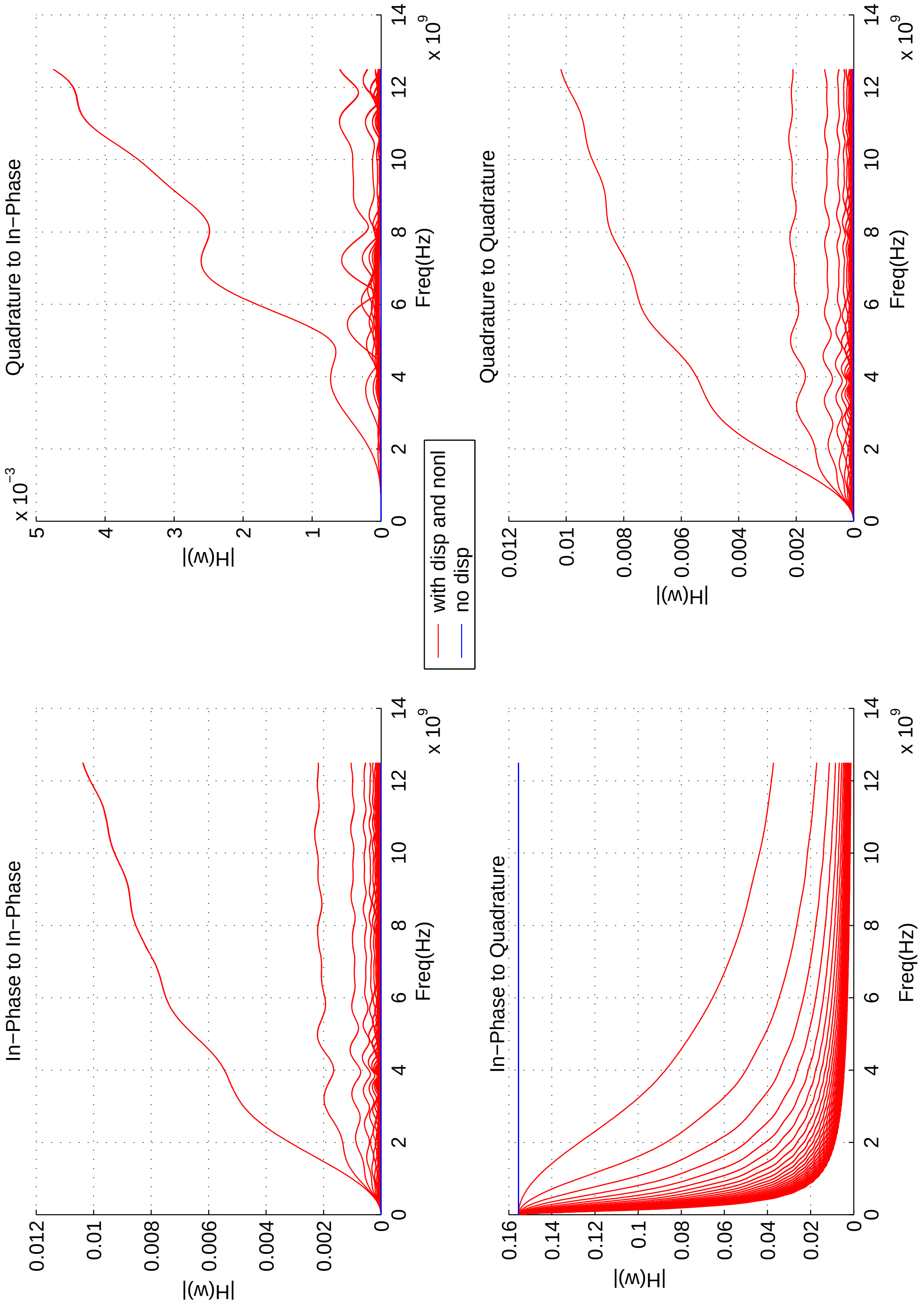

Figure 3.4: Inter-channel transfer functions - with full dispersion compensation
System parameters: # of channels: 49, Channel spacing: 25 GHz,
Launch Power: 1.13 mW, α = *0.25 dB/km ,* β_2 = *-21.6 ps*^{2}*/km,* β_3 = *0.128 ps*^{3}*/km,* γ = *2.0 1/(W·km), L: 80 km*

functions for different launched powers. Figure 3.5 and 3.6 show the inter and intra transfer functions for 20 different powers which are logarithmically equally spaced between 0.1 mW to 10 mW. Figure 3.7 shows the intra channel in-phase to quadrature transfer functions for different powers. Note that logarithmic y axis is used in Figure 3.7 for better understanding. To observe the actual effect of non-linearity, full dispersion compensation is applied after the fiber span. The number of channels is taken to be two which are separated by 100 GHz.

It can be observed from the Figure 3.5 and Figure 3.6 that the in-phase to quadrature transfer function shows an increase in amplitude as the launch power increases. This in turn means that ASE noise increases with launched power. However, the low-pass characteristics of the in-phase to quadrature noise transfer function do not change.

3.4 ASE noise propagation in Multi-Span WDM system

In this section, we analyze the noise propagation in a multi-span WDM system by calculating noise Power Spectral Density (PSD) at the end of the fiber.

A linear system can be described in time and frequency domain as

$$y(t) = h(t) * x(t) \tag{3.47}$$

$$Y(w) = H(w) \cdot X(w) \tag{3.48}$$

where $X(w)$ is the Fourier Transform of the input vector, $x(t)$, $H(w)$ is the Fourier Transform of the transfer function matrix, $h(t)$, $Y(w)$ is the Fourier Transform of the output vector, $y(t)$ and * denotes convolution operation.

PSD of a random process is defined as the Fourier Transform of the autocorrelation function of the process [17]. Assuming that $Z(t)$ is a stationary random process, PSD of $Z(t)$, $S_Z(w)$, can be found as follows

$$S_Z(w) = \mathfrak{F}[R_Z(t)] \tag{3.49}$$

$$= \mathfrak{F}[\mathrm{E}[Z(t) \star Z(t)]] \tag{3.50}$$

$$= \mathrm{E}[\mathfrak{F}[Z(t) \star Z(t)]] \tag{3.51}$$

$$= \mathrm{E}[Z^*(w) \cdot Z(w)] \tag{3.52}$$

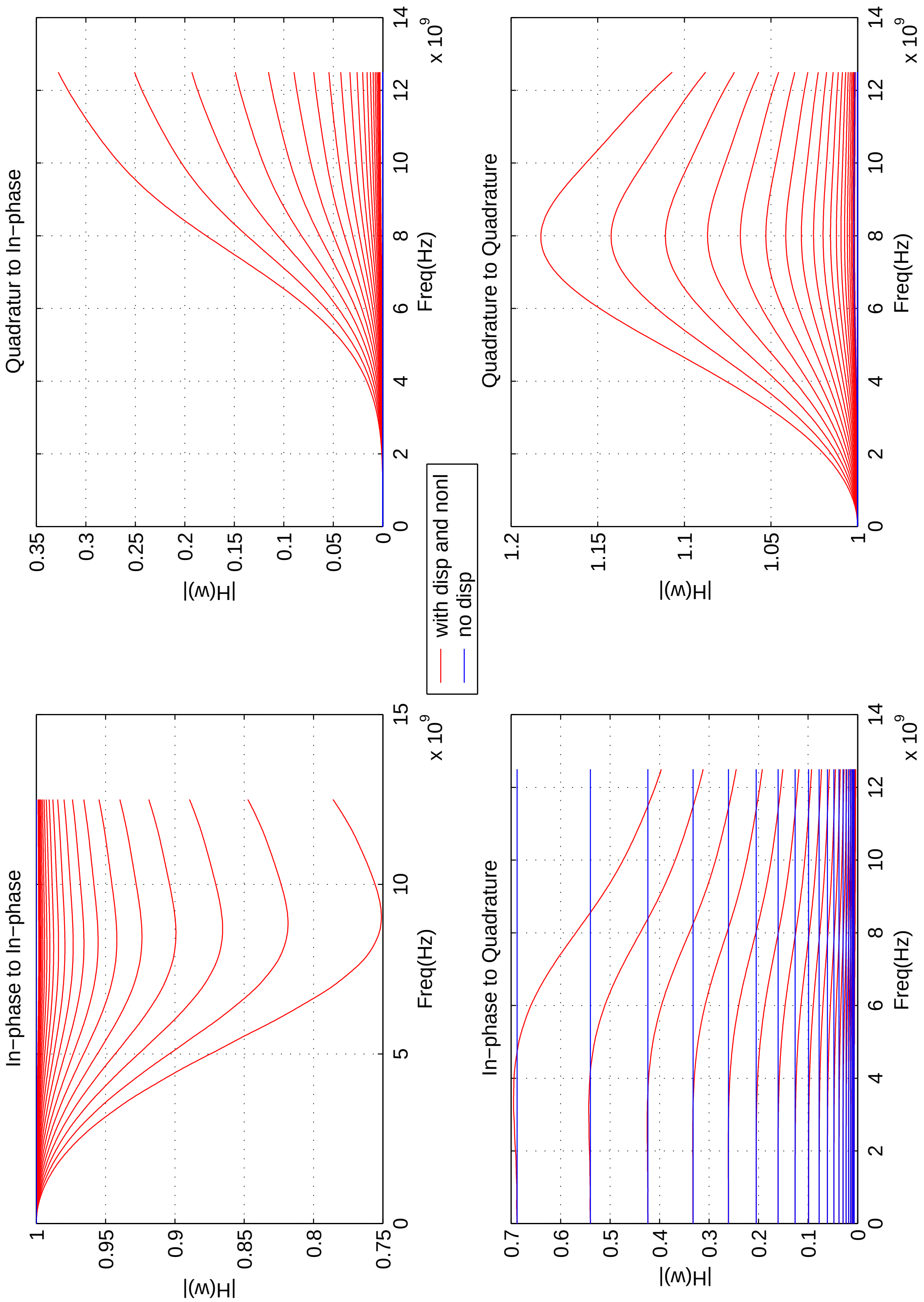

Figure 3.5: Intra-channel transfer functions as a function of launch power (0.1-10 mW) - with full dispersion compensation
System parameters: # of channels: 2, Channel spacing: 100 GHz,
Launch Power: 0.1-10 mW, α *= 0.25 dB/km ,* β_2 *= -21.6* ps^2/km*,* β_3 *= 0.128* ps^3/km*,* γ *= 2.0 1/(W·km), L: 80 km*

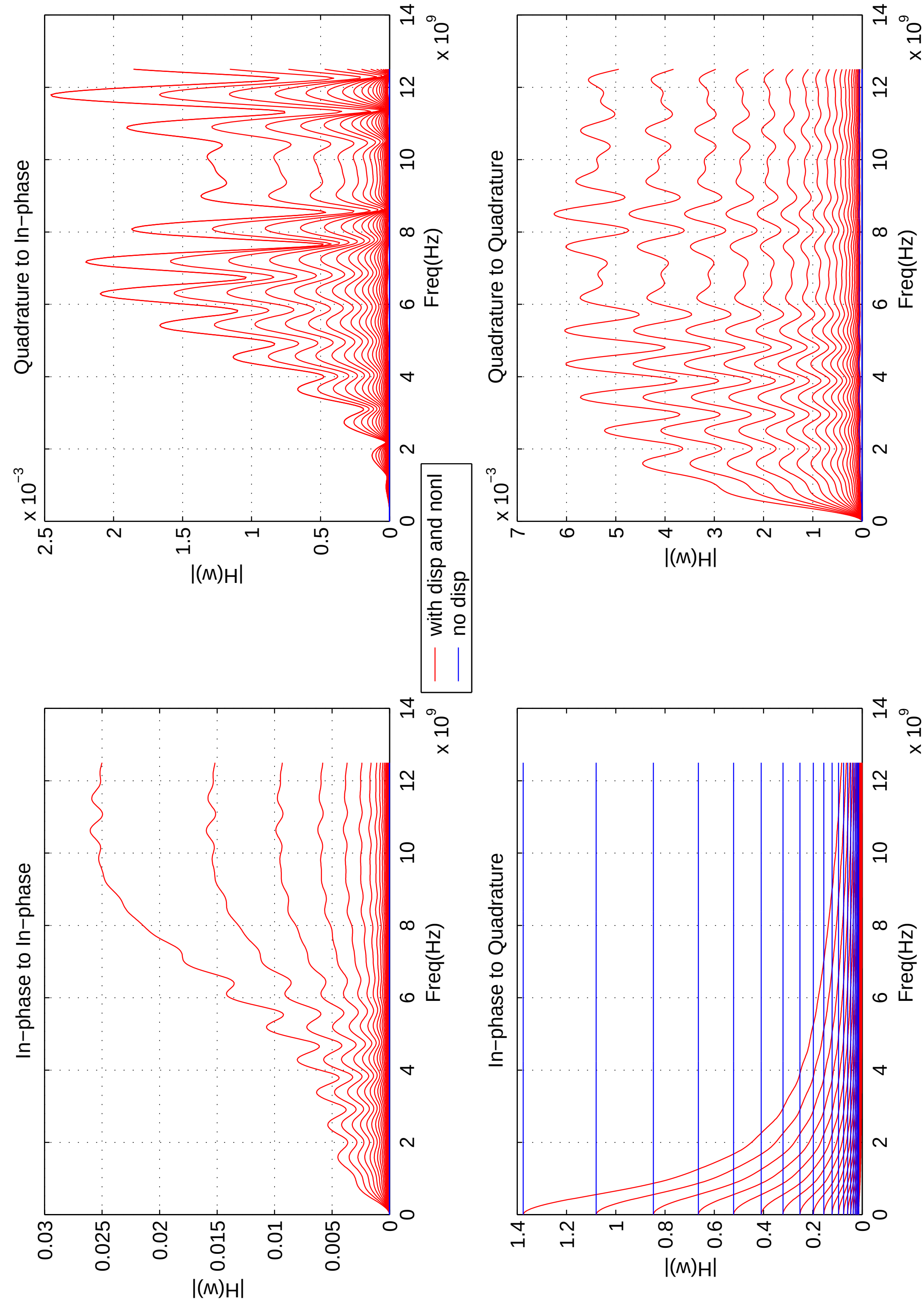

Figure 3.6: Inter-channel transfer functions as a function of launch power per channel (0.1-10 mW) - with full dispersion compensation

System parameters: # of channels: 2, Channel spacing: 100 GHz,
Launch Power: 0.1-10 mW, α *= 0.25 dB/km ,* β_2 *= -21.6 ps*^{2}*/km,* β_3 *= 0.128 ps*^{3}*/km,* γ *= 2.0 1/(W·km), L: 80 km*

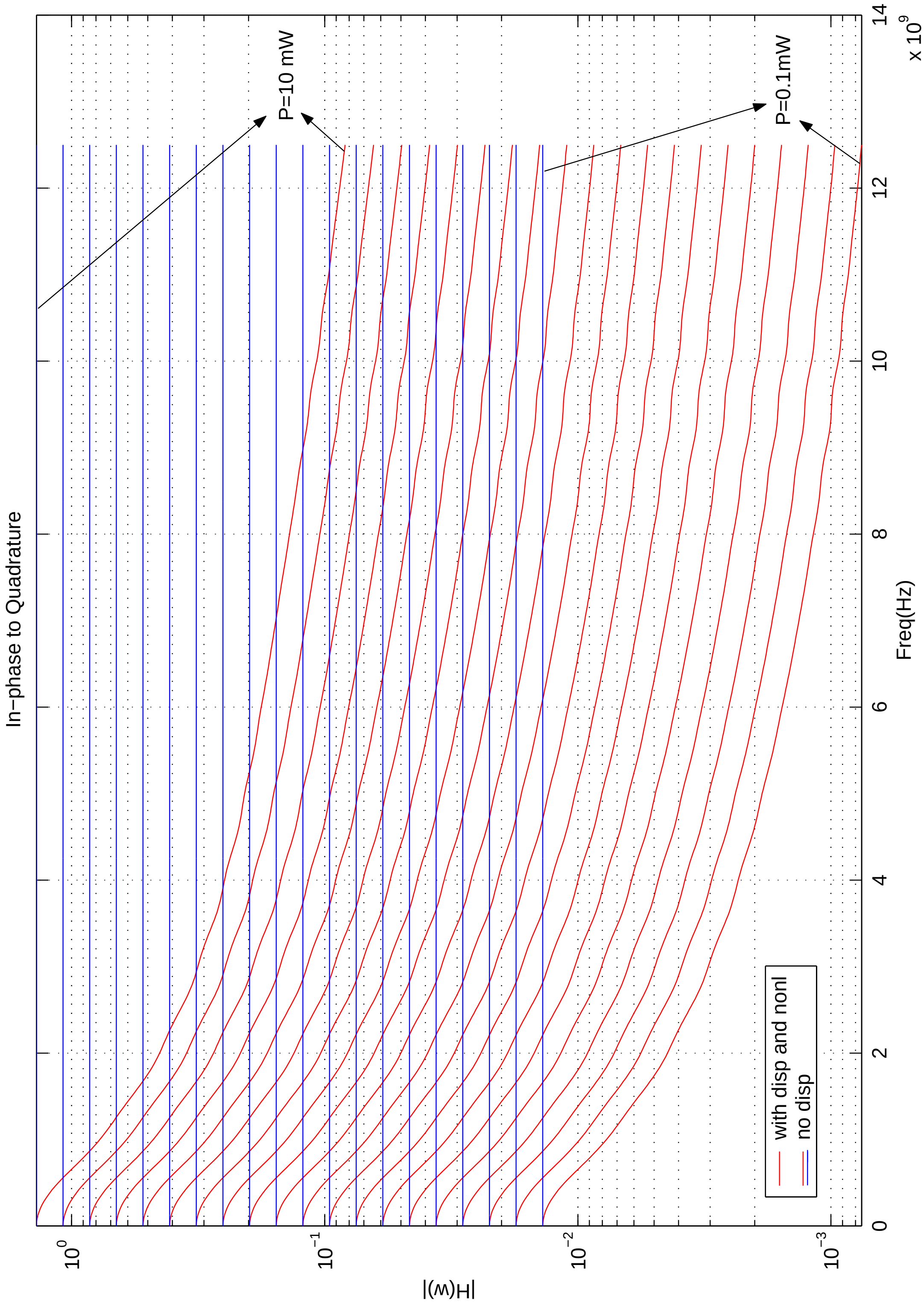

Figure 3.7: In-phase to quadrature inter-channel transfer functions as a function of launch power per channel (0.1-10 mW) - with full dispersion compensation
System parameters: # of channels: 2, Channel spacing: 100 GHz,
Launch Power: 0.1-10 mW, α = *0.25 dB/km ,* β_2 = *-21.6* ps^2/km*,* β_3 = *0.128* ps^3/km*,* γ = *2.0 1/(W·km), L: 80 km*

where $R_Z(t)$ is autocorrelation function of $Z(t)$, $\mathfrak{F}$ denotes Fourier Transform, E denotes probabilistic expectation operator, $\star$ denotes autocorrelation operation, * denotes complex conjugate operation and $j = \sqrt{-1}$. Note that in the computation of 3.49 we used the linearity property of the expectation operator. In order to calculate a system PSD, we use the same methodology. However, we get a power spectral density matrix rather than a single equation in general. For the system 3.47, the PSD matrix for $Y(w)$ is

$$
\begin{aligned}
S_Y(w) &= \mathrm{E}[Y(w) \cdot Y^*(w)] && (3.53)\\
&= \mathrm{E}[H(w) \cdot X(w) \cdot X^*(w) \cdot H^*(w)] && (3.54)\\
&= H(w) \cdot \underbrace{\mathrm{E}[X(w) \cdot X^*(w)]}_{S_X(w)} \cdot H^*(w) && (3.55)\\
&= H(w) \cdot S_X(w) \cdot H^*(w) && (3.56)
\end{aligned}
$$

By using same methodology and the formula 3.56 we can find the PSD matrix of the noise at the end of the fiber as

$$\mathbb{S}(z = L, w) = \mathbb{T}(z = L, w) \cdot \mathbb{S}(z = 0, w) \cdot \mathbb{T}^*(z = L, w) \tag{3.57}$$

where $\mathbb{T}(z = L, w)$ is the $2N \times 2N$ block transfer function matrix that collects all intra and inter transfer function matrices $T_{ki}(z = L, w)$ for $k, i = 1, 2 \ldots N$ and $\mathbb{S}(z, w)$ is the PSD matrix for all of the in-phase and quadrature ASE noise components of all the channels.

The PSD matrix $\mathbb{S}(z, w)$ value that enters in a span is equal to the summation of the PSD matrix value that comes from the previous span and the PSD matrix value generated by the amplifier itself. That is

$$\mathbb{S}_n(z, w) = \mathbb{S}_p(z, w) + \mathbb{S}_a(w) \tag{3.58}$$

where $\mathbb{S}_n(z, w)$ is the next PSD matrix value, $\mathbb{S}_p(z, w)$ is the previous PSD matrix value and $\mathbb{S}_a(w)$ is the PSD matrix value generated by the amplifier at the end of the span. For our computations, we assume that noise is uncorrelated between the channels at the beginning of every span. Also, we assume that the in-phase and quadrature components of the noise in the same channel are also uncorrelated. Thus, we can write PSD matrix for the noise generated by amplifiers as

$$\mathbb{S}_a(w) = N_{oa} \cdot \mathbb{I} \tag{3.59}$$

where $\mathbb{I}$ is $2N \times 2N$ identity matrix and N_{oa} is the common spectral density for all channels. Using 3.58 and 3.59, we can compute the PSD matrix for a multi-span WDM system.

Although there is a power transfer between the carrier power of the channels and to the ASE noise, it is small enough to assume that carrier powers entering the span is the same through the fiber. Thus, we will use the same block transfer function matrix $\mathbb{T}(z = L, w)$ for all of the spans in the calculations of PSD matrix.

The PSD matrix $\mathbb{S}(z, w)$ in fact contains wellworth information: the diagonal entries contain the spectral density of the in-phase and quadrature components of noise of all channels, and off-diagonal entries contains the cross-spectral densities of in-phase and quadrature components of noise of a channel and between other channels. This information will be used in the analysis of noise on the system performance later.

For a multi-span WDM system with M spans, we define the ASE noise amplification as

$$\mathbb{G}(z = ML, w) = \frac{\mathbb{S}(z = ML, w)}{MN_{oa}} \tag{3.60}$$

where $\mathbb{S}(z = ML, w)$ is the noise PSD matrix at the end of the fiber and N_{oa} is the spectral density of the ASE noise generated by OAs. The denominator of the equation 3.60 represents the noise spectral density at the end of the fiber, assuming that OAs exactly compensates for the loss along the WDM system in which noise accumulates linearly through the fiber. Although $\mathbb{G}(z = ML, w)$ is a matrix, its diagonal entries are more important than others since they actually show the noise amplification through the WDM system.

3.4.1 ASE noise propagation with dispersion but no Kerr non-linearity

Without Kerr non-linearity, all of the inter transfer functions become zero as it is shown in section 3.1.1. Also, it is shown in equation 3.30 that all intra-transfer function matrices are unitary. $\mathbb{T}(z = L, w)$ which collects all intra and inter transfer functions in a single matrix, is unitary since it is block diagonal with unitary matrices. That is

$$\mathbb{T}(z = L, w) \cdot \mathbb{T}^*(z = L, w) = \mathbb{I} \tag{3.61}$$

where $\mathbb{I}$ is $2N \times 2N$ identity matrix and * denotes complex conjugation transpose operation.

For this case, the PSD matrix at the end of the fiber span is

$$\mathbb{S}(z = L, w) = \mathbb{T}(z = L, w) \cdot \mathbb{S}_a(w) \cdot \mathbb{T}^*(z = L, w) \quad (3.62)$$

$$\Longrightarrow \mathbb{S}(z = L, w) = \mathbb{T}(z = L, w) \cdot N_{oa}\mathbb{I} \cdot \mathbb{T}^*(z = L, w) \quad (3.63)$$

$$\Longrightarrow \mathbb{S}(z = L, w) = N_{oa}\mathbb{T}(z = L, w) \cdot \mathbb{T}^*(z = L, w) \quad (3.64)$$

$$\Longrightarrow \mathbb{S}(z = L, w) = N_{oa}\mathbb{I} \quad (3.65)$$

so, we observe that the PSD matrix of ASE noise remains the same at the end of the fiber span for the case where there is no non-linearity. This makes us to conclude that ASE noise propagation through the fiber is linear and its spectral properties do not change.

For a WDM system with M fiber spans the PSD matrix at the end of the link becomes $M \cdot N_{oa}\mathbb{I}$ due to linear propagation of noise. Hence noise amplification at the end of the link is

$$\mathbb{G}(z = ML, w) = \frac{M \cdot N_{oa}\mathbb{I}}{MN_{oa}} \quad (3.66)$$

$$\Longrightarrow \mathbb{G}(z = ML, w) = \mathbb{I} \quad (3.67)$$

from which we conclude that there is no noise amplification through WDM system.

3.4.2 ASE noise propagation with Kerr non-linearity but no dispersion

For the case where dispersion is ignored, the intra and inter transfer functions can be calculated analytically as shown is section 3.1.1. In this case, transfer functions become frequency independent but depend on span length, launched signal power and loss coefficient of the fiber as shown in equation 3.34. Moreover, for no dispersion case while in-phase components of noise stay unchanged along the fiber, quadrature components of noise experience amplification along the fiber as shown in equation 3.31. The amount of amplification can be calculated analytically by using 3.57 and 3.58.

For a one span fiber, the noise amplification can be found by first gathering all intra and inter transfer function matrices in $\mathbb{T}(z = L, w)$ and then using equation 3.57. Note that PSD matrix of noise at the beginning of the fiber is $\mathbb{S}(z = 0, w) = \mathbb{S}_a = N_{oa} \cdot \mathbb{I}$. For an N -channel

WDM system, if we do necessary mathematical operations as stated by equations 3.57 and 3.60 to find $\mathbb{G}(z = L, w)$ and extract the diagonal entries of the matrix $\mathbb{G}(z = L, w)$, we get following equations for noise amplifications

$$\begin{aligned} \mathbb{G}_{II}(L, w) &= 1 \\ \mathbb{G}_{QQ}(L, w) &= 1 + 4(4N - 3)\gamma^2 L_{eff}^2 P^2 \end{aligned} \tag{3.68}$$

where P is the power of the channel carriers, N is the number of channels, L_{eff} is

$$L_{eff} = \frac{1 - \exp(-2\alpha L)}{2\alpha} \tag{3.69}$$

where L is the length of the fiber, α is the loss coefficient of the fiber and γ is the non-linearity coefficient of the fiber.

The above calculation is done for only one span WDM system. If we do the same operations for a WDM system with M spans by only considering the ASE noise added by the OA at the start of the fiber and ignoring all ASE noise additions by other OAs, we get the following equations for noise amplification

$$\begin{aligned} \mathbb{G}_{II}(L, w) &= 1 \\ \mathbb{G}_{QQ}(L, w) &= 1 + M^2 4(4N - 3)\gamma^2 L_{eff}^2 P^2 \end{aligned} \tag{3.70}$$

From equation 3.70 we observe that although in-phase component of noise do not experience any noise amplification, the quadrature component of noise amplification increases quadratically with the number of spans, M, in a WDM system. Despite the fact that we anticipate noise to be accumulated linearly, since noise is only introduced at the transmitter, the quadratic amplification can be explained by the correlations that exist between channels. If we examine the PSD matrix $\mathbb{S}(z = ML, w)$, we see that off-diagonal entries are non-zero. Thus we conclude that there is a correlation between in-phase and quadrature components of noise of channels. This is why quadrature component of noise amplifications is quadratic with respect to the number of spans M. If we set cross-correlations in PSD matrix $\mathbb{S}(z, w)$ zero after every span, we see that quadratic noise amplification is also linear with respect to the number of spans M.

To generalize the results, we have to include the effect of ASE noise generated by OAs between the spans. This result can easily be obtained by again using equations 3.57 and 3.58 and taking $\mathbb{S}(z = 0, w) = \mathbb{S}_a = N_{oa} \cdot \mathbb{I}$. Also, we can get the result by simply summing the PSD matrices at the end of the every fiber span. That is by summing the PSD matrices computed for $m = 1, 2, \cdots, M$, where M is the number of spans in WDM system, we can get the overall PSD matrix for the noise. This is because, we are assuming that noise generated by different OAs are un-correlated, revealed by the equation 3.58. In equation 3.58, we simply add the noise PSD matrices of previous span's PSD matrix and PSD matrix generated by OA itself to compute the PSD matrix that is entering the next fiber span because they are un-correlated. If we sum up the noise PSD matrices at the end of every span and use 3.60, we get the following noise amplification equations

$$\begin{aligned} \mathbb{G}_{II}(L, w) &= 1 \\ \mathbb{G}_{QQ}(L, w) &= 1 + \frac{2}{3}(2M^2 + 3M + 1)(4N - 3)\gamma^2 L_{eff}^2 P^2 \end{aligned} \tag{3.71}$$

We observe in equation 3.71 that quadrature noise amplification is quadratic, not cubic, with respect to M, number of spans in WDM system.

3.4.3 ASE noise propagation with Kerr non-linearity and dispersion

For the case where we both take the non-linearity and dispersion into account, we have stated that there is no general analytical solution for the transfer function in section 3.1.1 and shown a numerical method to compute the transfer function in section 3.2.

In this section, because we can compute the transfer functions numerically, we give the noise amplification results graphically. We use the same fiber parameters as in section 3.3. Additional system parameters are given under each graph. Note that noise amplification is given in dB units.

For simulation purposes, we use four dispersion compensation schemes at the end of every fiber span, which are

- nodispcomp: no dispersion compensation is performed anywhere in the WDM system.

- allinampdispcomp: 100 % Dispersion compensation after every span, but none at the receiver.

- allatRXdispcomp: no dispersion compensation after every span, but 100 % at the receiver.

- amp95restRXdispcomp: after every span of the fiber, 95 % of the dispersion is compensated. The remaining dispersion is compensated at the receiver.

We have shown in section 3.1.1 that transfer functions can be computed analytically for no-nonlinearity case. Also, we have shown in section 3.1.1 that inter transfer function matrices are zero matrices and that intra transfer function matrices are unitary in equation 3.30. Let's assume that, $\mathbb{T}(z = L, w)$ is the block transfer matrix that collects all inter and intra transfer function matrices. Then, we apply dispersion compensation schemes as follows

- for *allinampdispcomp* case, we first find the transfer function matrices by ignoring non-linearity and gather all transfer function matrices in $\mathrm{T}(z = L, w)$, which is block diagonal. To compensate the dispersion, we multiply $\mathbb{T}(z = L, w)$ by $\mathrm{T}^*(z = L, w)$ [2] from left to find the new block transfer function matrix

$$\mathcal{T}(z = L, w) = \mathrm{T}^*(z = L, w)\mathbb{T}(z = L, w) \tag{3.72}$$

  For this case, we use $\mathcal{T}(z = L, w)$ as the new block transfer function matrix and use it to evaluate the equation 3.57.

- for *allatRXdispcomp* case, we first find the transfer function matrices by ignoring non-linearity and assuming that the length of the fiber is ML, where M is the number of spans and L is the length of the fiber for one fiber span. Then, we gather all transfer function matrices in $\mathrm{T}(z = L, w)$. At the end of the fiber link we compute the new PSD matrix as

$$\mathbb{S}(z = ML, w) = \mathrm{T}^*(z = L, w)\mathbb{S}(z = ML, w)\mathrm{T}(z = L, w)^2 \tag{3.73}$$

[2] * denotes complex conjugate transpose operation.

- for *amp95restRXdispcomp* case, we again find the transfer function matrices by ignoring non-linearity and assuming that the fiber length is $0.95L$, where L is the actual length of the fiber for one fiber span. Then we gather all transfer function matrices in $\mathrm{T}_1(z = L, w)$. To compensate the dispersion at the end of the span we multiply $\mathbb{T}(z = L, w)$ by $\mathrm{T}_1^*(z = L, w)$ [3] to find the new block transfer function matrix

$$\mathcal{T}(z = L, w) = \mathrm{T}_1^*(z = L, w)\mathbb{T}(z = L, w) \tag{3.74}$$

and use $\mathcal{T}(z = L, w)$ for the PSD matrix computation in equation 3.57. Also we compute another transfer function matrix by ignoring non-linearity but assuming that fiber length is $0.05ML$, where M is the number of spans and L is the actual length of the fiber for one fiber span. After gathering all transfer function matrices in $\mathrm{T}_2(z = L, w)$ we compute the new PSD matrix at the end of the fiber as

$$\mathbb{S}(z = ML, w) = \mathrm{T}_2^*(z = L, w)\mathbb{S}(z = ML, w)\mathrm{T}_2(z = L, w)^3 \tag{3.75}$$

We now present the results for the ASE noise amplification as a function of frequency. Figure 3.8 and 3.9 shows the noise amplification for in-phase and quadrature components of ASE noise for the channel that sits in the middle of the WDM spectrum.

We observe in Figure 3.8 that in-phase noise amplification shows smooth behavior for *allinampdispcomp* and *amp95restRXdispcomp* dispersion compensation schemes. For *nodispcomp* and *allatRXdispcomp* schemes, on the other hand, in-phase noise amplification shows very chaotic behavior. However, for all dispersion compensation schemes we observe that in-phase noise amplification is not very significant despite the fact that it has chaotic behavior for some dispersion compensation schemes. Also, if we compare *nodispcomp* and *allatRXdispcomp* schemes we see that there is no significant difference with respect to in-phase noise amplification. This means that deferring dispersion compensation at the receiver has no significant impact on noise amplification. However, for the *allinampdispcomp* case where dispersion is fully compensated after every span, we observe that in-phase noise is attenuated as shown in Figure 3.8.

[3] * denotes complex conjugate transpose operation.

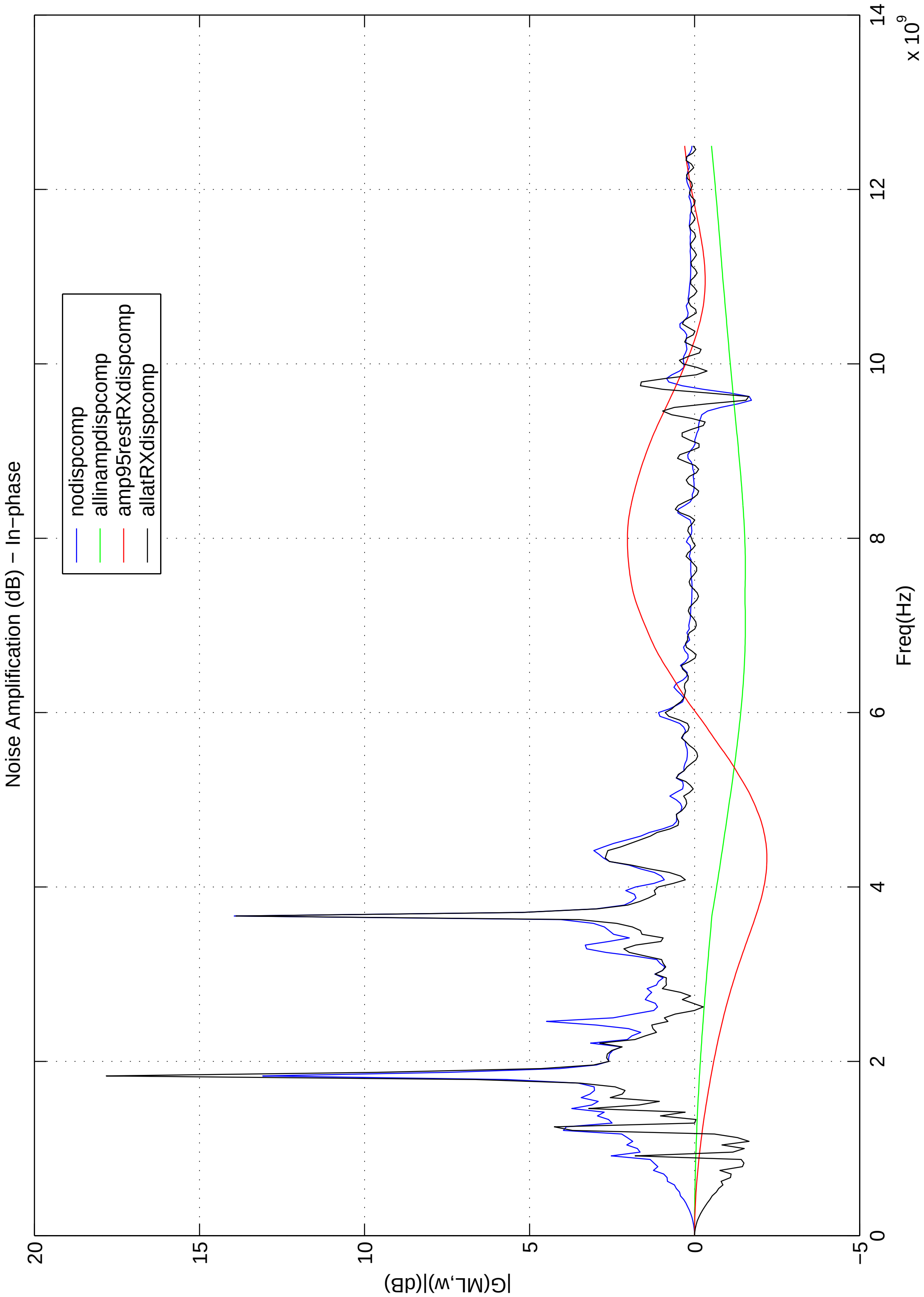

Figure 3.8: ASE noise amplification as a function of dispersion compensation scheme [In-phase]
System parameters: # of channels: 49, Channel spacing: 25 GHz,
Launch Power: 1.13 mW, α = *0.25 dB/km* , β_2 = *-21.6* ps^2/km, β_3 = *0.128* ps^3/km, γ = *2.0 1/(W·km), L: 80 km, # of spans: 20*

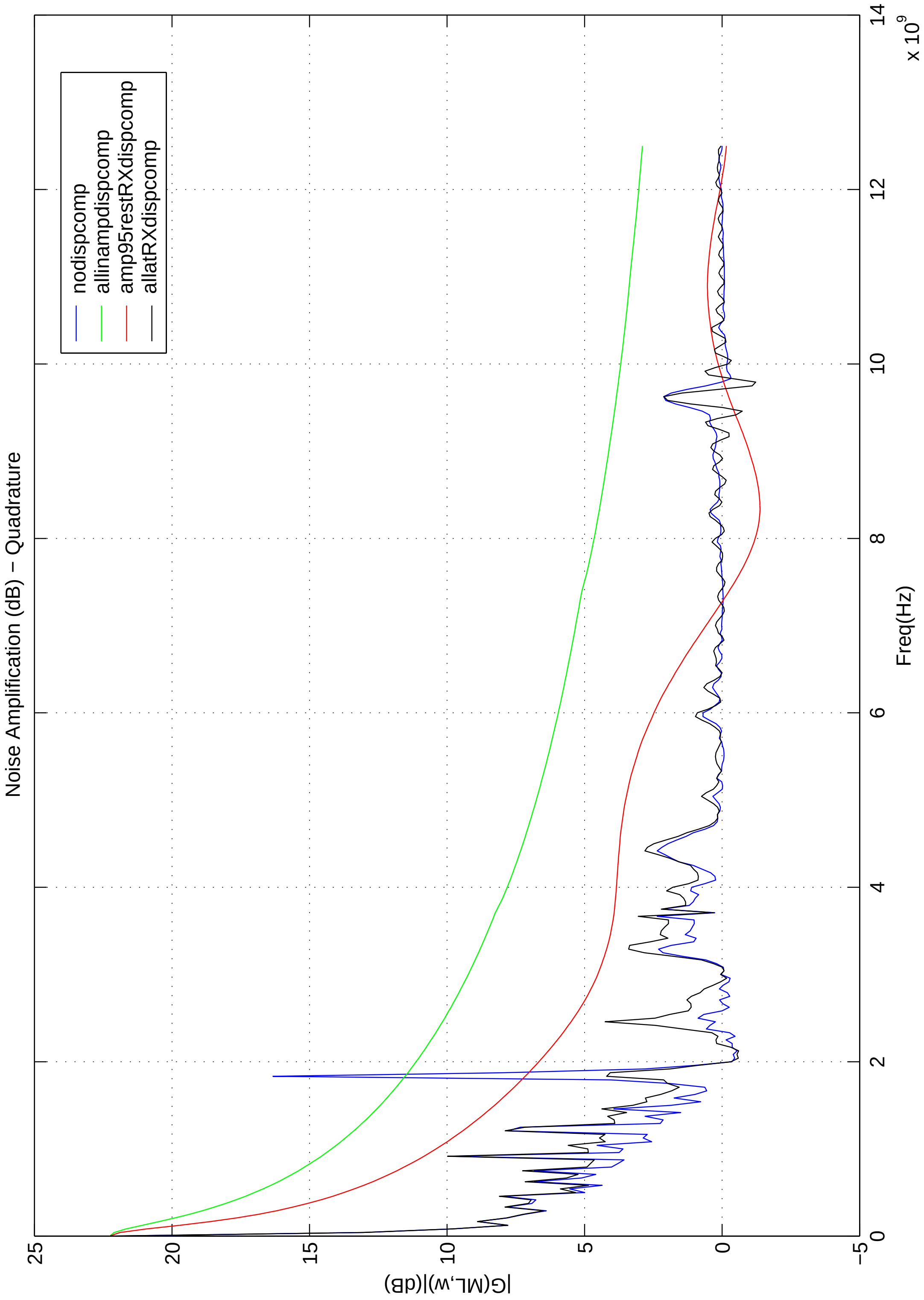

Figure 3.9: ASE noise amplification as a function of dispersion compensation scheme [Quadrature]
System parameters: # of channels: 49, Channel spacing: 25 GHz,
Launch Power: 1.13 mW, α *= 0.25 dB/km ,* β_2 *= -21.6 ps*^{2}*/km,* β_3 *= 0.128 ps*^{3}*/km,* γ *= 2.0 1/(W·km), L: 80 km, # of spans: 20*

Although in-phase noise amplification is not significant as shown in Figure 3.8, it is not the case for quadratic noise amplification. As shown in Figure 3.9, quadratic noise amplification is very significant at low frequencies. However, for all dispersion compensation schemes, the quadratic noise amplification shows a low pass characteristics. That is quadratic noise amplification decreases rapidly as offset frequency increases. Also, we observe in Figure 3.9 that the quadratic noise amplification is most significant for *allinampdispcomp* scheme. Note also that *allinampdispcomp* scheme is the only scheme that results in in-phase noise attenuation as shown in Figure 3.8. For quadratic noise, on the other hand, it resulted in most noise amplification. Like for in-phase noise, quadratic noise amplification shows chaotic behavior for *nodispcomp* and *allatRXdispcomp* schemes.

Let's now observe the affects of the number of channels in the system the ASE noise amplification. Figures 3.10, 3.11 and 3.12[4] show the in-phase and quadrature noise amplification for a WDM system with different number of channels. These figures were obtained by using the *amp95restRXdispcomp* scheme. In each figure, noise amplification of the channel that sits in the WDM spectrum is shown. In Figure 3.10, it is observed that in-phase noise amplification is not quite dependent on the number of channels. For quadratic noise, as depicted in Figures 3.11 and 3.12, we observe two different behaviors: whereas noise amplification at low offset frequencies increases with the number of channels, for high offset frequencies noise amplification do not change significantly with the number of channels.

Let's also observe the effect of launched power per channel on the noise amplification. Figures 3.13 and 3.14 show the in-phase and quadrature noise amplification for a WDM system with different launched channel powers that are logaritmically equally spaced between 0.1 mW and 10 mW. These figures were also obtained by using *amp95restRXdispcomp* scheme. As observed in Figures 3.13 and 3.14, both in-phase and quadrature noise amplification increase as the launched power increases for all offset frequencies. Also, we observe in Figure 3.14 that for high launched channel powers, quadratic noise amplification loses its low-pass characteristics.

[4]Figure 3.12 is same as Figure 3.11, but the amplification is shown with a log frequency

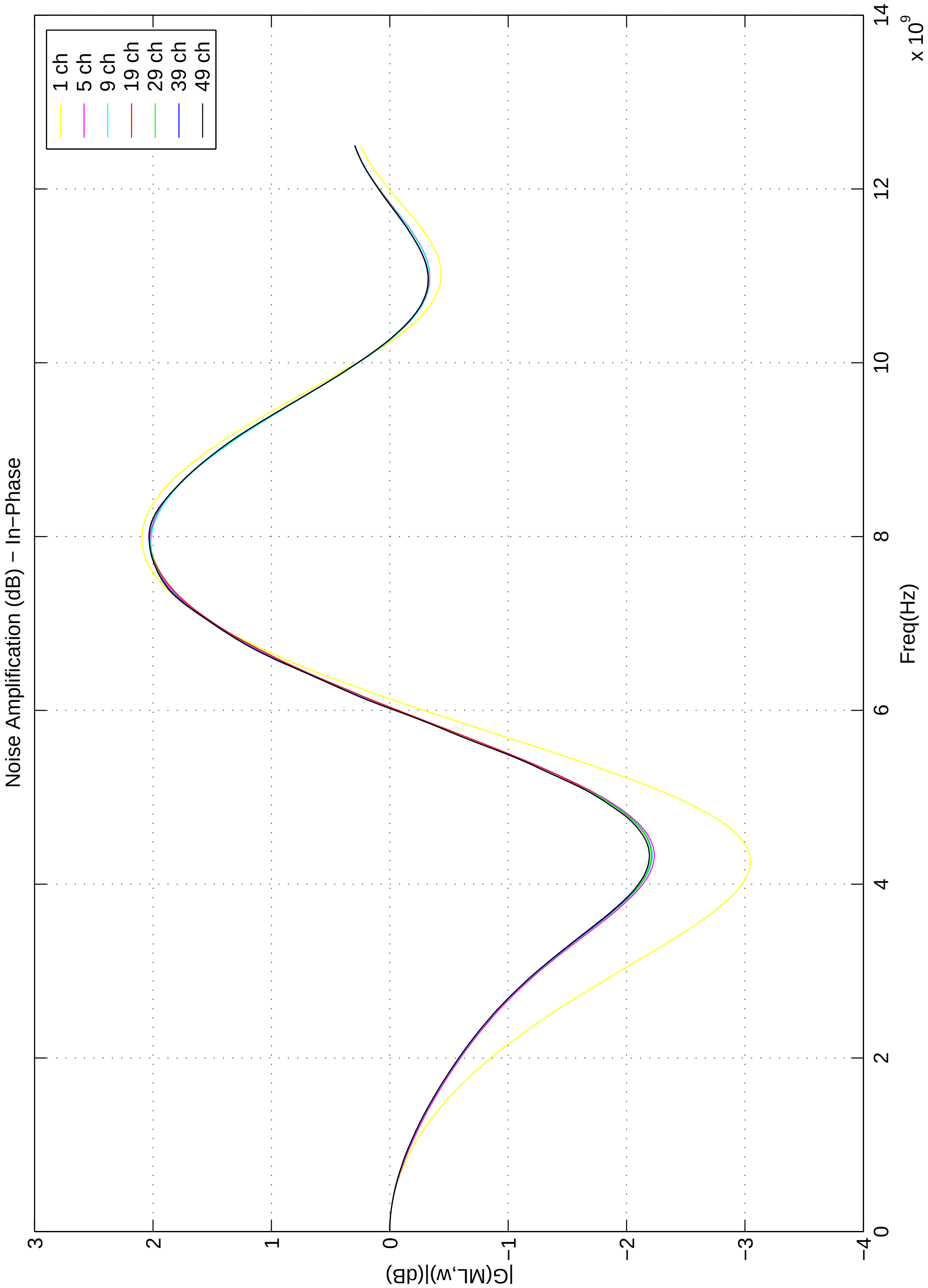

Figure 3.10: ASE noise amplification as a function of the number of channels [In-phase] (amp95RestRXdispComp)

System parameters: Channel spacing: 25 GHz, Launch Power: 1.13 mW, *α = 0.25 dB/km , β_2 = -21.6 ps^2/km, β_3 = 0.128 ps^3/km, γ = 2.0 1/(W·km), L: 80 km,* *# of spans: 20*

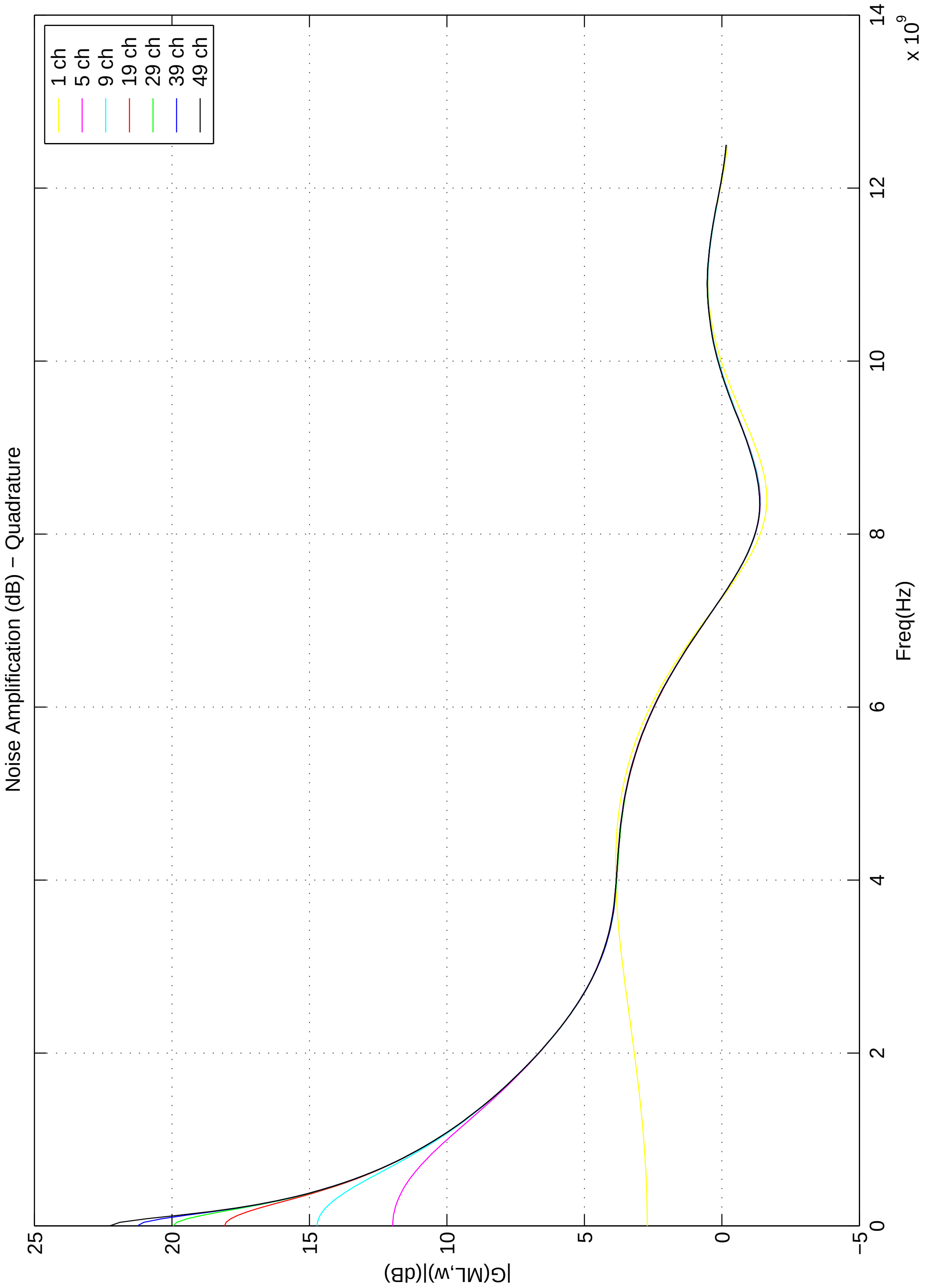

Figure 3.11: ASE noise amplification as a function of the number of channels [Quadrature] (amp95RestRXdispComp)
System parameters: Channel spacing: 25 GHz, Launch Power: 1.13 mW,
α = *0.25 dB/km* , β_2 = *-21.6 ps*^{2}*/km*, β_3 = *0.128 ps*^{3}*/km*, γ = *2.0 1/(W·km), L: 80 km,*
# of spans: 20

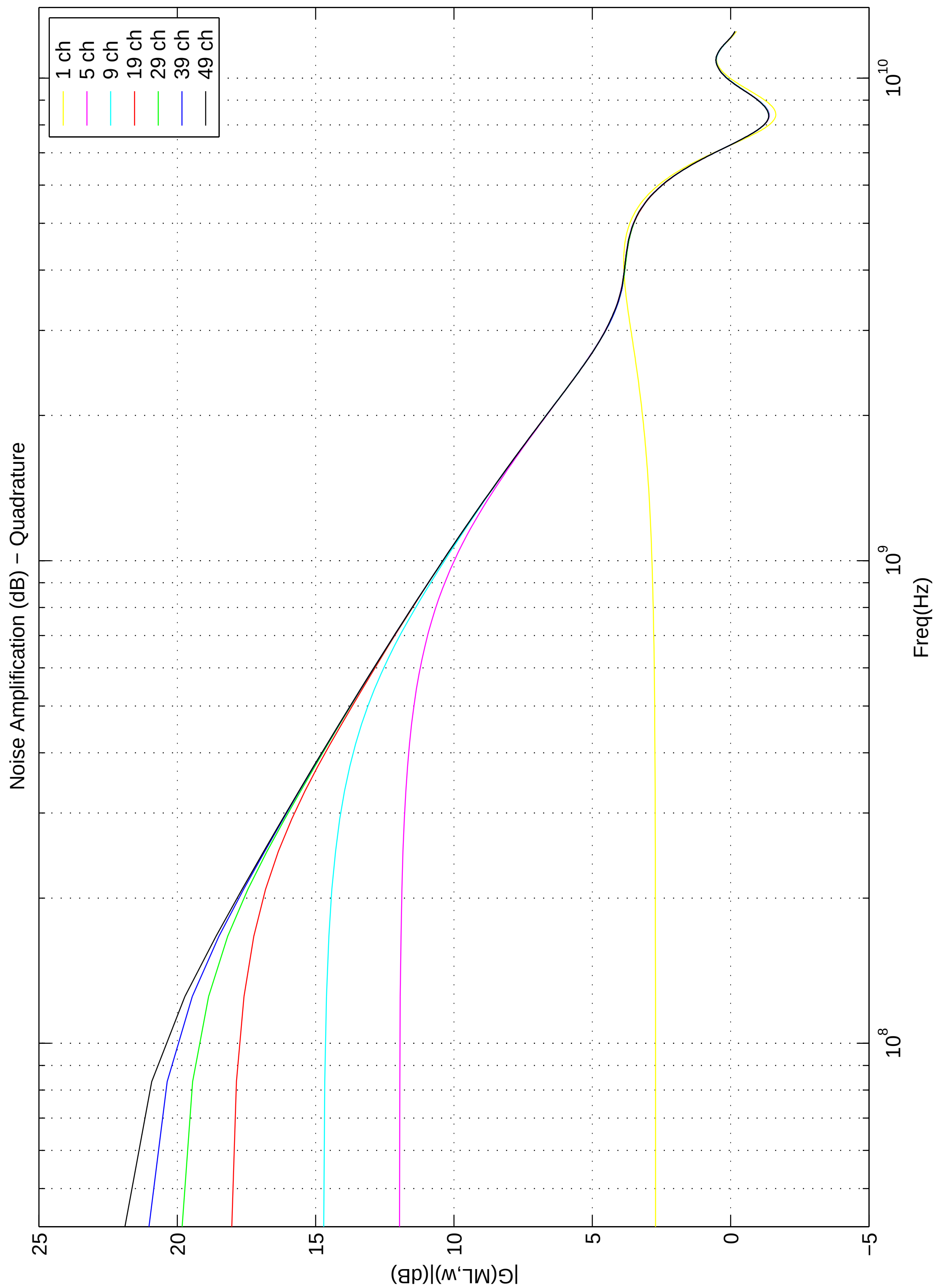

Figure 3.12: ASE noise amplification as a function of the number of channels [Quadrature] - Log frequency axis (amp95RestRXdispComp)
System parameters: Channel spacing: 25 GHz, Launch Power: 1.13 mW,
α = *0.25 dB/km* , β_2 = *-21.6 ps*^{2}*/km*, β_3 = *0.128 ps*^{3}*/km*, γ = *2.0 1/(W·km), L: 80 km,*
# of spans: 20

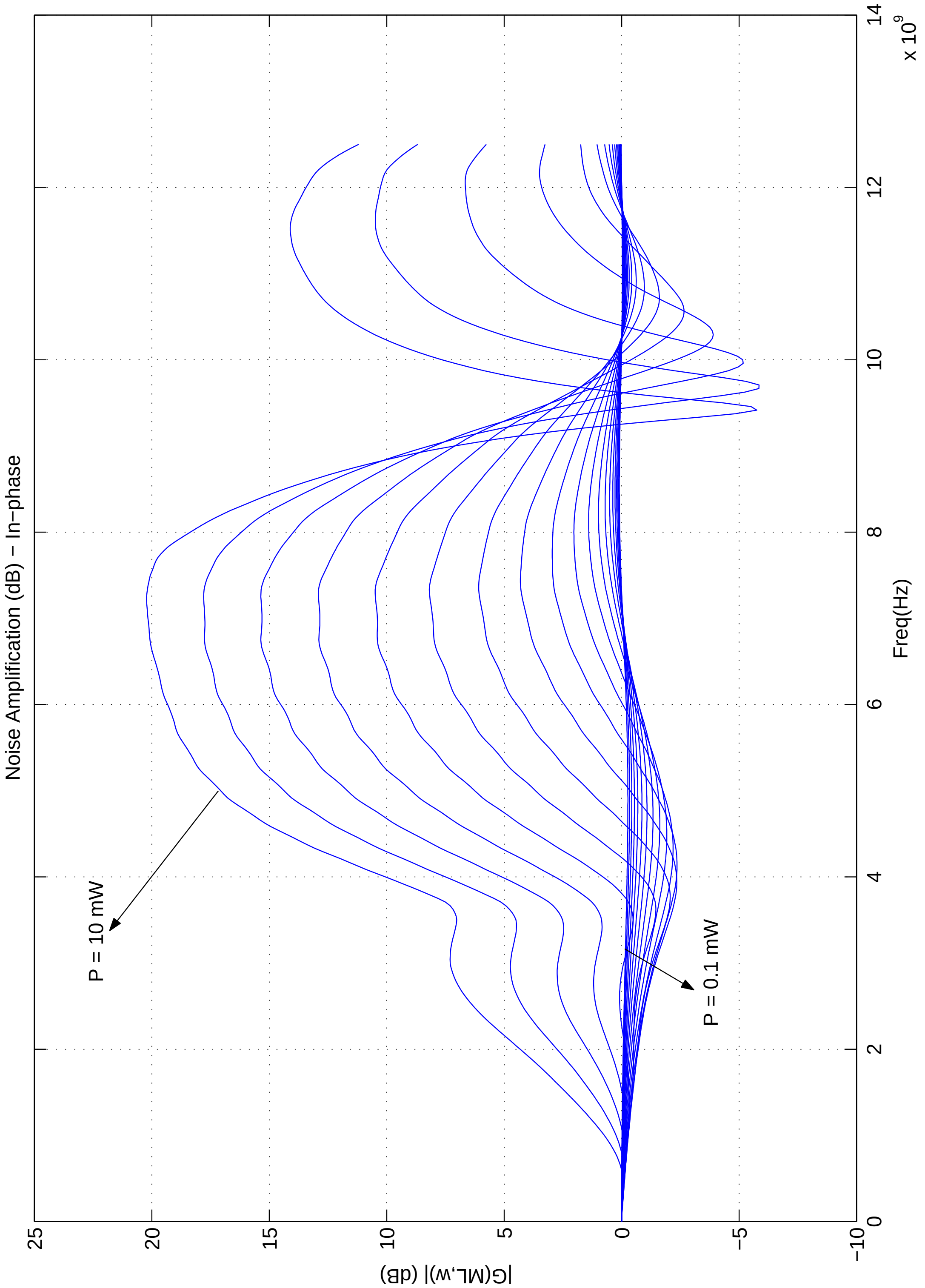

Figure 3.13: ASE noise amplification as a function of launch power per channel (0.1-10 mW) [In-phase] (amp95RestRXdispComp)
System parameters: # of channels: 49, Channel spacing: 25 GHz,
Launch Power: 0.1-10 mW, α *= 0.25 dB/km ,* β_2 *= -21.6* ps^2/km*,* β_3 *= 0.128* ps^3/km*,* γ *= 2.0 1/(W·km), L: 80 km, # of spans: 20*

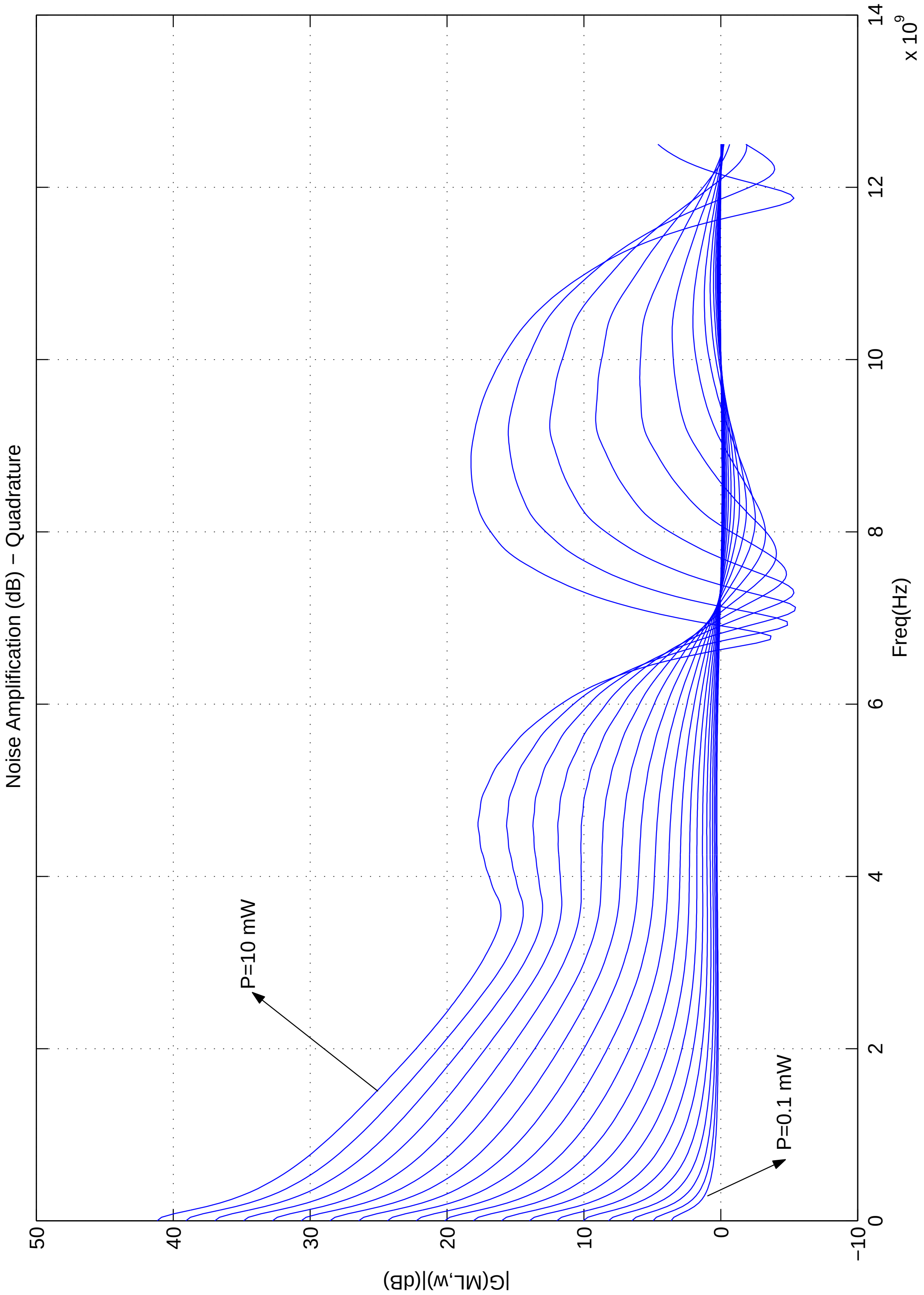

Figure 3.14: ASE noise amplification as a function of launch power per channel (0.1-10 mW) [Quadrature] (amp95RestRXdispComp)
System parameters: # of channels: 49, Channel spacing: 25 GHz,
Launch Power: 0.1-10 mW, α *= 0.25 dB/km ,* β_2 *= -21.6 ps*^{2}*/km,* β_3 *= 0.128 ps*^{3}*/km,* γ *= 2.0 1/(W·km), L: 80 km, # of spans: 20*

3.5 ASE noise Effect on Differential Modulation Schemes

In this section, we evaluate the effect of ASE noise on the system performance by computing the system's bit error ratio(BER). For the analysis, we specifically are interested in differential binary phase shift keying (DBPSK) and differential quadrature shift keying (DQPSK) modulation schemes. In the calculation of ASE noise effect on the system performance, we ignore all system dependent deficiencies, i.e. chromatic dispersion, non-ideality of the receiver, laser phase noise etc., thus enabling us to observe the pure effect of amplified ASE noise on the BER performance of the system.

3.5.1 BER performance evaluation methodology

In the evaluation of BER performance of the system we will use the $S(z = ML, w)$ matrix which gives the second order probabilistic characteristics of the amplified ASE noise. In particular, we will evaluate the BER performance of the channel that sits in the middle of the WDM spectrum since its the channel that is most effected by the amplified ASE noise.

Although $S(z = ML, w)$ gives the complete second order probabilistic characteristics of the ASE noise, more specific probabilistic characteristic of the noise such as joint probability density function for the time samples of ASE noise are required to compute BER performance. In the calculation of PSD matrix of noise in section 3.4 we assumed that in-phase and quadrature components of ASE noise generated by OAs are uncorrelated white Gaussian noise. Although the noise that impinges on the receiver is not strictly Gaussian, due to non-linear interaction of channels via Kerr non-linearity , we still assume that it is Gaussian. This is a result of the linearization that we have imposed on the system in the introductory part of this chapter. In a linear system a Gaussian stochastic process remains Gaussian throughout the process [17]. This is why we assume that the ASE noise impinging on the receiver is gaussian. However, note that the noise samples at the receiver are not un-correlated due to Kerr non-linearity.

For BER analysis, we assume that DPSK receiver is ideal and that the performance degradation is due only to ASE noise generated by OAs. The signal that impinges on the receiver is

$$r(t) = s(t) + n(t) \tag{3.76}$$

where $r(t)$ is the signal at the receiver, $s(t)$ is the noise free signal and $n(t)$ is the noise. In BER computation we assume that channels in WDM system are already separated by any means of electronic device. Also by the ideality of the receiver we assume that receiver has brick-wall filter, with a bandwidth equal to frequency separation between the channels, that separates channels from each other. In equation 3.76 both $r(t)$, $s(t)$ and $n(t)$ are complex quantities and have in-phase and quadrature components. That is

$$s(t) = s_i(t) + js_q(t) \text{ and } n(t) = n_i(t) + jn_q(t) \tag{3.77}$$

where $s_i(t)$ and $n_i(t)$ denote in-phase components, and $s_q(t)$ and $n_q(t)$ denote quadrature components of $s(t)$ and $n(t)$ respectively. The ideal receiver samples $r(t)$ at the center of each period and obtains

$$r[k] = r(kT_s) = s(kT_s) + n(kT_s) = s[k] + n[k] \tag{3.78}$$

where

$$s[k] = s_i[k] + s_q[k] \text{ and } n[k] = n_i[k] + n_q[k] \tag{3.79}$$

and T_s is the symbol period. Differential detector then performs the following operation

$$r_D[k] = r[k]r^*[k-1] \tag{3.80}$$

where * denotes complex conjugate operation. The decision of the symbol is then made by looking at the place of $r_D[k]$ in complex plane. For DBPSK, symbol decision is made by only looking at the real part of $r_D[k]$. For DQPSK, on the other hand, both real and imaginary parts are considered in the symbol decision.

The noise samples $n[k]$ impinging on the receiver are gaussian with zero mean. However, due to Kerr non-linearity, the in-phase $n_i[k]$ and the quadrature components $n_q[k]$ of noise are correlated with each other which can be inferred from non-zero cross spectral density, $S_{iq}(w)$. In addition, because spectral densities of in-phase, $S_{ii}(w)$, and quadratic, $S_{qq}(w)$, noise components are non-zero and non-constant, there is also correlation between two noise samples sampled at different times. If the Kerr non-linearity is ignored, the spectral densities of in-phase and quadrature noise components become frequency independent, i.e. white noise, and in-phase and quadrature noise components becomes uncorrelated.

The decision made by the differential detector depends on two consecutive bit symbols. As stated above there exists a correlation between and within noise samples. This means that $n_i[k]$, $n_q[k]$, $n_i[k-1]$ and $n_q[k-1]$ are correlated with each other. The correlation between noise samples can be computed by the use of spectral densities calculated in section 3.4. This is because spectral density function is the Fourier Transform of the correlation function [17]. So, correlation among noise samples can be found by the inverse Fourier Transform of spectral density function as follows

$$R_{ii}(\tau) = \mathrm{F}^{-1}(S_{ii}(w)) = \mathrm{E}[n_i(t)n_i(t+\tau)] \tag{3.81}$$

$$R_{qq}(\tau) = \mathrm{F}^{-1}(S_{qq}(w)) = \mathrm{E}[n_q(t)n_q(t+\tau)] \tag{3.82}$$

$$R_{iq}(\tau) = R_{qi}(\tau) = \mathrm{F}^{-1}(S_{iq}(w)) = \mathrm{E}[n_{iq}(t)n_{iq}(t+\tau)] \tag{3.83}$$

where F^{-1} denotes inverse Fourier Transform, S_{ii} and S_{qq} are the spectral densities of in-phase and quadrature components of noise respectively, S_{iq} is the cross spectral density between in-phase and quadrature components of noise; $R_{ii}(\tau)$, $R_{qq}(\tau)$, $R_{iq}(\tau)$ and $R_{qi}(\tau)$ are the correlation functions for in-phase and quadrature components of noise and E is the statistical expectation operator. Because we computed spectral densities at discrete frequency points, the computation of $R_{ii}(\tau)$, $R_{qq}(\tau)$ and $R_{iq}(\tau)$ becomes numerical rather than analytical. That is for a specific value ξ, $R(\xi)$ is computed by

$$R(\xi) = \int S(w)\exp(jw\xi) = \sum S(w_i)\exp(jw_i\xi)\Delta w \tag{3.84}$$

evaluating the integral in the inverse Fourier Transform by computing the summation shown in equation 3.84.

In the BER analysis, we will use Monte-Carlo simulations which require the generation of correlated noise samples $n_i[k]$, $n_q[k]$, $n_i[k-1]$ and $n_q[k-1]$. To do this, we first compute the covariance matrix of the noise samples as

$$
\begin{aligned}
\mathbb{C} =& \mathrm{E}[\mathbf{n}\mathbf{n}^T] \\
=& \begin{bmatrix}
\mathrm{E}[n_i[k]n_i[k]] & \mathrm{E}[n_i[k]n_q[k]] & \mathrm{E}[n_i[k]n_i[k]-1] & \mathrm{E}[n_i[k]n_q[k-1]] \\
\mathrm{E}[n_q[k]n_i[k]] & \mathrm{E}[n_q[k]n_q[k]] & \mathrm{E}[n_q[k]n_i[k]-1] & \mathrm{E}[n_q[k]n_q[k-1]] \\
\mathrm{E}[n_i[k-1]n_i[k]] & \mathrm{E}[n_i[k-1]n_q[k]] & \mathrm{E}[n_i[k-1]n_i[k]-1] & \mathrm{E}[n_i[k-1]n_q[k-1]] \\
\mathrm{E}[n_q[k-1]n_i[k]] & \mathrm{E}[n_q[k-1]n_q[k]] & \mathrm{E}[n_q[k-1]n_i[k]-1] & \mathrm{E}[n_q[k]n_q[k-1]]
\end{bmatrix} \\
=& \begin{bmatrix}
R_{ii}(0) & R_{iq}(0) & R_{ii}(T_s) & R_{iq}(T_s) \\
R_{qi}(0) & R_{qq}(0) & R_{qi}(T_s) & R_{qq}(T_s) \\
R_{ii}(T_s) & R_{iq}(T_s) & R_{ii}(0) & R_{iq}(0) \\
R_{qi}(T_s) & R_{qq}(T_s) & R_{qi}(0) & R_{qq}(0)
\end{bmatrix}
\end{aligned}
\tag{3.85}
$$

where $\mathbf{n}$ is

$$
\mathbf{n} = \begin{bmatrix} n_i[k] & n_q[k] & n_i[k-1] & n_q[k-1] \end{bmatrix}^{\dagger\,5} \tag{3.86}
$$

To generate noise samples with the covariance matrix given by 3.85 let's assume that

$$
\mathbf{n} = \mathbb{Q}g \tag{3.87}
$$

where $\mathbb{Q}$ is a 4×4 matrix and g is a 4×1 zero mean gaussian random vector. If covariance matrix of $\mathbf{n}$ is computed with $\mathbf{n}$ given by equation 3.87

$$
\begin{aligned}
\mathrm{E}[\mathbf{n}\mathbf{n}^\dagger] &= \mathrm{E}[(\mathbb{Q}g)(\mathbb{Q}g)^\dagger] \\
&= \mathrm{E}[\mathbb{Q}gg^\dagger\mathbb{Q}^\dagger] \\
&= \mathbb{Q} \quad \underbrace{\mathrm{E}[gg^\dagger]}_{\text{Identity Matrix}} \quad \mathbb{Q}^\dagger \\
&= \mathbb{Q}\mathbb{Q}^\dagger
\end{aligned}
\tag{3.88}
$$

where E is the statistical expectation operator, and † denotes matrix transpose operation. If 3.85 and 3.88 is compared it is inferred that

[5] † denotes matrix transpose operation.

$$\mathbb{C} = \mathbb{Q}\mathbb{Q}^{\dagger} \tag{3.89}$$

For a given $\mathbb{C}$ matrix, $\mathbb{Q}$ can be computed by using Cholesky decomposition [5].

The signal at the receiver is given by the equation 3.4. So our BER analysis methodology is as follows:

- Create large random noise vectors $\mathbf{n}$ by first computing covariance matrix, $\mathbb{C}$, then finding $\mathbb{Q}$ and multiplying $\mathbb{Q}$ with g where g is zero mean gaussian random vector

- Add the noise vector $\mathbf{n}$ to the desired large signal whose power at the sample time is P

- Apply differential detector operation as given by the equation 3.80

- Count the number of errors and compute the ratio of number of symbols to find Symbol Error Ratio (SER)

For DBPSK modulation scheme BER is equal to SER. Each symbol in DQPSK modulation scheme is represented by two bits. Because it is unlikely that two of the bits for DQPSK symbol is in error in the same time, due to Gray coding, the symbol error and BER is equal for DQPSK modulation scheme. This in turn means that BER is half of the SER since there are twice as many bits as symbols for DQPSK modulation scheme.

3.5.2 BER performance results for DBPSK/DQPSK

In this section, we provide BER results for DBPSK/DQPSK modulation schemes with different system settings. As we have stated earlier it is assumed that system degradation is only due to ASE noise and receiver has ideal characteristics.

The frequency separation between the channels are taken to be 25 GHz and symbol rate is taken to be 12.5 Gs/sec. For all simulations, we assume that noise spectral density is such that when Kerr non-linearity is ignored and launched power per channel is 1 mW, system BER is 10^{-4}. For DBPSK modulation scheme the analytical formula that gives systems BER is given by

$$BER = \frac{1}{2}\exp(-\frac{E_b}{N_o}) \tag{3.90}$$

where E_b is the energy per bit and N_o is the noise spectral density [20]. The analytical formula for the Signal to Noise Ratio (SNR) for a differential phase shift keying modulation is given by

$$SNR = \frac{E_b}{N_o}\log 2(M)\frac{T_s}{BW} \tag{3.91}$$

where M is the number of bits per symbol, T_s is the number of symbols per second and BW is the bandwidth of the noise [20]. SNR also equals to

$$SNR = \frac{P_s}{P_n} \tag{3.92}$$

where P_s is the signal power and P_n is the noise power. The power of the noise equals the area under the spectral density function. However, because noise accumulates linearly for Kerr non-linearity case, spectral density of the noise at the end of the fiber is constant, i.e. N_o, and equal for both in-phase and quadrature noise. Thus, the power of the noise at the end of the fiber is $2N_oBW$ where BW is the bandwidth of the noise.

The value of the noise spectral density, N_o, at the end of the fiber for DBPSK and DQPSK modulation schemes can be found by using 3.91 and 3.92. The ratio E_b/N_o can be obtained by MATLAB's *berawgn* function.

Figures 3.15, 3.16, 3.17 and 3.18 show the BER results of single and multi channel systems as a function of launched channel power which is logarithmically equally spaced between 0.1 mW and 10 mW. All of the simulations are done by using 10^7 noise samples. In each figure there are four subplots that show simulation results for different dispersion compensation schemes. In each subplot there are four curves that show simulation results for different system settings

- *No noise amp*: BER is evaluated by ignoring Kerr non-linearity in the system. For this case $\mathbb{C}$ matrix given by equation 3.85 becomes diagonal since there is no correlation among noise samples. Also note that in this case noise accumulates linearly and BER equals to 10^{-4} when the launched power per channel is 1 mW.

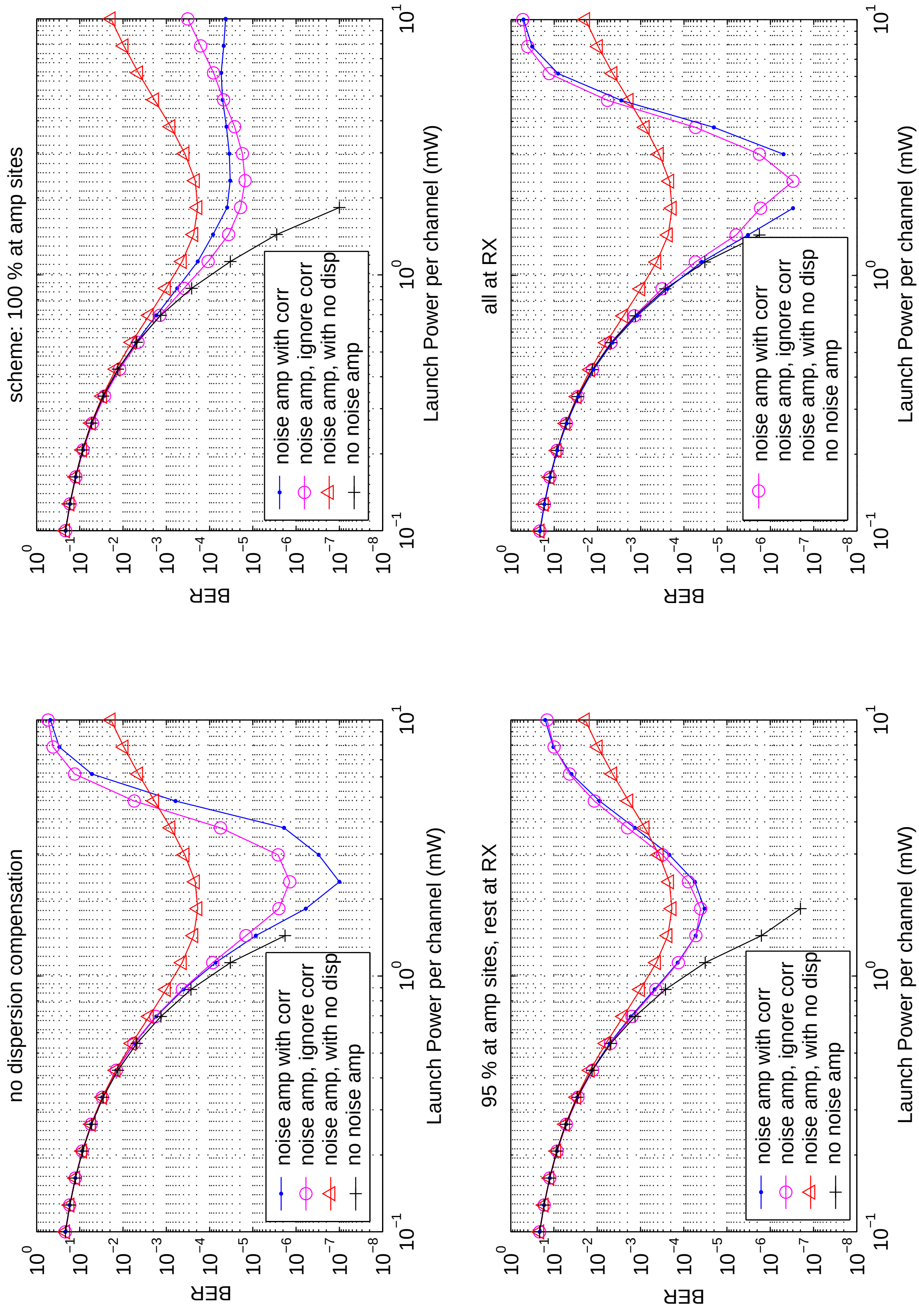

Figure 3.15: DBPSK BER performance - impact of dispersion compensation scheme and noise correlation - single channel system
System parameters: # of channels: 1, Channel spacing: 25 GHz,
Symbol rate: 12.5 Gs/sec, Launch Power: 0.1-10 mW, α *= 0.25 dB/km ,* β_2 *= -21.6* ps^2/km, $\beta_3 = 0.128$ ps^3/km, $\gamma = 2.0$ *1/(W·km),* L *: 80 km, # of spans: 20*

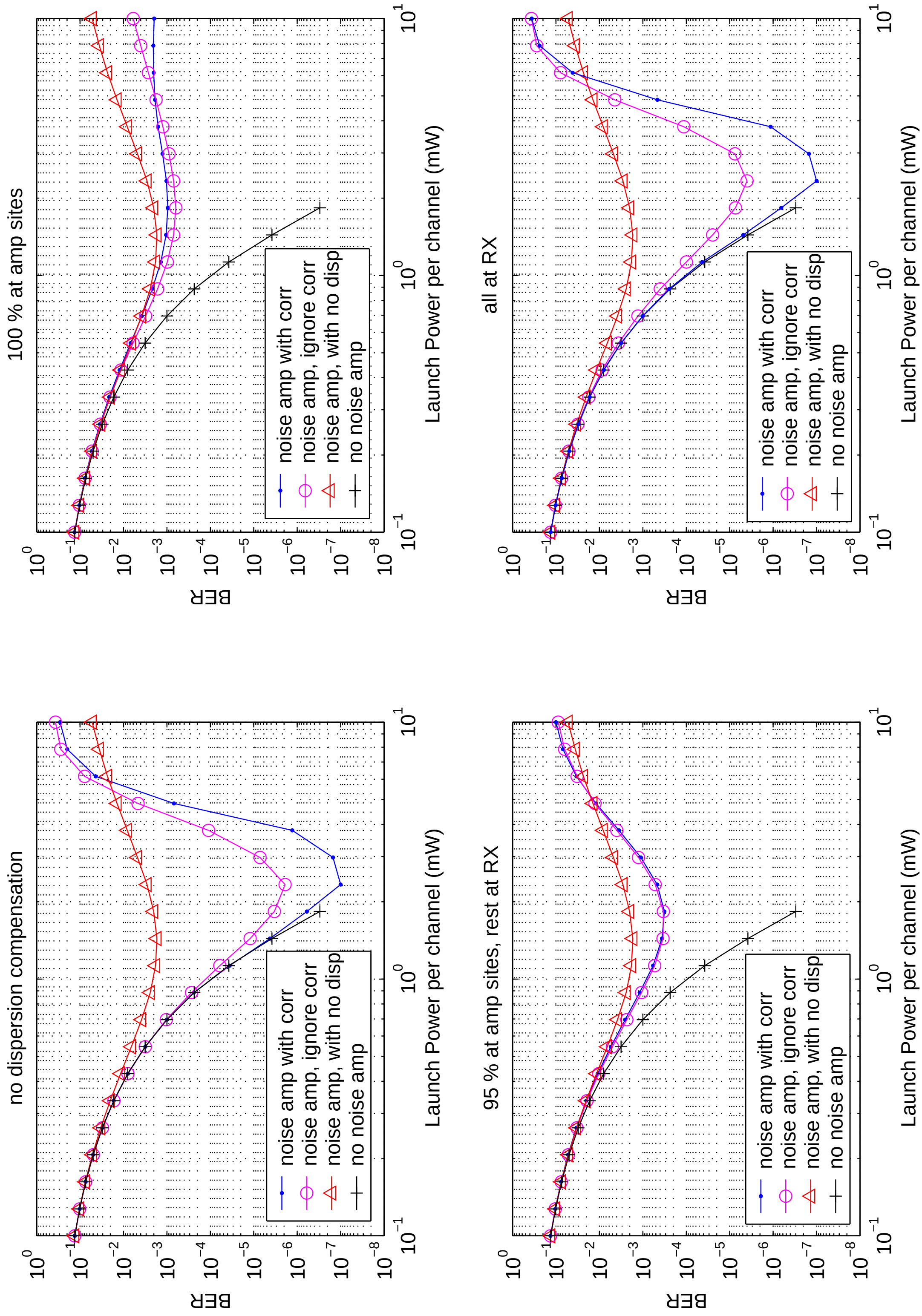

Figure 3.16: DQPSK BER performance - impact of dispersion compensation scheme and noise correlation - single channel system

System parameters: # of channels: 1, Channel spacing: 25 GHz, Symbol rate: 12.5 Gs/sec, Launch Power: 0.1-10 mW, α *= 0.25 dB/km ,* β_2 *= -21.6 ps*^{2}*/km,* $\beta_3 = 0.128$ *ps*^{3}*/km,* $\gamma = 2.0$ *1/(W·km),* L *: 80 km, # of spans: 20*

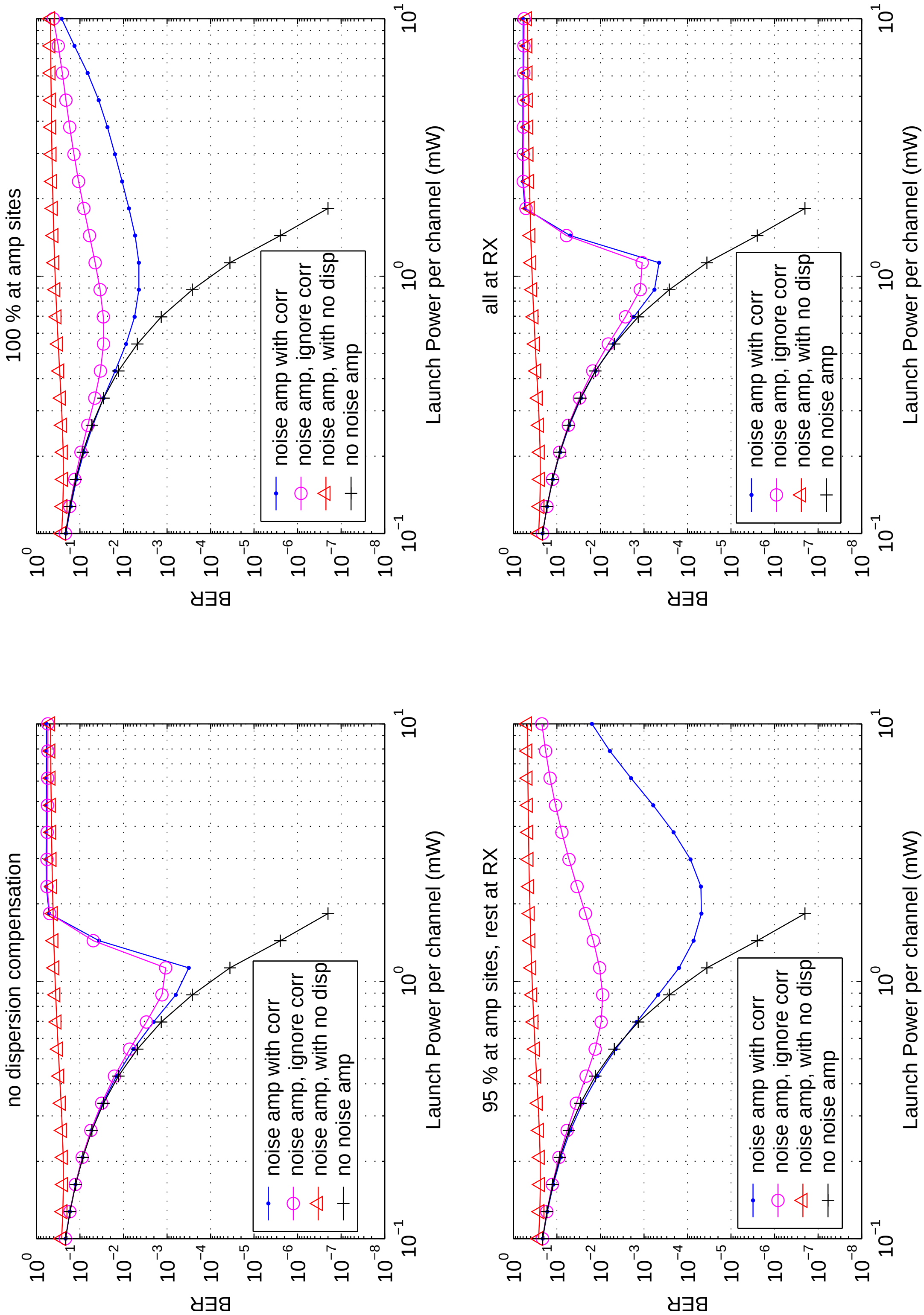

Figure 3.17: DBPSK BER performance - impact of dispersion compensation scheme and noise correlation - multi channel system

System parameters: # of channels: 49, Channel spacing: 25 GHz,
Symbol rate: 12.5 Gs/sec, Launch Power: 0.1-10 mW, α *= 0.25 dB/km ,* β_2 *= -21.6* ps^2/km*,* $\beta_3 = 0.128$ ps^3/km*,* $\gamma = 2.0$ *1/(W·km),* L *: 80 km, # of spans: 20*

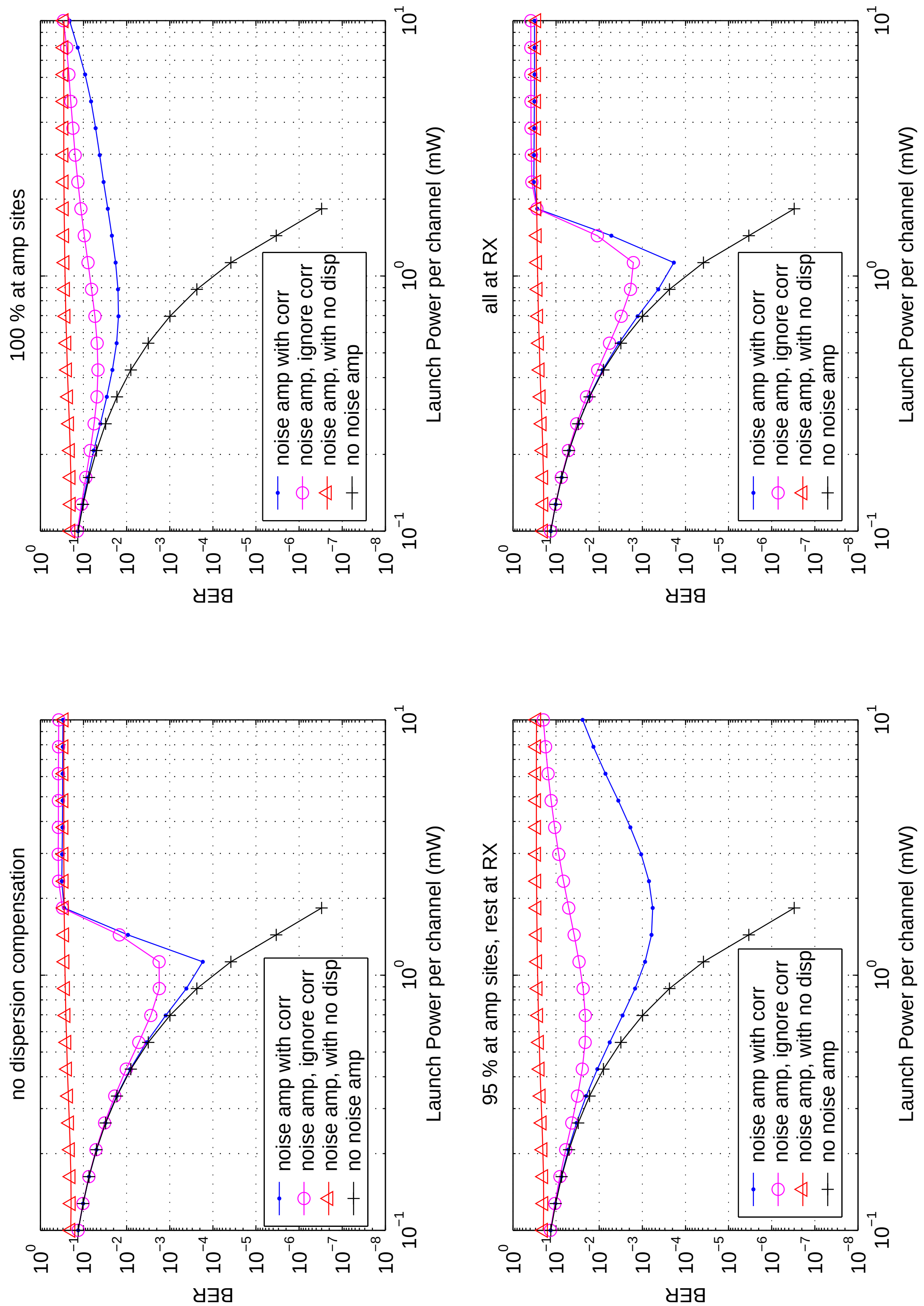

Figure 3.18: DQPSK BER performance - impact of dispersion compensation scheme and noise correlation - multi channel system
System parameters: # of channels: 49, Channel spacing: 25 GHz,
Symbol rate: 12.5 Gs/sec, Launch Power: 0.1-10 mW, α *= 0.25 dB/km ,* β_2 *= -21.6* ps^2/km*,* β_3 *= 0.128* ps^3/km*,* γ *= 2.0 1/(W·km), L : 80 km, # of spans: 20*

- *Noise amp, ignore cor*: In this case, Kerr non-linearity is taken into account but the correlations among the noise samples at the receiver are taken to be zero. That is, all of the off-diagonal entries of $\mathbb{C}$ matrix given by equation 3.85, set to be zero before generating random noise samples.

- *Noise amp with cor*: In this case, both Kerr non-linearity and correlations among and within noise samples are taken into account. This analysis shows the actual BER result for the system.

- *Noise amp with no disp*: In this case, dispersion is ignored but Kerr non-linearity is taken into account. Note that dispersion compensation has no significance since there is no dispersion in the system for this case. Without dispersion, ASE noise experiences frequency independent amplification. In this case, correlations among noise samples become zero. However, correlations within noise samples, i.e. in-phase and quadrature noise components for the same noise sample, are non-zero. For this case, $\mathbb{C}$ matrix given by equation 3.85 becomes block diagonal.

If we look closer to the Figures 3.15, 3.16, 3.17 and 3.18 that show BER performance of the system we observe that

- For all cases where Kerr non-linearity is taken into account, there exists an optimal launch power for which BER is the smallest. It is observed that system performance increases as power per channel increases to some point. However, increasing the channel power over that point results in worse system performance. This situation can be explained by Signal to Noise Ratio (SNR). As the channel power increases, the SNR increases yielding better system performance. However, the effect of non-linearity becomes much worse resulting in system performance degradation as the power per channel increases.

- For all cases, inclusion of the dispersion results in better system performance.

- For the single channel case, application of *amp95restRXdispcomp* and *allinampdisp-comp* schemes show similar result as *nodispcomp* and *allatRXdispcomp* do.

- If the optimal power is considered, the best system performance is obtained for the dispersion compensation schemes *nodispcomp* and *allatRXdispcomp* for the single channel case. For the multi channel case, the best system performance
  - for DBPSK modulation is obtained for the *amp95restRXdispcomp* scheme.
  - for DQPSK modulation is obtained for the *nodispcomp* and *allatRXdispcomp* schemes.
- The existence of correlations between noise samples do not effect the system performance significantly for the single channel case. For the multi channel case, on the other hand, the existence of correlations among noise samples greatly effect the system performance, for both DBPSK and DQPSK modulation schemes, especially if *amp95restRXdispcomp* scheme is used.

As stated above, while the correlations between noise samples improve the system performance for multi channel system, its impact on single channel system is not very significant. To fully observe the effect of noise correlation on system performance for multi channel systems, we give the Figures 3.19,3.20, 3.21 and 3.22 that show system BER performance for different number of channels. While correlations are taken into account in Figures 3.19 and 3.20, to better observe the noise correlation effect correlations among noise samples are ignored in Figures 3.21 and 3.22.

From Figures 3.19, 3.20, 3.21 and 3.22 we observe that

- For the case where correlation effect is taken into account, the inclusion of additional channels have no significant effect on the system performance if either *amp95restRXdispcomp* or *allinampdispcomp* scheme is used. However system, performance degrades for *nodispcomp* and *allatRXdispcomp* schemes as new channels are added to the system.
- For the case where the correlations are ignored, the inclusion of additional channels degrades the system performance for all dispersion compensation schemes.
- Whereas the correlations among noise signals greatly improves the system performance for *amp95restRXdispcomp* or *allinampdispcomp* schemes, there is no significant

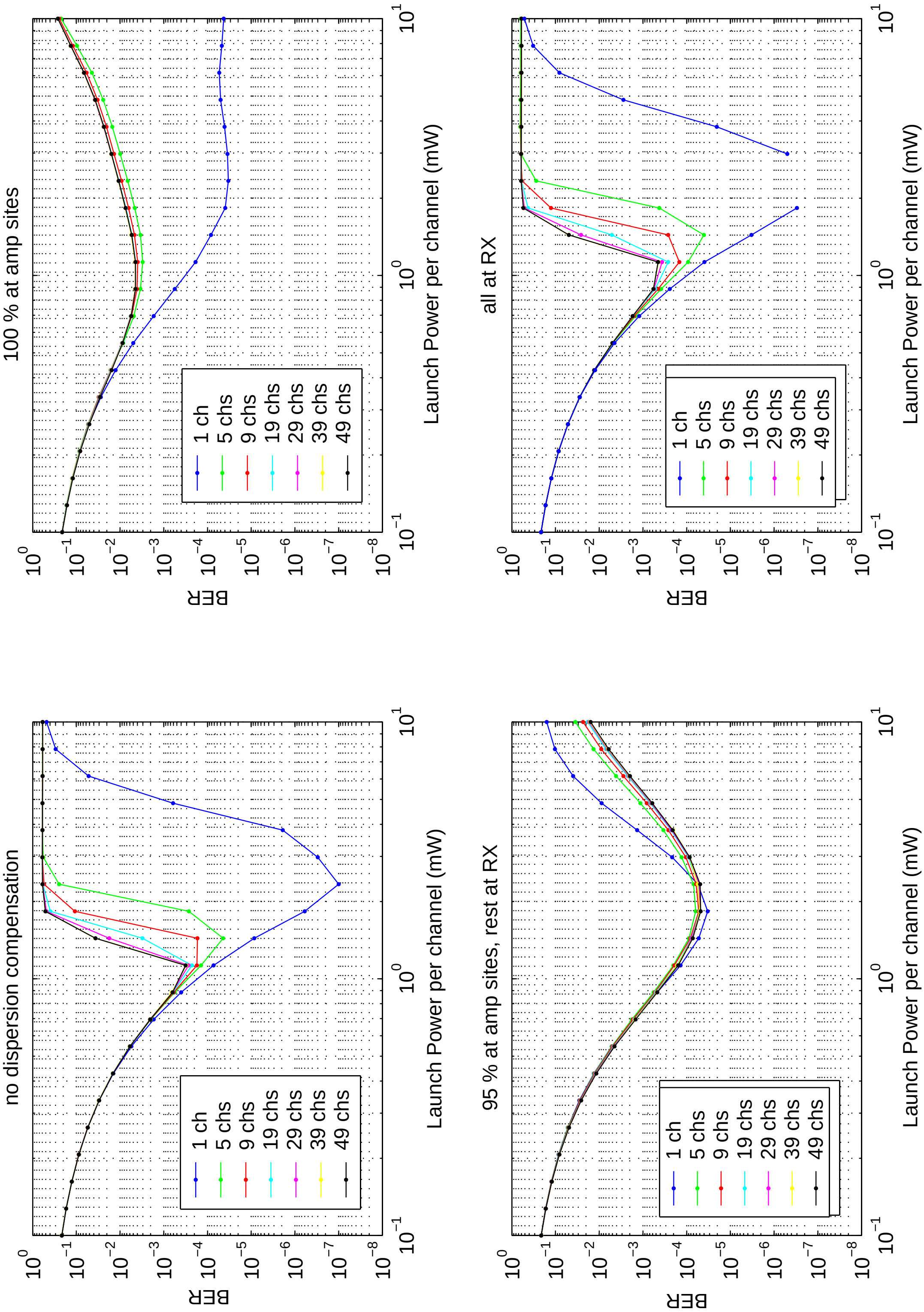

Figure 3.19: DBPSK BER performance - impact of dispersion compensation scheme and the number of channels - with correlations

System parameters: # of channels: 1-49, Channel spacing: 25 GHz, Symbol rate: 12.5 Gs/sec, Launch Power: 0.1-10 mW, α *= 0.25 dB/km ,* β_2 *= -21.6 ps*^{2}*/km,* β_3 *= 0.128 ps*^{3}*/km,* γ *= 2.0 1/(W·km), L : 80 km, # of spans: 20*

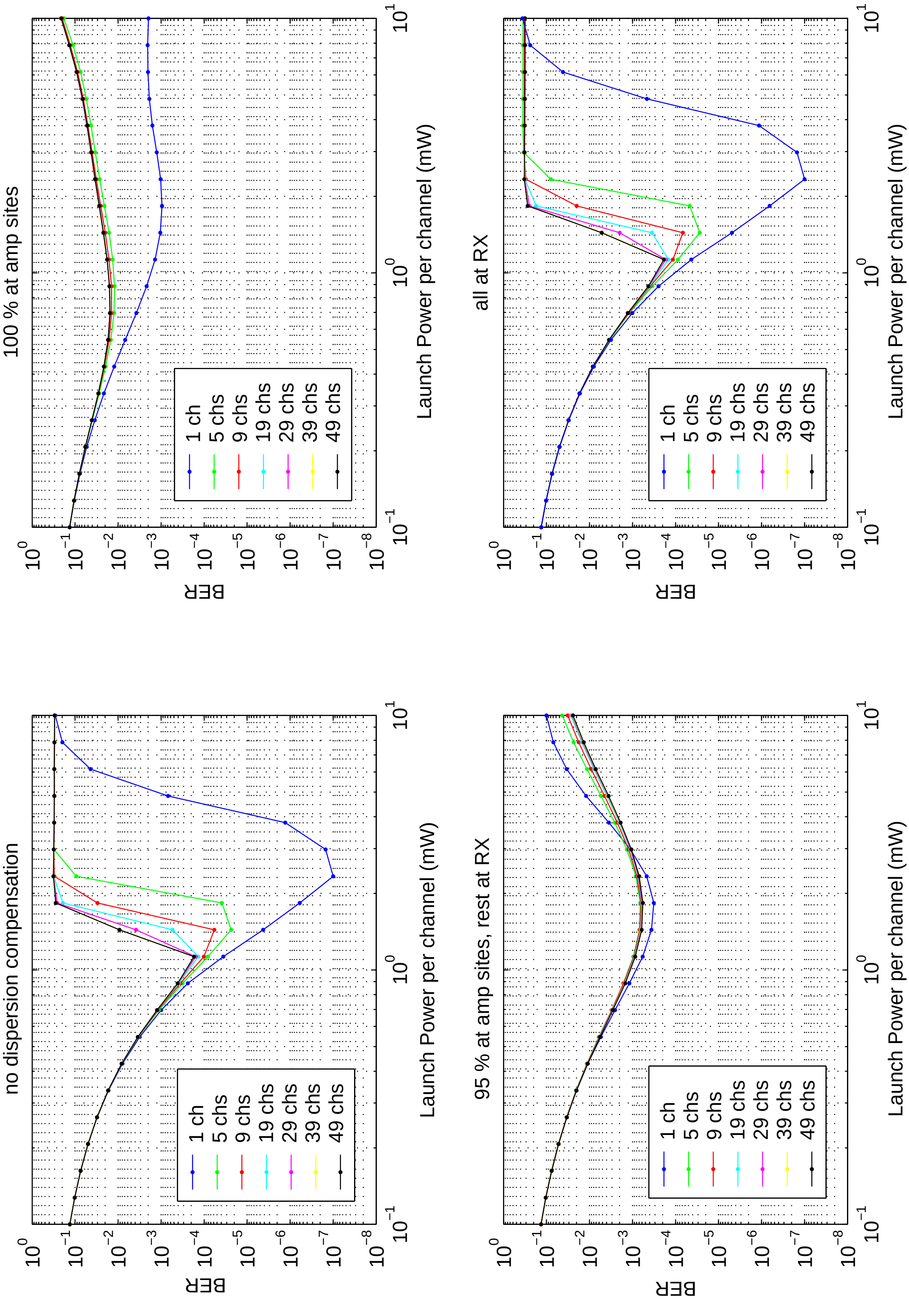

Figure 3.20: DQPSK BER performance - impact of dispersion compensation scheme and the number of channels - with correlations
System parameters: # of channels: 1-49, Channel spacing: 25 GHz,
Symbol rate: 12.5 Gs/sec, Launch Power: 0.1-10 mW, α = *0.25 dB/km ,* β_2 = *-21.6* ps^2/km, $\beta_3 = 0.128\ ps^3/km$, $\gamma = 2.0\ 1/(W \cdot km)$, L *: 80 km, # of spans: 20*

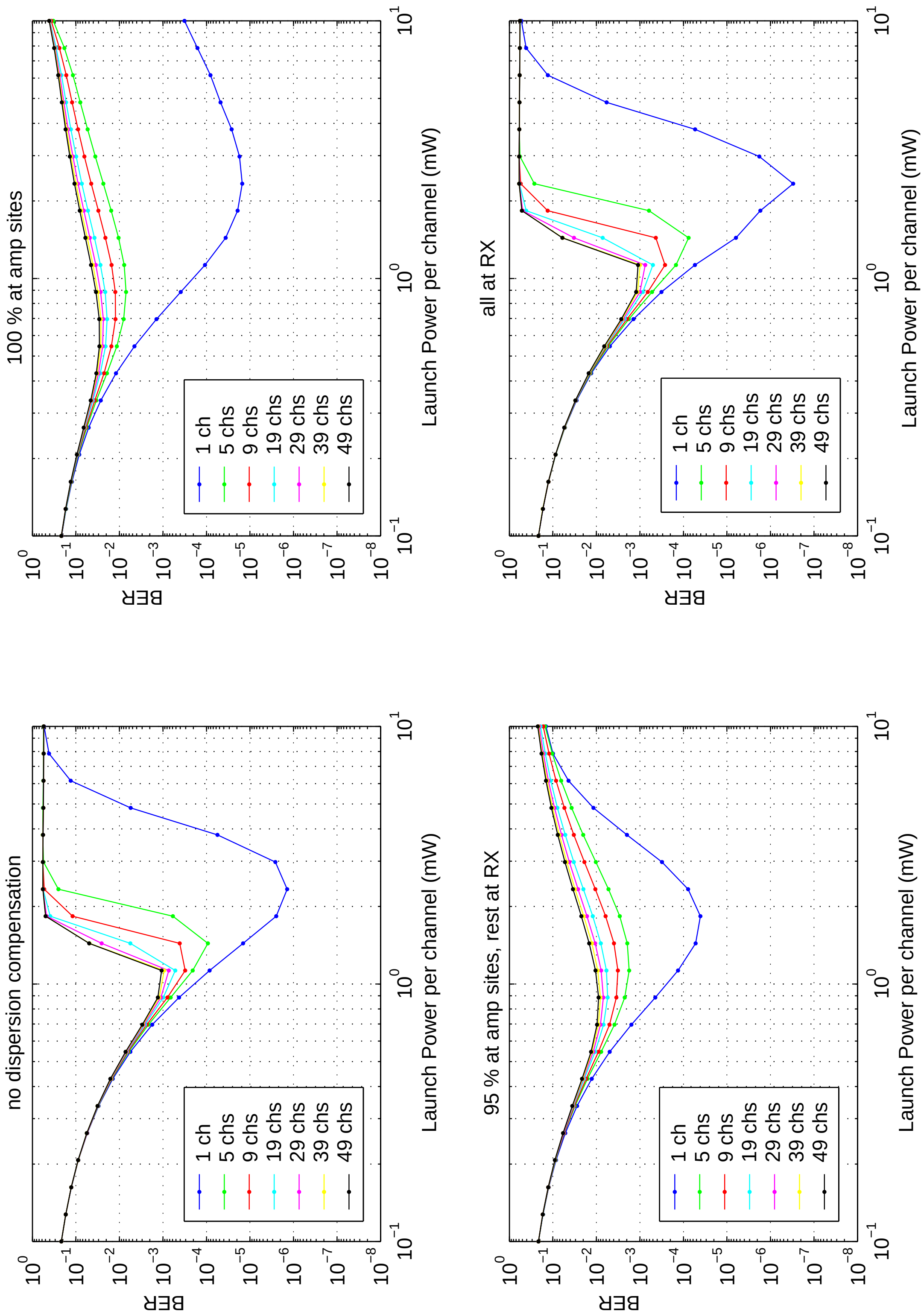

Figure 3.21: DBPSK BER performance - impact of dispersion compensation scheme and the number of channels - ignoring correlations
System parameters: # of channels: 1-49, Channel spacing: 25 GHz,
Symbol rate: 12.5 Gs/sec, Launch Power: 0.1-10 mW, α *= 0.25 dB/km ,* β_2 *= -21.6 ps*^{2}*/km,* $\beta_3 = 0.128$ *ps*^{3}*/km,* $\gamma = 2.0$ *1/(W·km), L : 80 km, # of spans: 20*

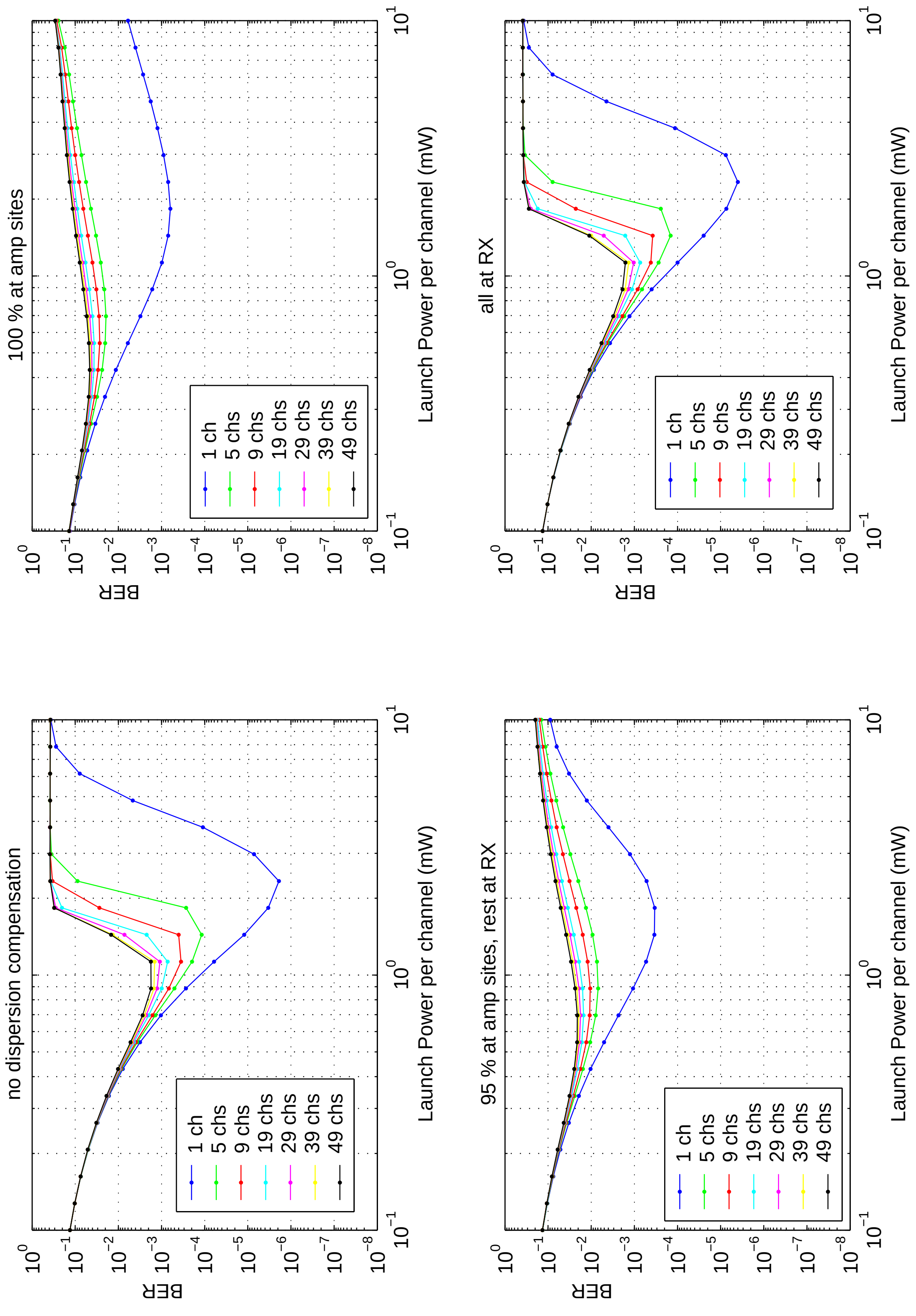

Figure 3.22: DQPSK BER performance - impact of dispersion compensation scheme and the number of channels - ignoring correlations
System parameters: # of channels: 1-49, Channel spacing: 25 GHz,
Symbol rate: 12.5 Gs/sec, Launch Power: 0.1-10 mW, α *= 0.25 dB/km ,* β_2 *= -21.6 ps*^{2}*/km,* β_3 *= 0.128 ps*^{3}*/km,* γ *= 2.0 1/(W·km), L : 80 km, # of spans: 20*

effect of correlations on the system performance for *nodispcomp* and *allatRXdispcomp* schemes.

In this chapter, we have considered the effect of noise on WDM system with unmodulated carriers. In the analysis, we have first computed transfer functions between channels and used these transfer functions in the computation of spectral density of the noise at the end of the fiber. At last, we have computed the covariance matrix from spectral density function and made a Monte-Carlo simulation to compute the systems BER performance.

In the next chapter, we will extend the noise analysis on WDM system performance by considering modulated carriers.

Chapter 4

MODULATED CARRIER CASE

The noise analysis for modulated carrier case is much like the un-modulated carrier case. The first step is to solve the NLSE equation, which is given by equation 2.1, by only considering large desired signals. In chapter 3, where the carriers are assumed to be un-modulated, the solution of NLSE is obtained by ignoring FWM products that result as a consequence of Kerr non-linearity. The ignorance of FWM products made the solution of NLSE equation easier by obtaining coupled partial differential equations for each carrier envelope. In this chapter, however, because a more general, modulated carrier, case is considered, FWM products will not be ignored and NLSE equation will be solved directly by using numerical methods.

For modulated carrier case, signal envelope U can be expressed as

$$U = \sum_{k=1}^{N} m_k(t) e^{jw_k t} \tag{4.1}$$

where N is the number of channels, $m_k(t)$ is the envelope of the k^{th} channel and w_k is the offset frequency of the k^{th} channel from the carrier frequency of the complex envelope U.

To find the equation that characterisizes the noise $a(z,t)$, we will follow the steps given in chapter 2:

1. In the first step, NLSE equation given by 2.1 will be solved by ignoring any disturbances such as noise in the WDM system. The solution methodology for NLSE equation will be given later in the chapter. For the time being let assume that the solution is $A(z,t)$.

2. In the second step, we express the general solution of NLSE $U(z,t)$ as a summation of noise free solution $A(z,t)$ and the noise $a(z,t)$ as

$$U(z,t) = A(z,t) + a(z,t) \tag{4.2}$$

3. In the third step, we insert $U(z,t)$ into the NLSE equation given by 4.3, and perform first order linearization with respect to $a(z,t)$.

$$\begin{aligned}\frac{\partial U(z,t)}{\partial z} =& -\alpha U(z,t) - j\frac{1}{2}\beta_2\frac{\partial^2 U(z,t)}{\partial t^2} + \frac{1}{6}\beta_3\frac{\partial^3 U(z,t)}{\partial t^3} \\ &+ j\gamma|U(z,t)|^2 U(z,t)\end{aligned} \tag{4.3}$$

We assumed that $A(z,t)$ is a solution of 4.3. Next, insert $A(z,t)+a(z,t)$ in place of $U(z,t)$ in equation 4.3

$$\begin{aligned}\frac{\partial A(z,t)+a(z,t)}{\partial z} =& -\alpha(A(z,t)+a(z,t)) \\ &- j\frac{1}{2}\beta_2\frac{\partial^2 (A(z,t)+a(z,t))}{\partial t^2} + \frac{1}{6}\beta_3\frac{\partial^3 (A(z,t)+a(z,t))}{\partial t^3} \\ &+ j\gamma|(A(z,t)+a(z,t))|^2(A(z,t)+a(z,t))\end{aligned} \tag{4.4}$$

Rearranging the equation 4.4, we get

$$\begin{aligned}\frac{\partial A(z,t)}{\partial z} + \frac{\partial a(z,t)}{\partial z} =& -\alpha A(z,t) - j\frac{1}{2}\beta_2\frac{\partial^2 A(z,t)}{\partial t^2} + \frac{1}{6}\beta_3\frac{\partial^3 A(z,t)}{\partial t^3} \\ &+ j\gamma|A(z,t)|^2 A(z,t) \\ &- \alpha a(z,t) - j\frac{1}{2}\beta_2\frac{\partial^2 a(z,t)}{\partial t^2} + \frac{1}{6}\beta_3\frac{\partial^3 a(z,t)}{\partial t^3} \\ &+ j\gamma[(|a(z,t)|^2 + A(z,t)a^*(z,t) + a(z,t)A^*(z,t))(A(z,t)+a(z,t))] \\ &+ j\gamma|A(z,t)|^2 a(z,t)\end{aligned} \tag{4.5}$$

where * denotes complex conjugate operation. Subtracting equation 4.3 from 4.5, by replacing $U(z,t)$ in equation 4.3 with $A(z,t)$, we obtain

$$\begin{aligned}\frac{\partial a(z,t)}{\partial z} =& -\alpha a(z,t) - j\frac{1}{2}\beta_2\frac{\partial^2 a(z,t)}{\partial t^2} + \frac{1}{6}\beta_3\frac{\partial^3 a(z,t)}{\partial t^3} \\ &+ 2j\gamma|A(z,t)|^2 a(z,t) + j\gamma A^2(z,t)a^*(z,t)\end{aligned} \tag{4.6}$$

If equation 4.6 is compared with the equation 3.7, it is observed that while for un-modulated carrier case noise does not depend on the input spectrum $U(z,t)$, for modulated carrier case noise depends on the input spectrum $U(z,t)$. In chapter 3, the system BER performance is computed by assuming that noise at the end of the fiber is stationary. However, for the modulated carrier case as it is given by the equation 4.6, noise at the end of fiber is not stationary because it depends on the input spectrum $A(z,t)$. As a consequence of this, while the correlation between noise samples for un-modulated carrier case depends only to the signal sampling period; for modulated carrier case, correlations between noise samples depends not only to the sampling period but also to the sampling time.

As in for un-modulated carrier case, let's decompose noise $a(z,t)$ and $A(z,t)$ into its real (in-phase) and imaginary(quadrature) components

$$a(z,t) = a_r(z,t) + ja_i(z,t), A(z,t) = A_r(z,t) + jA_i(z,t) \tag{4.7}$$

where $a_r(z,t)$ and $A_r(z,t)$ are the in-phase components of $a(z,t)$ and $A(z,t)$, $a_i(z,t)$ and $A_i(z,t)$ are the quadrature components of $a(z,t)$ and $A(z,t)$ and $j = \sqrt{-1}$. By using equation 4.7, equation 4.6 can be written in vector form as

$$\begin{aligned}\frac{d}{dz}\begin{bmatrix} a_r(z,t) \\ a_i(z,t) \end{bmatrix} =& -\alpha \begin{bmatrix} a_r(z,t) \\ a_i(z,t) \end{bmatrix} + \frac{1}{2}\beta_2 \begin{bmatrix} 0 & \frac{\partial^2}{\partial t^2} \\ -\frac{\partial^2}{\partial t^2} & 0 \end{bmatrix} \begin{bmatrix} a_r(z,t) \\ a_i(z,t) \end{bmatrix} + \frac{1}{6}\beta_3 \begin{bmatrix} \frac{\partial^3}{\partial t^3} & 0 \\ 0 & 0\frac{\partial^3}{\partial t^3} \end{bmatrix} \begin{bmatrix} a_r(z,t) \\ a_i(z,t) \end{bmatrix} \\ &+ \gamma \begin{bmatrix} -2A_r(z,t)A_i(z,t) & -A_r(z,t)^2 - 3A_i(z,t)^2 \\ 3A_r(z,t)^2 + A_i(z,t)^2 & 2A_r(z,t)A_i(z,t) \end{bmatrix} \begin{bmatrix} a_r(z,t) \\ a_i(z,t) \end{bmatrix}\end{aligned} \tag{4.8}$$

Note that in equation 4.8 $A(z,t)$ is the deterministic, noise free, solution of NLSE equation described by 2.1 and $a(z,t)$ is the stochastic perturbation as a consequence of noise.

Equation 4.8 is a linear Partial Differential Equation(PDE) and can be solved by using some means of numerical methods if $a(z=0,t)$ is known. However, since $a(z,t)$ is not a deterministic signal $a(z=0,t)$ is unknown. Although $a(z=0,t)$ is not known, equation 4.8 can be used to find stochastic characteristics of noise $a(z,t)$.

4.1 Covariance Matrix Formulation for Noise Analysis

Because $a(z,t)$ depends on input spectrum $A(z,t)$, As described by the equation 4.6, $a(z,t)$ is nonstationary. To fully characterize $a(z,t)$ it is required to know stochastic properties of $a(z,t)$ between time $t=-\infty$ and $t=\infty$, which is practically impossible. Thus we limit the time to T_s for practical purposes .

Although both $a(z,t)$ and $A(z,t)$ are continuous functions, some discretization have to be done for simulation purposes. In our analysis, we discretize the time into N_t time points as $t_1, t_2, \cdots, t_{N_t-1}, t_{N_t} \in [0, T_s]$. In this case, $a(z,t)$ and $A(z,t)$ can be expressed in vector form as

$$\mathbf{a_c(z)} = \begin{bmatrix} a(z,t_1) & a(z,t_2) & \cdots & a(z,t_{N_t}) \end{bmatrix}^{\dagger} \tag{4.9}$$

$$\mathbf{A_c(z)} = \begin{bmatrix} A(z,t_1) & A(z,t_2) & \cdots & A(z,t_{N_t}) \end{bmatrix}^{\dagger} \tag{4.10}$$

where $\mathbf{a_c(z)}$ and $\mathbf{A_c(z)}$ are complex-valued vector functions of z and † denotes matrix transpose operation. Note that time dependence of $a(z,t)$ and $A(z,t)$ disappeared due to the time discretization.

In order to use 4.9 and 4.10 in equation 4.8, we first decompose $a(z,t)$ and $A(z,t)$ into their real and imaginary parts

$$\mathbf{a_c(z)} = \mathbf{a_r(z)} + j\mathbf{a_i(z)} \tag{4.11}$$

$$\mathbf{A_c(z)} = \mathbf{A_r(z)} + j\mathbf{A_i(z)} \tag{4.12}$$

and gather real and imaginary parts in one column vector as

$$\mathbf{a_c(z)} = \begin{bmatrix} \mathbf{a_r(z)}^{\dagger} & \mathbf{a_i(z)}^{\dagger} \end{bmatrix}^{\dagger} \tag{4.13}$$

$$\mathbf{A_c(z)} = \begin{bmatrix} \mathbf{A_r(z)}^{\dagger} & \mathbf{A_i(z)}^{\dagger} \end{bmatrix}^{\dagger} \tag{4.14}$$

where † denotes matrix transpose operation. Also let's define

$$\mathbb{A}(z) = \begin{bmatrix} -2\mathfrak{D}[A_r(z)]\mathfrak{D}[A_i(z)] & -\mathfrak{D}[A_r(z)]^2 - 3\mathfrak{D}[A_i(z)]^2 \\ 3\mathfrak{D}[A_r(z)]^2 + \mathfrak{D}[A_i(z)]^2 & 2\mathfrak{D}[A_r(z)]\mathfrak{D}[A_i(z)] \end{bmatrix} \tag{4.15}$$

and

$$\mathbb{B}_2 = \begin{bmatrix} 0 & \mathbb{D}_2 \\ -\mathbb{D}_2 & 0 \end{bmatrix}, \mathbb{B}_3 = \begin{bmatrix} \mathbb{D}_3 & 0 \\ 0 & \mathbb{D}_3 \end{bmatrix} \tag{4.16}$$

where $\mathbb{D}_2$ and $\mathbb{D}_3$ are second and third order differentiation operators respectively and $\mathfrak{D}$ is the diagonal operator which converts an $N \times 1$ column vector χ to a $N \times N$ square matrix whose main diagonal is χ and off-diagonal entries are 0.

By using 4.13, 4.15 and 4.16, equation 4.8 can be expressed as

$$\frac{d\mathbf{a}(z)}{dz} = -\alpha\mathbf{a}(z) + \frac{1}{2}\beta_2\mathbb{B}_2\mathbf{a}(z) + \frac{1}{6}\beta_3\mathbb{B}_3\mathbf{a}(z) + \gamma\mathbb{A}(z)\mathbf{a}(z) \tag{4.17}$$

A stochastic process like $a(z,t)$ can be seen as a sequence of random variables, that is to say each discrete time point $a(z,t_k)$ is a random variable. Thus, $\mathbf{a}(z)$ in equation 4.17 can be treated as a random vector. Because in our case $a(z,t)$ is a non-stationary stochastic process, correlations among each time sample of noise $a(z,t_k)$ play a critical role in the analysis of noise. In this case, it is not enough to solve 4.17 alone, but a more complete analysis is required. In the noise analysis for modulated carrier case, we will use covariance matrix formulation as described below.

Let the covariance matrix for $\mathbf{a}(z)$ random vector be defined as

$$\mathbf{K}(z) = \mathrm{E}[\mathbf{a}(z)\mathbf{a}(z)^\dagger] \tag{4.18}$$

where E denotes the probabilistic expectation operator and † denotes matrix transpose operation. Note that $\mathbf{K}(z)$ is real and symmetric matrix. If we take the derivative of $\mathbf{K}(z)$ with respect to z, we get

$$\begin{aligned} \frac{\mathbf{K}(z)}{dz} &= \frac{d\mathrm{E}[\mathbf{a}(z)\mathbf{a}(z)^\dagger]}{dz} \\ &= \mathrm{E}\left\{\frac{d[\mathbf{a}(z)\mathbf{a}(z)^\dagger]}{dz}\right\} \\ &= \mathrm{E}\left\{\frac{d\mathbf{a}(z)}{dz}\mathbf{a}(z)^\dagger + \mathbf{a}(z)\frac{d\mathbf{a}(z)^\dagger}{dz}\right\} \end{aligned} \tag{4.19}$$

If we insert equation 4.17 to the equation 4.19 and apply the expectation operator, we get the following equation for covariance matrix $\mathbf{K}(z)$

$$\begin{aligned}\frac{d\mathbf{K}(z)}{dz} =& -2\alpha\mathbf{K}(z) + \frac{1}{2}\beta_2[\mathbb{B}_2\mathbf{K}(z) + \mathbf{K}(z)\mathbb{B}_2^\dagger] + \frac{1}{6}\beta_3[\mathbb{B}_3\mathbf{K}(z) + \mathbf{K}(z)\mathbb{B}_3^\dagger] \\ &+ \gamma[\mathbb{A}(z)\mathbf{K}(z) + \mathbf{K}(z)\mathbb{A}(z)^\dagger]\end{aligned} \tag{4.20}$$

which is a linear differential equation with respect to $\mathbf{K}(z)$ and can be solved to find $\mathbf{K}(z = L)$ by using numerical schemes provided that $\mathbf{K}(z = 0)$ is given. Throughout the chapter we will refer to equation 4.20 as COVODE.

Note that $\mathbf{K}(z)$ itself contains a wellworth information about the noise characteristics. If it is diagonal then it models a white noise. If the diagonals have the same value then it models stationary white noise and if they are different, it models non-stationary white noise. For our case, although the noise that enters the fiber $\mathbf{K}(z = 0)$ is stationary, at the end of the fiber, $\mathbf{K}(z = L)$ has in general non-zero off diagonal and non-constant diagonal entries. That is to say noise at the end of the fiber is non-stationary and colored.

Note that solution of equation 4.20 requires the knowledge of $\mathbf{A}(z)$. Thus, in our analysis we will first solve NLSE equation described by 2.1 and then use the values of $\mathbf{A}(z)$ to solve equation 4.19. In the next two subsections, we will give the solution methodology for both NLSE and COVODE equation.

4.2 Numerical Solution of NLSE

NLSE equation given by 2.1 is a non-linear PDE. In order to obtain efficient and accurate solution of NLSE equation, one has to use high-order integration schemes in space and time.

If we discretize the time for large desired signal $A(z, t)$, as done in section 4.1 as $t_1, t_2, \cdots, t_{N_t-1}, t_{N_t} \in [0, T_s]$, we get the following set of partial differential equations

$$\begin{bmatrix} A(z,t_1) \\ A(z,t_2) \\ \vdots \\ A(z,t_{N_t}) \end{bmatrix} = \begin{bmatrix} -\alpha A(z,t_1) - j\frac{1}{2}\beta_2\frac{\partial^2 A(z,t_1)}{\partial t^2} + \frac{1}{6}\beta_3\frac{\partial^3 A(z,t_1)}{\partial t^3} + j\gamma|A(z,t_1)|^2 A(z,t_1) \\ -\alpha A(z,t_2) - j\frac{1}{2}\beta_2\frac{\partial^2 A(z,t_2)}{\partial t^2} + \frac{1}{6}\beta_3\frac{\partial^3 A(z,t_2)}{\partial t^3} + j\gamma|A(z,t_2)|^2 A(z,t_2) \\ \vdots \\ -\alpha A(z,t_{N_t}) - j\frac{1}{2}\beta_2\frac{\partial^2 A(z,t_{N_t}}{\partial t^2} + \frac{1}{6}\beta_3\frac{\partial^3 A(z,t_{N_t}}{\partial t^3} + j\gamma|A(z,t_{N_t}|^2 A(z,t_{N_t}) \end{bmatrix} \tag{4.21}$$

and if 4.21 is transformed into the frequency domain, we obtain

$$\begin{bmatrix} A(z,w_1) \\ A(z,w_2) \\ \vdots \\ A(z,w_{N_t}) \end{bmatrix} = \begin{bmatrix} -\alpha - j\frac{1}{2}\beta_2 w_1^2 + \frac{1}{6}\beta_3 w_1^3 & 0 & \cdots & 0 \\ 0 & -\alpha - j\frac{1}{2}\beta_2 w_2^2 + \frac{1}{6}\beta_3 w_2^3 & \cdots & 0 \\ \vdots & \vdots & \ddots & \vdots \\ 0 & 0 & \cdots & -\alpha - j\frac{1}{2}\beta_2 w_{N_f}^2 + \frac{1}{6}\beta_3 w_{N_{tf}}^3 \end{bmatrix} \begin{bmatrix} A(z,w_1) \\ A(z,w_2) \\ \vdots \\ A(z,w_{N_t}) \end{bmatrix} + \mathfrak{F} \begin{bmatrix} j\gamma|A(z,t_1)|^2 A(z,t_1) \\ j\gamma|A(z,t_2)|^2 A(z,t_2) \\ \vdots \\ j\gamma|A(z,t_{N_t}|^2 A(z,t_{N_t}) \end{bmatrix} \tag{4.22}$$

where $\mathfrak{F}$ is the FFT operation. Note that frequencies and time points in equation 4.21 are discrete and it should also be noted that the above transformation is done by the FFT operation, not done by the use of normal Fourier Transform. Equation 4.21 can be written as

$$\frac{d\widehat{\mathbf{A}}(\mathbf{z})}{dz} = L\widehat{\mathbf{A}}(\mathbf{z}) + NL[\widehat{\mathbf{A}}(\mathbf{z})] \tag{4.23}$$

where L is the diagonal matrix and NL is the non-linear operator . Since L has diagonal entries that are summations of quadratic and cubic functions of frequency, L has widely varying values which makes L stiff. This stiffness and non-linearity preclude the use of high-order integration schemes due to stability issues [11, 18].

Although numerical computations for the linear part of the equation 4.23 can be done trivially, since L is a diagonal matrix, it is not the case for the non-linear part. However, computations for non-linear part of the equation 4.23 can be done in time domain because non-linear operator in time domain becomes vector products, i.e. diagonal matrices. In this case, two FFT should be used : first, the computations for non-linear part is done in time domain, then the result is converted into frequency domain by using FFT. Secondly computations for linear part is done. For the next z-step, to go to time domain, another FFT is used.

Generally the most used computational method to solve NLSE equation is the $split-step$ method [25]. The method is based on the operator splitting such that the linear and non-linear parts of the NLSE equation are treated separately. Although $split - step$ method gives sufficient results for small step-sizes, for large step-sizes the method may give erroneous results due to stability issues.

In order to obtain more accurate results one has to solve equation 4.23 by solving linear and non-linear parts concurrently. For computational purposes, it is not efficient to use *implicit* integration scheme to solve 4.23 because it requires the solution of non-linear equations at every step. However, because the linear part of the equation 4.23 is $stiff$, it is also not efficient to use *explicit* integration schemes due to stability issues of the explicit methods. A more general method used in the solution of non-linear PDEs such as 4.23 is IMEX schemes [27]. The idea behind the IMEX schemes is to use an implicit method for the linear part integration and use an explicit method for the non-linear part integration. In this case, stability issues disappear and no non-linear equation solution is required at every step. Because IMEX schemes give more accurate results, in the solution of 4.23 we will use IMEX schemes. More specifically, we rearrange equation 4.23 and integrate from z_k to z_{k+1} as

$$\frac{d\widehat{\mathbf{A}}(\mathbf{z})}{dz} = L\widehat{\mathbf{A}}(\mathbf{z}) + NL[\widehat{\mathbf{A}}(\mathbf{z})] \tag{4.24}$$

$$\Longrightarrow d\widehat{\mathbf{A}}(\mathbf{z}) = L\widehat{\mathbf{A}}(\mathbf{z})dz + NL[\widehat{\mathbf{A}}(\mathbf{z})]dz \tag{4.25}$$

$$\Longrightarrow \int_{z_k}^{z_{k+1}} d\widehat{\mathbf{A}}(\mathbf{z}) = \int_{z_k}^{z_{k+1}} L\widehat{\mathbf{A}}(\mathbf{z})dz + \int_{z_k}^{z_{k+1}} NL[\widehat{\mathbf{A}}(\mathbf{z})]dz \tag{4.26}$$

$$\Longrightarrow \widehat{\mathbf{A}}(\mathbf{z_{k+1}}) - \widehat{\mathbf{A}}(\mathbf{z_k}) = \underbrace{\int_{z_k}^{z_{k+1}} L\widehat{\mathbf{A}}(\mathbf{z})dz}_{\text{implicit integration}} + \underbrace{\int_{z_k}^{z_{k+1}} NL[\widehat{\mathbf{A}}(\mathbf{z})]dz}_{\text{explicit integration}} \tag{4.27}$$

For simplicity, we use Adams Bashforth (AB) method for explicit integration and Adams Moulton (AM) method for implicit integration. If third order Adams methods are used, equation 4.27 would become

$$\begin{aligned} \widehat{\mathbf{A}}(\mathbf{z_{k+1}}) - \widehat{\mathbf{A}}(\mathbf{z_k}) = & \frac{h}{12}\{5L\widehat{\mathbf{A}}(\mathbf{z_{k+1}}) + 8L\widehat{\mathbf{A}}(\mathbf{z_k}) - L\widehat{\mathbf{A}}(\mathbf{z_{k-1}}) \\ & + \frac{h}{12}\{23NL[\widehat{\mathbf{A}}(\mathbf{z_{k+1}})] - 16NL[\widehat{\mathbf{A}}(\mathbf{z_k})] + 5NL[\widehat{\mathbf{A}}(\mathbf{z_{k-1}})]\} \end{aligned} \tag{4.28}$$

where h is the step size. Note that while linear part of the equation 4.28 is done in frequency domain, non-linear part of 4.28 should be done in time domain due to computational cost as cited above.

In our simulation beside using IMEX schemes, we use different IMEX schemes for different frequency components as done by Fornberg and Driscoll [11] . In this method, the frequency components of $\widehat{A}(z)$ are separated into three parts as *low*, *medium* and *high*. The main idea behind this separation is to increase accuracy by using different IMEX schemes for different frequency components. The method they applied and we used in our simulation is: for low frequencies $AB7/AB7$, for medium frequencies $AB7/AM6$ and for high frequencies $AB7/AM2^*$ for the non-linear/linear part of equation 4.23, where ABk and AMk being the k^{th} order Adams Bashforth and Moulton methods.

$AM2^*$ is a second order integration scheme defined as

$$\widehat{\mathbf{A}}(\mathbf{z_{k+1}}) - \widehat{\mathbf{A}}(\mathbf{z_k}) = \frac{h}{2}\{\frac{3}{2}L\widehat{\mathbf{A}}(\mathbf{z_{k+1}}) + \frac{1}{2}L\widehat{\mathbf{A}}(\mathbf{z_k})\} \tag{4.29}$$

where h is the step size. Note that while the normal $AM2$ (trapezoid) method is one step method, $AM2^*$ method is a second order method. Although $AM2^*$ has greater error constant (1/3) than the $AM2$ method (1/12), $AM2^*$ has a stability region that extends to the right-hand plane containing the imaginary axis as shown in Figure 4.1.

The frequency separation is done by looking at the values of the diagonal L matrix and we determine in which stability region of AB and AM methods they belong to. The L matrix has almost purely imaginary values with a very small real part. The real part comes from the attenuation constant and imaginary values come from the second and third order dispersion constants. Thus, it is reasonable to look only at the imaginary axis to classify frequency components as low, medium and high. The stability regions for $AB7$ and $AM6$ methods are shown in Figure 4.2.

For a specific frequency component w, L matrix has the value

$$-\alpha - j\frac{1}{2}\beta_2(jw^2) + \frac{1}{6}\beta_3(jw^3) = -\alpha + j\{\frac{1}{2}\beta_2 w^2 - \frac{1}{6}\beta_3 w^3\} \tag{4.30}$$

For our simulation purposes, we take the following criterion to classify frequency components w

- w is low if $h(j\{\frac{1}{2}\beta_2 w^2 - \frac{1}{6}\beta_3 w^3\}) <= 0.02$
- w is medium if $0.02 < h(j\{\frac{1}{2}\beta_2 w^2 - \frac{1}{6}\beta_3 w^3\}) <= 0.5$ and
- w is high if $h(j\{\frac{1}{2}\beta_2 w^2 - \frac{1}{6}\beta_3 w^3\}) > 0.5$

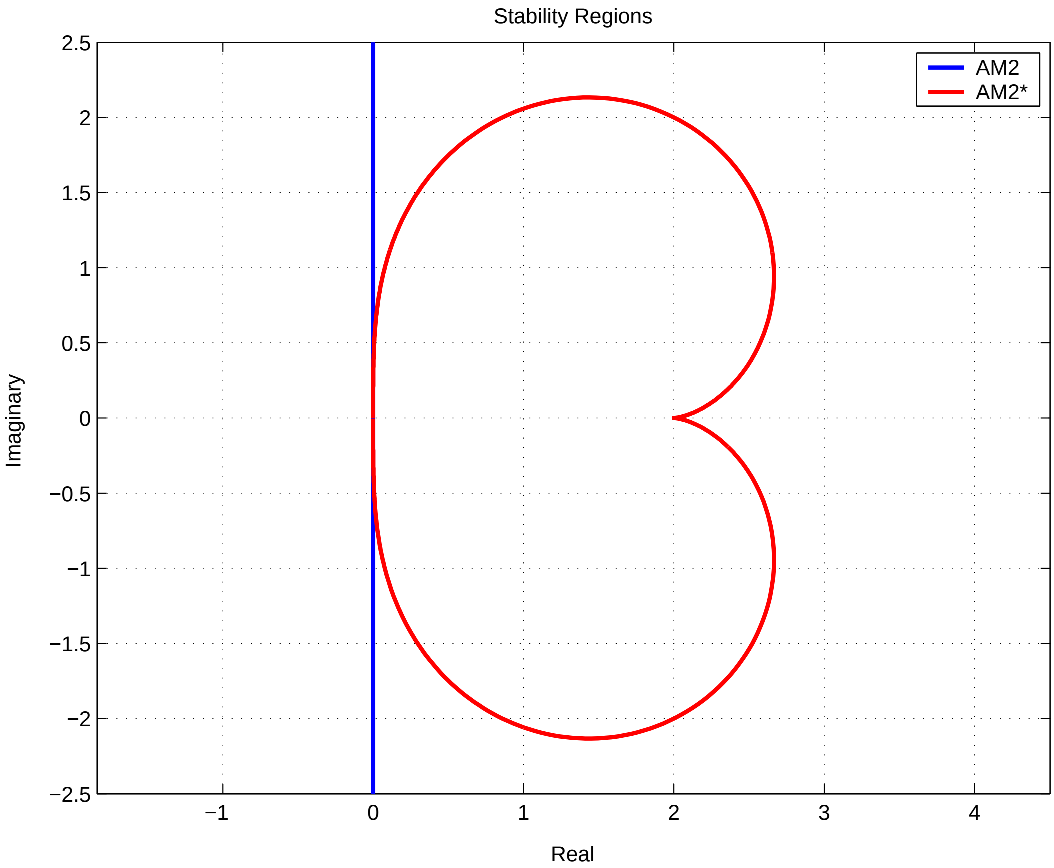

Figure 4.1: Stability Region for AM2 and AM2*

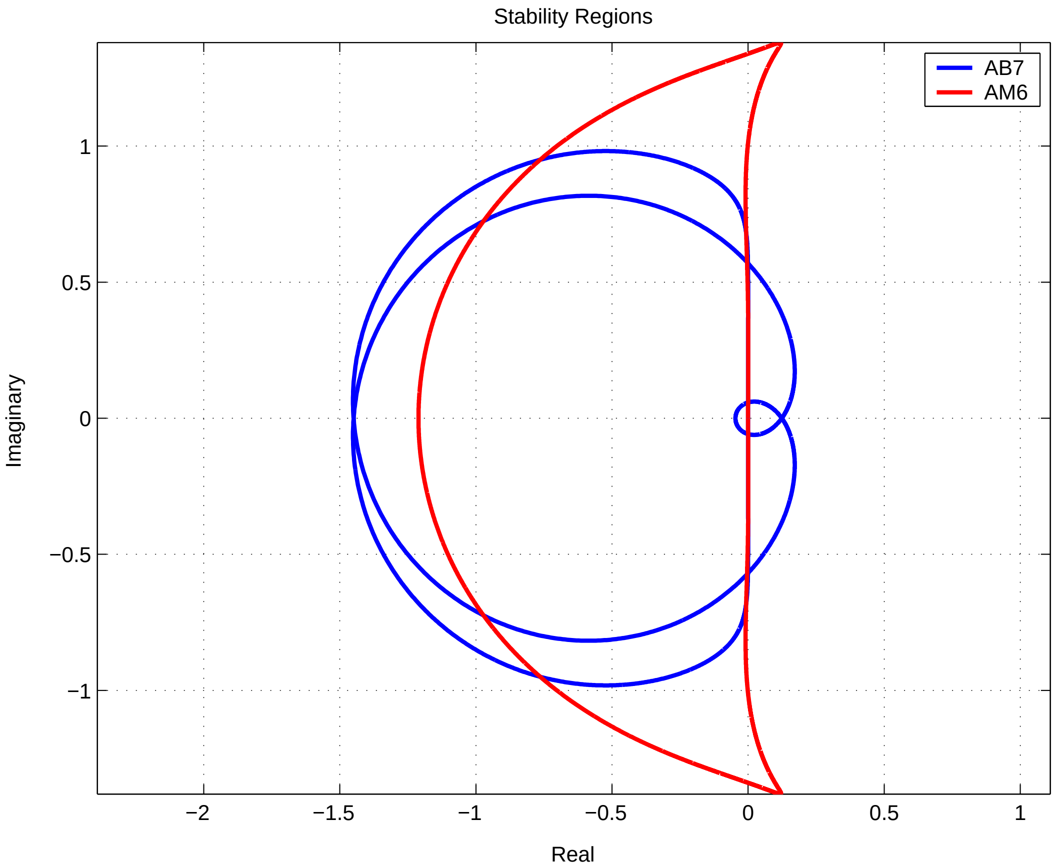

Figure 4.2: Stability Region for AB7 and AM6

where h is the step size.

In addition to use different IMEX schemes for different frequency components, in our simulation we also select the step size for numerical integration adaptively. The step size selection is based on limiting the non-linear phase shift Φ_{NL} such that $\gamma \Delta z P_p < \Phi_{NL|max}$ where γ is the Kerr non-linearity constant and P_p is the instantaneous optical peak power [3, 24]. Also, we set an upper limit on Δz so that no stability issues are concerned.

The use of adaptive step size requires the use of adaptive AB and AM methods. In this case the coefficients of AB and AM should be calculated at every step. From this point on, the variable coefficient calculation methodology will be given and the coefficient calculation methodology will be applied for $AM2^*$ method as an example at the end of the section.

Let's assume that the differential equation that we seek a solution for, has the form

$$\dot{y} = \frac{dy}{dx} = f(x, y) \tag{4.31}$$

and assume that we already know the previous k values of y and x. That is y_j and x_j are known for $j = n-k+1, n-k+2, \cdots, n-1, n$. Let's also define $h_n = x_{n+1} - x_n$ to denote the step size for the n^{th} step and $f_j = f(x_j, y_j)$. Our aim is to find y_{n+1}. If we integrate 4.31 from x_n to x_{n+1}

$$\begin{aligned}
\frac{dy}{dx} &= f(x, y) && (4.32)\\
\Longrightarrow dy &= f(x, y)dx && (4.33)\\
\Longrightarrow \int_{x_n}^{x^{n+1}} dy &= \int_{x_n}^{x^{n+1}} f(x, y)dx && (4.34)\\
\Longrightarrow y_{n+1} &= y_n + \int_{x_n}^{x^{n+1}} f(x, y)dx && (4.35)
\end{aligned}$$

The main idea in the integration of $\int_{x_n}^{x^{n+1}} f(x, y)dx$ is to find a polynomial that interpolates (x_j,f_j) and use that polynomial in the evaluation of the integral.

For AB methods, the polynomial $p(x)$ that interpolates (x_j,f_j) for $j = n-k+1, n-k+2, \cdots, n-1, n$ can be found by using Newton's interpolation formula [10]

$$p(x) = \sum_{j=0}^{k-1} \prod_{i=0}^{j-1} (x - x_{n-i}) \delta^j f[x_n, x_{n-1}, \cdots, x_{n-j}] \tag{4.36}$$

where divided differences $\delta^j f[x_n, x_{n-1}, \cdots, x_{n-j}]$ are defined as [10]

$$\delta^0 f[x_n] = f_n \tag{4.37}$$
$$\delta^j f[x_n, \cdots, x_{n-j}] = \frac{\delta^{j-1} f[x_n, \cdots, x_{n-j+1}] - \delta^{j-1} f[x_{n-1}, \cdots, x_{n-j}]}{x_n - x_{n-j}} \tag{4.38}$$

If we insert $p(x)$ in place of $f(x, y)$ in the integral $\int_{x_n}^{x^{n+1}} f(x, y)dx$ in 4.35, and evaluate the integral, the next value of y, y_{n+1}, is found as

$$y_{n+1} = y_n + h_n \sum_{j=0}^{k-1} g_j(n)\Phi_j^*(n) \tag{4.39}$$

Note that the above derivation is for AB methods. However, the derivation for AM methods are exactly the same. The only difference is to include the point (x_{n+1}, f_{n+1}) in the interpolation formula $p(x)$

$$p(x) = \sum_{j=0}^{k} \prod_{i=0}^{j-1} (x - x_{n-i})\delta^j f[x_n, x_{n-1}, \cdots, x_{n-j}] + \prod_{i=0}^{k-1} (x - x_{n-i})\delta^k f[x_{n+1}, x_n, \cdots, x_{n-k+1}] \tag{4.40}$$

If we insert $p(x)$ in place of $f(x, y)$ in the integral $\int_{x_n}^{x^{n+1}} f(x, y)dx$ in 4.35, and evaluate the integral, the next value of y, y_{n+1}, is found as

$$y_{n+1} = y_n + h_n \sum_{j=0}^{k-1} g_j(n)\Phi_j^*(n) + h_n g_k(n)\Phi_k(n + 1) \tag{4.41}$$

The formulae that give the values of $g_j(n), \Phi_j(n),$ and $\Phi_j^*(n)$ are given below [10]

$$\begin{aligned} \Phi_0(n) &= \Phi_0^*(n) = f_n \\ \Phi_{j+1}(n) &= \Phi_j(n) - \Phi_j^*(n - 1) \\ \Phi_j^*(n) &= \beta_j(n)\Phi_j(n) \end{aligned} \tag{4.42}$$

where $\beta_j(n)$ coefficients are defined as

$$\begin{aligned} \beta_0(n) &= 1 \\ \beta_j(n) &= \beta_{j-1}(n)\frac{x_{n+1} - x_{n-j+1}}{x_n - x_{n-j}} \end{aligned} \tag{4.43}$$

The values of $g_j(n)$ can be found by the formula $g_j(n) = c_{j1}(x_{n+1})$ where $c_{jq}(x_{n+1})$ is defined as

$$\begin{aligned} c_{0q}(x_{n+1}) &= \frac{1}{q} \\ c_{1q}(x_{n+1}) &= \frac{1}{q(q+1)} \\ c_{jq}(x_{n+1}) &= c_{j-1,q}(x_{n+1}) - c_{j-1,q+1}(x_{n+1})\frac{h_n}{x_{n+1} - x_{n-j+1}} \end{aligned}$$

Coefficient calculation for $AM2^*$ method is given here to show how the above derivation is used.

$AM2^*$ method is a second order implicit method which is given by the equation 4.29. The interpolation points for $AM2^*$ method are (x_{n-2}, y_{n-2}) and (x_{n+1}, y_{n+1}). If we apply Newton interpolation formula to find the interpolation polynomial for $AM2^*$, we get

$$p(x) = \delta^0 f[x_{n-1}] + (x - x_{n-1})\delta^0 f[x_{n+1}, x_{n-1}] \tag{4.44}$$

$$\Longrightarrow p(x) = f_{n-1} + (x - x_{n-1})\frac{f_{n+1} - f_{n-1}}{x_{n+1} - x_{n-1}} \tag{4.45}$$

If $p(x)$ is substituted in equation 4.27 in place of $f(x, y)$, we obtain

$$y_{n+1} = y_n + \int_{x_n}^{x^{n+1}} p(x)dx \tag{4.46}$$

$$\Longrightarrow y_{n+1} = y_n + f_{n-1}(x_{n+1} - x_n) + \frac{f_{n+1} - f_{n-1}}{x_{n+1} - x_{n-1}}\left\{\frac{x_{n+1}^2 - x_n^2}{2} - x_{n-1}(x_{n+1} - x_n)\right\} \tag{4.47}$$

$$\begin{aligned} \Longrightarrow y_{n+1} = y_n + f_{n-1}&\left\{\underbrace{(x_{n+1} - x_n) - \frac{x_{n+1}^2 - x_n^2 - 2x_{n-1}(x_{n+1} - x_n)}{2(x_{n+1} - x_{n-1})}}_{\text{coefficient formula for} f_{n-1}}\right\} + \\ &+ f_{n+1}\left\{\underbrace{\frac{x_{n+1}^2 - x_n^2 - 2x_{n-1}(x_{n+1} - x_n)}{2(x_{n+1} - x_{n-1})}}_{\text{coefficient formula for} f_{n+1}}\right\} \end{aligned} \tag{4.48}$$

4.48 shows the coefficient formula for variable step-size $AM2^*$ method. If fixed step-size is used, equation 4.48 would be simplified as 4.29.

In our simulation, we implement the fully variable step sized IMEX schemes in the solution of NLSE equation. Also, for different frequencies we applied different IMEX schemes as stated above. The computational complexity of the solution of NLSE equation is $O(N_z N_t \log(N_t))$ where N_z is the number of z-steps and N_t is the number of time points taken between $[0, T_s]$, T_s being the signal time. The log factor comes from the FFT operation.

4.3 Numerical Solution of COVODE

Unlike the NLSE equation, COVODE is a linear PDE. Right hand side of COVODE contains both z dependent coefficient matrices, as a result of non-linearity, and z independent coefficient matrices, as a result of attenuation and dispersion. In the solution of COVODE equation, we use the same methodology as done in the solution of NLSE equation. This is because COVODE equation has the same stiffness problem that NLSE equation has. More precisely, in the solution of COVODE we use $AB7$ for the low frequency components and the z varying linear terms ($\mathbb{A}(z)$), and use $AM6$ for the medium frequency components and $AM2^*$ for the high frequency components. The frequency separation mechanism is exactly the same as done in the solution of NLSE equation.

In the solution of COVODE equation, the operations for the z varying part is done in time domain whereas the operations for the linear part is done in frequency domain as in the solution of NLSE equation. This in turn requires the use of FFT operations in the solution. The transformation of the $\mathbf{K}(z)$ matrix from time domain to the frequency domain is done as follows. $\mathbf{K}(z)$ in time domain is

$$\begin{aligned}\mathbf{K_t}(z) &= \mathrm{E}[\mathbf{a}(z)\mathbf{a}(z)^\dagger] \\ &= \mathrm{E}\left\{\begin{bmatrix}\mathbf{a}_r(z) \\ \mathbf{a}_i(z)\end{bmatrix}\begin{bmatrix}\mathbf{a}_r(z)^\dagger & \mathbf{a}_i(z)^\dagger\end{bmatrix}\right\} \\ &= \begin{bmatrix}\mathrm{E}[\mathbf{a}_r(z)\mathbf{a}_r(z)^\dagger] & \mathrm{E}[\mathbf{a}_r(z)\mathbf{a}_i(z)^\dagger] \\ \mathrm{E}[\mathbf{a}_i(z)\mathbf{a}_r(z)^\dagger] & \mathrm{E}[\mathbf{a}_i(z)\mathbf{a}_i(z)^\dagger]\end{bmatrix}\end{aligned} \tag{4.49}$$

where $\mathbf{K_t}(z)$ denotes time domain covariance matrix, E is the probabilistic expectation operator and † denotes matrix transpose operation. $\mathbf{K}(z)$ in frequency domain can be found by first taking the Fourier Transforms of $\mathbf{a}_r(z)$ and $\mathbf{a}_i(z)$, and then applying the expectation operator. However, note that both $\mathbf{a}_r(z)$ and $\mathbf{a}_i(z)$ are discrete vectors as a function of z. Thus, the frequency counterpart of these vectors can be found by the use of FFT operation which actually corresponds to a matrix multiplication. Let's define the FFT matrix as $\mathfrak{F}$, $\mathbf{K}(z)$ in frequency domain then becomes

$$\begin{aligned}\mathbf{K_f}(z) &= \mathrm{E}\left\{\begin{bmatrix}\mathfrak{F}\mathbf{a}_r(z)\\ \mathfrak{F}\mathbf{a}_i(z)\end{bmatrix}\begin{bmatrix}(\mathfrak{F}\mathbf{a}_r(z))^* & (\mathfrak{F}\mathbf{a}_i(z))^*\end{bmatrix}\right\}\\ &= \begin{bmatrix}\mathfrak{F} & 0\\ 0 & \mathfrak{F}\end{bmatrix}\underbrace{\begin{bmatrix}\mathrm{E}[\mathbf{a}_r(z)\mathbf{a}_r(z)^\dagger] & \mathrm{E}[\mathbf{a}_r(z)\mathbf{a}_i(z)^\dagger]\\ \mathrm{E}[\mathbf{a}_i(z)\mathbf{a}_r(z)^\dagger] & \mathrm{E}[\mathbf{a}_i(z)\mathbf{a}_i(z)^\dagger]\end{bmatrix}}_{\mathbf{K_t}(z)}\begin{bmatrix}\mathfrak{F}^* & 0\\ 0 & \mathfrak{F}^*\end{bmatrix}\end{aligned} \tag{4.50}$$

where $\mathbf{K_f}(z)$ denotes covariance matrix in frequency domain, E is the expectation operator, $\mathfrak{F}$ is the FFT matrix, * denotes the complex conjugate transpose operation and † denotes matrix transpose operation. Complex conjugate transpose operation is done because for complex vectors χ covariance matrix is defined as $\mathrm{E}[\chi\chi^*]$, E being the expectation operator.

Equation 5.3 gives a formula for the covariance matrix $\mathbf{K}(z)$ to go back and forth between time domain and frequency domain. Although matrix multiplication is used for FFT operation in the derivation of equation 5.3, MATLAB's fft function is used in actual implementation.

In frequency domain, time domain differentiation matrices $\mathbb{D}_2$ and $\mathbb{D}_3$ in $\mathbb{B}_2$ and $\mathbb{B}_3$ becomes diagonal matrices and have the value

$$\mathbb{D}_2 = \begin{bmatrix}(jw_1)^2 & 0 & \cdots & 0\\ 0 & (jw_2)^2 & 0 & \vdots\\ \vdots & 0 & \ddots & 0\\ 0 & \cdots & 0 & (jw_{N_t})^2\end{bmatrix} \text{ and } \mathbb{D}_3 = \begin{bmatrix}(jw_1)^3 & 0 & \cdots & 0\\ 0 & (jw_2)^3 & 0 & \vdots\\ \vdots & 0 & \ddots & 0\\ 0 & \cdots & 0 & (jw_{N_t})^3\end{bmatrix} \tag{4.51}$$

where $w_1, w_2, \cdots, w_{N_t}$ are the frequency components of $A(z,t)$. In the solution of COVODE we first solve the NLSE equation as described in section 4.2 and use the values of $\mathbf{A}(z)$ to construct $\mathbb{A}(z)$ matrix. Also, we use the same z-step sizes found in the solution of NLSE equation. If we apply explicit integration to z varying and low order frequency components, and implicit integration to medium and high order frequency components in the solution of COVODE, at every z-step we need to solve a matrix equation given by

$$\mathbf{E}\mathbf{K}_f(z_n) + \mathbf{K}_f(z_n)\mathbf{E}^* = \mathbf{F}(z_n) \tag{4.52}$$

where * denotes complex conjugate transpose, $\mathbf{K}_f(z_n)$ denotes the covariance matrix in frequency domain at z_n and $\mathbf{E}$ has the form

$$\mathbf{E} = \begin{bmatrix} \mathbf{D}_d & \mathbf{D}_o \\ -\mathbf{D}_o & \mathbf{D}_d \end{bmatrix} \tag{4.53}$$

where $\mathbf{D}_d$ and $\mathbf{D}_o$ are z independent diagonal matrices. Equation 4.52 is a continuous Lyapunov matrix equation [2]. The solution for equation 4.52 can be found by the method of Barters and Stewart [23] with computational cost $O(N_t^3)$, where N_t is the number of discrete time points taken between $[0, T_s]$, T_s being the signal time. Although Bartels-Stewart algorithm can be used in the solution of equation 4.52, 4.52 can also be solved in $O(N_t^2)$ time without using Bartels-Stewart algorithm due to special form of $\mathbf{E}$ matrix.

The $\mathbf{E}$ matrix in equation 4.52 can be written as

$$\mathrm{E} = \begin{bmatrix} \begin{pmatrix} c_1 & 0 & \cdots & 0 \\ 0 & c_2 & \cdots & 0 \\ \vdots & \vdots & \ddots & \vdots \\ 0 & 0 & \cdots & c_{N_t} \end{pmatrix} & \begin{pmatrix} d_1 & 0 & \cdots & 0 \\ 0 & d_2 & \cdots & 0 \\ \vdots & \vdots & \ddots & \vdots \\ 0 & 0 & \cdots & d_{N_t} \end{pmatrix} \\ -\begin{pmatrix} d_1 & 0 & \cdots & 0 \\ 0 & d_2 & \cdots & 0 \\ \vdots & \vdots & \ddots & \vdots \\ 0 & 0 & \cdots & d_{N_t} \end{pmatrix} & \begin{pmatrix} c_1 & 0 & \cdots & 0 \\ 0 & c_2 & \cdots & 0 \\ \vdots & \vdots & \ddots & \vdots \\ 0 & 0 & \cdots & c_{N_t} \end{pmatrix} \end{bmatrix} \tag{4.54}$$

Also, we can write $\mathbf{K}_f(z_n)$ and $\mathbf{F}(z_n)$ matrices in vector form as

$$\mathbf{K}_f(z_n) = \begin{bmatrix} \vdots & \vdots & \vdots & \vdots & \vdots \\ \mathbf{K}_f(z_n)_1 & \cdots & \mathbf{K}_f(z_n)_{N_t+1} & \cdots & \mathbf{K}_f(z_n)_{N_t+N_t} \\ \vdots & \vdots & \vdots & \vdots & \vdots \end{bmatrix} \tag{4.55}$$

$$\mathbf{F}(z_n) = \begin{bmatrix} \vdots & \vdots & \vdots & \vdots & \vdots \\ \mathbf{F}(z_n)_1 & \cdots & \mathbf{F}(z_n)_{N_t+1} & \cdots & \mathbf{F}(z_n)_{N_t+N_t} \\ \vdots & \vdots & \vdots & \vdots & \vdots \end{bmatrix} \tag{4.56}$$

If we write the $\mathbf{E}$, $\mathbf{K}_f(z_n)$ and $\mathbf{F}(z_n)$ matrices as shown by the equations 4.54, 4.55 and 4.56, the Lyapunov equation 4.52 can be solved by considering the two columns of $\mathbf{K}_f(z_n)$ simultaneously. That is, the solution of 4.52 can be found by solving the following equation for every $j = 1, 2, \cdots, N_t$

$$\underbrace{\begin{bmatrix} \mathbf{E} + c_j^{\ddagger}\mathbf{I} & d_j^{\ddagger}\mathbf{I} \\ -d_j^{\ddagger}\mathbf{I} & \mathbf{E} + c_j^{\ddagger}\mathbf{I} \end{bmatrix}}_{\mathbf{E}_2} \begin{bmatrix} \mathbf{K}_f(z_n)_j \\ \mathbf{K}_f(z_n)_{j+N_t} \end{bmatrix} = \begin{bmatrix} \mathbf{F}(z_n)_j \\ \mathbf{F}(z_n)_{j+N_t} \end{bmatrix} \tag{4.57}$$

where ‡ denotes complex conjugate operation. The inverse of $\mathbf{E}_2$ is given by

$$\mathbf{E}_2^{-1} = \begin{bmatrix} \mathbf{G}^{-1} & 0 \\ 0 & \mathbf{G}^{-1} \end{bmatrix} \begin{bmatrix} \mathbf{E} + c_j^{\ddagger}\mathbf{I} & -d_j^{\ddagger}\mathbf{I} \\ d_j^{\ddagger}\mathbf{I} & \mathbf{E} + c_j^{\ddagger}\mathbf{I} \end{bmatrix} \tag{4.58}$$

where

$$\mathbf{G} = \Big((\mathbf{E} + c_j^{\ddagger}\mathbf{I})^2 + (d_j^{\ddagger})^2\mathbf{I} \Big) \tag{4.59}$$

Because $\mathbf{E}$ has a special structure, its inverse can be found trivially. The inverse of the $\mathbf{E}$ matrix shown by the equation 4.53 is given by

$$\mathbf{E}^{-1} = \begin{bmatrix} (\mathbf{D}_d^2 + \mathbf{D}_o^2)^{-1} & 0 \\ 0 & (\mathbf{D}_d^2 + \mathbf{D}_o^2)^{-1} \end{bmatrix} \begin{bmatrix} \mathbf{D}_d & -\mathbf{D}_o \\ \mathbf{D}_o & \mathbf{D}_d \end{bmatrix} \tag{4.60}$$

Because $\mathbf{G}$ matrix has the same structure as $\mathbf{E}$ matrix, the inverse of $\mathbf{G}$ matrix can be computed by using 4.60. The special structure of $\mathbf{E}$ is a result of the use of implicit integration schemes for the loss and dispersion terms of COVODE, and performing solution in frequency domain.

The computational complexity of the solution of COVODE equation is $O(N_z N_t^2 \log(N_t))$ where N_z is the number of z steps, which is adaptively found by the solution of NLSE equation, and N_t is the number of discrete time points taken between

$[0, T_s]$, T_s being the signal time. The log term in computational cost comes from the use of FFT operations.

4.4 Covariance Matrix Computation With Transfer Functions

In the propagation of noise covariance matrix one can also use the transfer function methodology which is stated below.

Likewise in the un-modulated carrier case, we can obtain a transfer function matrix for the differential equation that is given by 4.8

$$\frac{d}{dz}\begin{bmatrix} a_r(z,t) \\ a_i(z,t) \end{bmatrix} = -\alpha \begin{bmatrix} a_r(z,t) \\ a_i(z,t) \end{bmatrix} + \frac{1}{2}\beta_2 \begin{bmatrix} 0 & \frac{\partial^2}{\partial t^2} \\ -\frac{\partial^2}{\partial t^2} & 0 \end{bmatrix} \begin{bmatrix} a_r(z,t) \\ a_i(z,t) \end{bmatrix} + \frac{1}{6}\beta_3 \begin{bmatrix} \frac{\partial^3}{\partial t^3} & 0 \\ 0 & \frac{\partial^3}{\partial t^3} \end{bmatrix} \begin{bmatrix} a_r(z,t) \\ a_i(z,t) \end{bmatrix}$$
$$+ \gamma \begin{bmatrix} -2A_r(z,t)A_i(z,t) & -A_r(z,t)^2 - 3A_i(z,t)^2 \\ 3A_r(z,t)^2 + A_i(z,t)^2 & 2A_r(z,t)A_i(z,t) \end{bmatrix} \begin{bmatrix} a_r(z,t) \\ a_i(z,t) \end{bmatrix} \tag{4.61}$$

that characterisize noise propagation along the fiber.

A linear time-invariant(LTI) system can be modeled in frequency domain as

$$Y(w) = H(w)X(w) \tag{4.62}$$

where $X(w)$ denotes the Fourier transform of the system input, $x(t)$, $H(w)$ denotes the system transfer function and $Y(w)$ denotes the Fourier transform of the system output,$y(t)$. However, equation 4.61 is a linear, with respect to z, time-varying system(LTV). A LTV system can also be modeled in frequency domain. In this case the transfer function becomes also *time* dependent. That is

$$Y(w,t) = H(w,t)X(w) \tag{4.63}$$

where where $X(w)$ denotes the Fourier transform of the system input, $x(t)$, $H(w,t)$ denotes the system transfer function.$y(t)$, system output, can be obtained from $Y(w,t)$ in 4.63 by using inverse Fourier transform

$$y(t) = \int_{-\infty}^{\infty} Y(w,t)\exp(jwt)dw \tag{4.64}$$

For equation 4.61 we can find a transfer function matrix that transfer the initial noise envelope to the noise envelope at the end of the fiber span. That is

$$\begin{bmatrix} \mathcal{A}_r(z,w,t) \\ \mathcal{A}_i(z,w,t) \end{bmatrix} = \begin{bmatrix} \mathcal{H}_{RR}(z,w,t) & \mathcal{H}_{IR}(z,w,t) \\ \mathcal{H}_{RI}(z,w,t) & \mathcal{H}_{II}(z,w,t) \end{bmatrix} \begin{bmatrix} \mathcal{A}_r(z=0,w,t) \\ \mathcal{A}_r(z=0,w,t) \end{bmatrix} \tag{4.65}$$

where $\mathcal{A}_r(z,w,t)$ and $\mathcal{A}_i(z,w,t)$ denote Fourier transforms of noise in-phase, $a_r(z,t)$, and quadrature, $a_i(z,t)$, parts respectively, $\mathcal{H}_{RR}(z,w,t)$ denotes the transfer function from noise in-phase component to noise in-phase component, $\mathcal{H}_{IR}(z,w,t)$ denotes the transfer function from noise quadrature component to noise in-phase component, $\mathcal{H}_{RI}(z,w,t)$ denotes the transfer function from noise in-phase component to quadrature component and $\mathcal{H}_{II}(z,w,t)$ denotes the transfer function from noise quadrature component to quadrature component. Please note that in this case transfer functions also become z dependent.

Equation 4.61 can be written in Fourier domain as

$$\begin{aligned} \frac{\partial}{\partial z}\begin{bmatrix} \mathcal{A}_r(z,w,t) \\ \mathcal{A}_i(z,w,t) \end{bmatrix} &= -\alpha \begin{bmatrix} \mathcal{A}_r(z,w,t) \\ \mathcal{A}_i(z,w,t) \end{bmatrix} \\ &+ \frac{1}{2}\beta_2 \begin{bmatrix} 0 & (jw)^2 + 2(jw)\frac{\partial}{\partial t} + \frac{\partial^2}{\partial t^2} \\ -((jw)^2 + 2(jw)\frac{\partial}{\partial t} + \frac{\partial^2}{\partial t^2}) & 0 \end{bmatrix} \begin{bmatrix} \mathcal{A}_r(z,w,t) \\ \mathcal{A}_i(z,w,t) \end{bmatrix} \\ &+ \frac{1}{6}\beta_3 \begin{bmatrix} (jw)^3 + 3(jw)^2\frac{\partial}{\partial t} + 3(jw)\frac{\partial^2}{\partial t^2} + \frac{\partial^3}{\partial t^3} & 0 \\ 0 & (jw)^3 + 3(jw)^2\frac{\partial}{\partial t} + 3(jw)\frac{\partial^2}{\partial t^2} + \frac{\partial^3}{\partial t^3} \end{bmatrix} \begin{bmatrix} \mathcal{A}_r(z,w,t) \\ \mathcal{A}_i(z,w,t) \end{bmatrix} \\ &+ \gamma \begin{bmatrix} -2A_r(z,t)A_i(z,t) & -A_r(z,t)^2 - 3A_i(z,t)^2 \\ 3A_r(z,t)^2 + A_i(z,t)^2 & 2A_r(z,t)A_i(z,t) \end{bmatrix} \begin{bmatrix} \mathcal{A}_r(z,w,t) \\ \mathcal{A}_i(z,w,t) \end{bmatrix} \end{aligned} \tag{4.66}$$

where $\mathcal{A}_r(z,w,t)$ and $\mathcal{A}_i(z,w,t)$ denote Fourier transforms of noise in-phase and quadrature components respectively, $A_r(z,t)$ and $A_i(z,t)$ are the noise-free large desired signal envelopes, w denotes the Fourier frequency and $j = sqrt(-1)$. Equation 4.66 should be satisfied at every Fourier frequency point,w_i. For specific w_i let define

$$\begin{bmatrix} \mathbb{A}_r(z,t) \\ \mathbb{A}_i(z,t) \end{bmatrix} = \begin{bmatrix} \mathcal{A}_r(z,w_i,t) \\ \mathcal{A}_i(z,w_i,t) \end{bmatrix} \tag{4.67}$$

By using the definition 4.67, equation 4.66 can be written as

$$\frac{\partial}{\partial z}\begin{bmatrix}\mathbb{A}_r(z,t)\\ \mathbb{A}_i(z,t)\end{bmatrix} = -\alpha\begin{bmatrix}\mathbb{A}_r(z,t)\\ \mathbb{A}_i(z,t)\end{bmatrix}$$
$$+\frac{1}{2}\beta_2\begin{bmatrix}0 & (jw_i)^2+2(jw_i)\frac{\partial}{\partial t}+\frac{\partial^2}{\partial t^2}\\ -((jw_i)^2+2(jw_i)\frac{\partial}{\partial t}+\frac{\partial^2}{\partial t^2}) & 0\end{bmatrix}\begin{bmatrix}\mathbb{A}_r(z,t)\\ \mathbb{A}_i(z,t)\end{bmatrix}$$
$$+\frac{1}{6}\beta_3\begin{bmatrix}(jw_i)^3+3(jw_i)^2\frac{\partial}{\partial t}+3(jw_i)\frac{\partial^2}{\partial t^2}+\frac{\partial^3}{\partial t^3} & 0\\ 0 & (jw_i)^3+3(jw_i)^2\frac{\partial}{\partial t}+3(jw_i)\frac{\partial^2}{\partial t^2}+\frac{\partial^3}{\partial t^3}\end{bmatrix}\begin{bmatrix}\mathbb{A}_r(z,t)\\ \mathbb{A}_i(z,t)\end{bmatrix}$$
$$+\gamma\begin{bmatrix}-2A_r(z,t)A_i(z,t) & -A_r(z,t)^2-3A_i(z,t)^2\\ 3A_r(z,t)^2+A_i(z,t)^2 & 2A_r(z,t)A_i(z,t)\end{bmatrix}\begin{bmatrix}\mathbb{A}_r(z,t)\\ \mathbb{A}_i(z,t)\end{bmatrix} \tag{4.68}$$

The solution of 4.68 can be obtained by integration the right hand side of the solution both in time and frequency domain. The frequency domain is required to compute the differentiation(s) used in the equation. Writing equation 4.68 in frequency domain we obtain

$$\frac{\partial}{\partial z}\begin{bmatrix}\mathfrak{A}_r(z,\xi)\\ \mathfrak{A}_i(z,\xi)\end{bmatrix} = -\alpha\begin{bmatrix}\mathfrak{A}_r(z,\xi)\\ \mathfrak{A}_i(z,\xi)\end{bmatrix}$$
$$+\frac{1}{2}\beta_2\begin{bmatrix}0 & (jw_i)^2+2(jw_i)\frac{\partial}{\partial t}+\frac{\partial^2}{\partial t^2}\\ -((jw_i)^2+2(jw_i)\frac{\partial}{\partial t}+\frac{\partial^2}{\partial t^2}) & 0\end{bmatrix}\begin{bmatrix}\mathfrak{A}_r(z,\xi)\\ \mathfrak{A}_i(z,\xi)\end{bmatrix}$$
$$+\frac{1}{6}\beta_3\begin{bmatrix}(jw_i)^3+3(jw_i)^2\frac{\partial}{\partial t}+3(jw_i)\frac{\partial^2}{\partial t^2}+\frac{\partial^3}{\partial t^3} & 0\\ 0 & (jw_i)^3+3(jw_i)^2\frac{\partial}{\partial t}+3(jw_i)\frac{\partial^2}{\partial t^2}+\frac{\partial^3}{\partial t^3}\end{bmatrix}\begin{bmatrix}\mathfrak{A}_r(z,\xi)\\ \mathfrak{A}_i(z,\xi)\end{bmatrix}$$
$$+\mathcal{F}\left\{\gamma\begin{bmatrix}-2A_r(z,t)A_i(z,t) & -A_r(z,t)^2-3A_i(z,t)^2\\ 3A_r(z,t)^2+A_i(z,t)^2 & 2A_r(z,t)A_i(z,t)\end{bmatrix}\begin{bmatrix}\mathbb{A}_r(z,t)\\ \mathbb{A}_r(z,t)\end{bmatrix}\right\} \tag{4.69}$$

where $\mathfrak{A}_r(z,\xi)$ and $\mathfrak{A}_i(z,\xi)$ are the Fourier transforms of $\mathbb{A}_r(z,t)$ and $\mathbb{A}_r(z,t)$ respectively and $\mathcal{F}$ denotes Fourier transform. The solution of 4.69 can be find

- integrating the z dependent part in time domain
- then going to frequency domain by using FFT transform
- integration the w_i dependent part and computing the next value of $\mathfrak{A}_r(z,\xi)$ and $\mathfrak{A}_i(z,\xi)$
- computing $\mathbb{A}_r(z,t)$ and $\mathbb{A}_r(z,t)$ by using inverse FFT transform

For specific w_i we can compute the envelope of $\mathcal{A}_r(z, w_i, t)$ and $\mathcal{A}_i(z, w_i, t)$ by solving 4.69. To compute the system transfer function matrix we will use identity matrix for the initial condition in the solution of 4.69. In the solution for the z dependent part integration, we will use second-order AdamsBashforth and use trapezoid rule for the w_i dependent part.

In the solution of 4.69 we need to solve a linear system of equations at each z-step. The coefficient matrices in the solution of linear systems take the following form

$$\mathcal{D} = \begin{bmatrix} \mathcal{D}1 & \mathcal{D}2 \\ -\mathcal{D}2 & \mathcal{D}1 \end{bmatrix} \tag{4.70}$$

where $\mathcal{D}\infty$ and $\mathcal{D}\in$ are diagonal matrices. The inverse of D matrix can be find by using the block matrix inversion formula which is given by

$$\begin{bmatrix} A & B \\ C & D \end{bmatrix}^{-1} = \begin{bmatrix} (A - BD^{-1}C)^{-1} & -A^{-1}B(D - CA^{-1}B)^{-1} \\ -D^{-1}C(A - BD^{-1}C)^{-1} & (D - CA^{-1}B)^{-1} \end{bmatrix} \tag{4.71}$$

Because in our case $A = D$ and $B = -C$ and all matrices are diagonal, the computation of the inverse of $\mathcal{D}$ matrix takes $\mathcal{O}(N)$, time where N is the size of the $\mathcal{D}1$ and $\mathcal{D}2$ matrices. We will use the block matrix inversion formula in the solution of 4.69.

To compute the covariance among noise sample we will use the transfer function matrix. Let assume that a LTV system receives $x(t)$ as input and produce $y(t)$ as output and let $H(w, t)$ be the time dependent system transfer function. Then $y(t)$ can be written as

$$y(t) = \int_{-\infty}^{\infty} H(w, t)X(w) \exp(jwt)dw \tag{4.72}$$

where $X(w)$ is the Fourier transform of $x(t)$. Because the samples are taken at discrete time points, for the inverse Fourier transform in 4.72 we will use discrete values as

$$y(t) = \sum_i H(w_i, t)X(w_i) \exp(jw_it)\Delta w \tag{4.73}$$

By using 4.73 we can compute the covariance of two sample $y(t)$ time points as

$$
\begin{aligned}
E[y(t_1)y(t_2)^*] &= E\left[\left(\sum_i H(w_i,t_1)X(w_i)\exp(jw_it_1)\Delta w\right)\left(\sum_k H(w_k,t_2)X(w_k)\exp(jw_kt_2)\Delta w\right)^*\right] \\
&= E\left[\sum_i\sum_k H(w_i,t_1)X(w_i)X(w_k)^*H(w_k,t_2)^*\exp(j(w_it_1-w_kt_2)(\Delta w)^2\right] \\
&= \sum_i\sum_k H(w_i,t_1)E[X(w_i)X(w_k)^*]H(w_k,t_2)^*\exp(j(w_it_1-w_kt_2)(\Delta w)^2
\end{aligned}
\tag{4.74}
$$

where * denotes complex conjugate operation, E is the statistical expectation operator and $j=\sqrt{-1}$. If $X(w)$ is white stationary noise, then equation 4.77 takes the following simplified form

$$
E[y(t_1)y(t_2)^*] = \sum_i H(w_i,t_1)E[X(w_i)X(w_i)^*]H(w_i,t_2)^*\exp(j(w_it_1-w_it_2)(\Delta w)^2 \tag{4.75}
$$

Equation 4.73 can be written in vector form as

$$
\underbrace{\begin{bmatrix} y(t_1) \\ y(t_2) \\ \vdots \\ y(t_N) \end{bmatrix}}_{\mathbb{Y}} = \underbrace{\begin{bmatrix} H(w_1,t_1)\exp(jw_1t_1)\Delta w & H(w_2,t_1)\exp(jw_2t_1)\Delta w & \cdots & H(w_1,t_N)\exp(jw_1t_N)\Delta w \\ H(w_1,t_2)\exp(jw_1t_2)\Delta w & H(w_2,t_2)\exp(jw_2t_2)\Delta w & \cdots & H(w_1,t_2)\exp(jw_1t_2)\Delta w \\ \vdots & \vdots & \ddots & \vdots \\ H(w_1,t_N)\exp(jw_1t_N)\Delta w & H(w_2,t_N)\exp(jw_2t_N)\Delta w & \cdots & H(w_N,t_N)\exp(jw_Nt_N)\Delta w \end{bmatrix}}_{\mathbb{H}} \underbrace{\begin{bmatrix} X(w_1) \\ X(w_2) \\ \vdots \\ X(w_N) \end{bmatrix}}_{\mathbb{X}} \tag{4.76}
$$

where N denotes the number of discrete time points. Assuming that $\mathbb{Y}$, $\mathbb{H}$ and $\mathbb{X}$ are given like in equation 4.76, we can find the covariance matrix for $\mathbb{Y}$ as

$$
\begin{aligned}
E[\mathbb{Y}\mathbb{Y}^*] &= E[(\mathbb{H}\mathbb{X})(\mathbb{H}\mathbb{X})^*] \\
&= E[\mathbb{H}\mathbb{X}\mathbb{X}^*\mathbb{H}^*] \\
&= \mathbb{H}E[\mathbb{X}\mathbb{X}^*]\mathbb{H}^*
\end{aligned}
\tag{4.77}
$$

where E is the statistical expectation operator and * denotes complex conjugate operation. If $x(t)$ is white stationary process, then 4.77 takes the following form

$$
\begin{aligned}
E[\mathbb{Y}\mathbb{Y}^*] &= \mathbb{H}E[\mathbb{X}\mathbb{X}^*]\mathbb{H}^* \\
&= \eta\mathbb{H}\mathbb{H}^*
\end{aligned}
\tag{4.78}
$$

E is the statistical expectation operator, η is the spectral density of $X(w)$ and * denotes complex conjugate operation.

Following the methodology stated above, by using transfer function matrices $\mathcal{H}_{RR}(z,w,t)$, $\mathcal{H}_{IR}(z,w,t)$, $\mathcal{H}_{RI}(z,w,t)$ and $\mathcal{H}_{II}(z,w,t)$ and given initial noise covariance matrix at $z=0$, we can find the noise covariance matrix at the end of the fiber link. Let assume that at $z=L$, L being the fiber span length, $\mathbb{H}_{RR}$, $\mathbb{H}_{IR}$, $\mathbb{H}_{RI}$ and $\mathbb{H}_{II}$ denote the t and w dependent transfer function matrices likewise in equation 4.76. Then, noise vector at the end of the fiber link can be calculated as

$$\begin{aligned}\mathbf{a}_r(z=L) &= \mathbb{H}_{RR}\cdot a_r(z=0,w)+\mathbb{H}_{IR}\cdot\mathbf{a}_i(z=0,w)\\ \mathbf{a}_i(z=L) &= \mathbb{H}_{RI}\cdot a_r(z=0,w)+\mathbb{H}_{II}\cdot\mathbf{a}_i(z=0,w)\end{aligned}\tag{4.79}$$

or equivalently

$$\begin{bmatrix}\mathbf{a}_r(z=L)\\ \mathbf{a}_i(z=L)\end{bmatrix}=\begin{bmatrix}\mathbb{H}_{RR} & \mathbb{H}_{IR}\\ \mathbb{H}_{RI} & \mathbb{H}_{II}\end{bmatrix}\begin{bmatrix}\mathbf{a}_r(z=0,w)\\ \mathbf{a}_i(z=0,w)\end{bmatrix}\tag{4.80}$$

where $\mathbf{a}_r(z=L)$ and $\mathbf{a}_i(z=L)$ are the noise in-phase and quadrature component vectors in time domain and $\mathbf{a}_r(z=0,w)$ and $\mathbf{a}_i(z=0,w)$ are the Fourier transforms of noise in-phase and quadrature component vectors. By using 4.80 we can find the noise covariance matrix at the end of the fiber as

$$\begin{aligned}E\left\{\begin{bmatrix}\mathbf{a}_r(z=L)\\ \mathbf{a}_i(z=L)\end{bmatrix}\begin{bmatrix}\mathbf{a}_r(z=L)\\ \mathbf{a}_i(z=L)\end{bmatrix}^*\right\} &= E\left\{\left(\begin{bmatrix}\mathbb{H}_{RR} & \mathbb{H}_{IR}\\ \mathbb{H}_{RI} & \mathbb{H}_{II}\end{bmatrix}\begin{bmatrix}\mathbf{a}_r(z=0,w)\\ \mathbf{a}_i(z=0,w)\end{bmatrix}\right)\left(\begin{bmatrix}\mathbb{H}_{RR} & \mathbb{H}_{IR}\\ \mathbb{H}_{RI} & \mathbb{H}_{II}\end{bmatrix}\begin{bmatrix}\mathbf{a}_r(z=0,w)\\ \mathbf{a}_i(z=0,w)\end{bmatrix}\right)^*\right\}\\ &= \begin{bmatrix}\mathbb{H}_{RR} & \mathbb{H}_{IR}\\ \mathbb{H}_{RI} & \mathbb{H}_{II}\end{bmatrix}E\left\{\begin{bmatrix}\mathbf{a}_r(z=0,w)\\ \mathbf{a}_i(z=0,w)\end{bmatrix}\begin{bmatrix}\mathbf{a}_r(z=0,w)\\ \mathbf{a}_i(z=0,w)\end{bmatrix}^*\right\}\begin{bmatrix}\mathbb{H}_{RR} & \mathbb{H}_{IR}\\ \mathbb{H}_{RI} & \mathbb{H}_{II}\end{bmatrix}^*\\ &= \begin{bmatrix}\mathbb{H}_{RR} & \mathbb{H}_{IR}\\ \mathbb{H}_{RI} & \mathbb{H}_{II}\end{bmatrix}\underbrace{\begin{bmatrix}\mathbf{K_f}^{rr}(z=0) & \mathbf{K_f}^{ri}(z=0)\\ \mathbf{K_f}^{ir}(z=0) & \mathbf{K_f}^{ii}(z=0)\end{bmatrix}}_{\mathbf{K_f}(z=0)}\begin{bmatrix}\mathbb{H}_{RR} & \mathbb{H}_{IR}\\ \mathbb{H}_{RI} & \mathbb{H}_{II}\end{bmatrix}^*\end{aligned}\tag{4.81}$$

where $\mathbf{K_f}^{rr}$, $\mathbf{K_f}^{ri}$, $\mathbf{K_f}^{ir}$ and $\mathbf{K_f}^{ii}$ are given in 5.3. Assuming that noise entering the fiber is white and stationary and has uncorrelated in-phase and quadrature components, 4.81 can be simplified as

$$E\left\{\begin{bmatrix}\mathbf{a}_r(z=L)\\ \mathbf{a}_i(z=L)\end{bmatrix}\begin{bmatrix}\mathbf{a}_r(z=L)\\ \mathbf{a}_i(z=L)\end{bmatrix}^*\right\}=\eta\begin{bmatrix}\mathbb{H}_{RR} & \mathbb{H}_{IR}\\ \mathbb{H}_{RI} & \mathbb{H}_{II}\end{bmatrix}\begin{bmatrix}\mathbb{H}_{RR} & \mathbb{H}_{IR}\\ \mathbb{H}_{RI} & \mathbb{H}_{II}\end{bmatrix}^* \tag{4.82}$$

where η denotes the noise spectral density. Equation 4.82 holds since the frequency domain covariance matrix, $\mathbf{K_f}(z=0)$, becomes identity matrix.

For the equation 4.61, we have computed the transfer function matrices and used equation 4.82 in the computation of noise covariance matrix at the end of the fiber. The results obtained by using the transfer function matrices matched the results that are obtained by COVODE equation.

4.5 Simulation Results

In this section, we give simulation results for noise propagation in a WDM system with modulated carriers. As denoted by the equation 4.20, noise propagation depends on the input spectrum $A(z,t)$. Thus, to compute the noise propagation along the fiber we first solve NLSE equation as described in section 4.2 and then apply numerical techniques described in section 4.3 .

The initial condition for the noise covariance matrix $\mathbf{K}(z=0)$ is taken to be identity matrix. In this case, we assume that noise is white and stationary Gaussian as a function of time and that real and imaginary parts of the noise are uncorrelated. In simulations, we assume that noise added to the system with the first OA and no noise addition is done by the last OA which is located in the receiver. Also, we assumed that noise added by different OAs are uncorrelated with each other and that OAs in the fiber link compensate the loss for one fiber span completely.

Note that in the solutions of both NLSE and COVODE equation we use the FFT operation. However, the use of FFT operation requires that the signal is periodic. For our simulations, we assume that each channel in WDM spectrum modulates periodic signals with a period of $8T_b$, where T_b is the duration of a single bit. In our simulation, we use $T_b = 12.5$ Gb/sec. The discrete time points, N_t, are taken to be 256 due to the efficiency in FFT operation and Nyquist sampling rate criteria.

In simulation, we model the bits by using raised cosine pulse whose equation is given by

$$rcos(t) = sinc(\frac{t}{T})\frac{\cos(\frac{\pi\beta t}{T})}{1-\frac{4\beta^2t^2}{T^2}} \tag{4.83}$$

where T is the bit duration and β is the roll-off factor. The advantages of using raised cosine pulse in the simulation are the reduced symbol interference in time domain and finite bandwidth in frequency domain. In the simulation, we take roll-off factor, β, to be 0.6 .

For our simulation, we set the channel separation to 25 GHz, power per channel to 10 mW and take the fiber length 80 km. The fiber parameters for the simulation are $\alpha = 0.25$ dB/km, $\beta_2 =$ -21.6 ps^2/km, $\beta_3 = 0.128$ ps^3/km and $\gamma = 1.2$ 1/Wkm.

Note that in all of the figures, we give the noise amplification with respect to the noise which is obtained by ignoring non-linearity in the fiber.

4.5.1 Fiber without Kerr non-linearity

In this case there is no signal noise interaction and noise characteristics do not change along the fiber. Although there are some distortion on the noise as a consequence of dispersion the second order characteristics of the noise do not change. That is, the noise at the end of the fiber link is still white and stationary. In this case 4.20 can be solved analytically by considering the two columns of $\mathbf{K}(z)$ simultaneously.

4.5.2 Combination of Unmodulated Carriers

We now present the noise amplification for un-modulated carriers. Figure 4.3 shows the noise amplification as a function of frequency for a WDM system with 1, 3 and 5 channels. Figure 4.3 shows the main diagonal of $\mathbf{K}_f(z = L)$ before the channel select filter. Although the noise before the channel select filter is non-stationary, after the channel select filter (WDM demux) noise becomes stationary as observed by the diagonal structure of covariance matrix shown in Figure 4.4. Figure 4.4 shows the noise covariance matrix after the channel select filter where the simulation is done for 5 channeled WDM system.

It is observed in Figure 4.3 that for the 5 channel case noise amplification reaches about ~ 4 dB. However the noise amplification decrease rapidly as one moves away channel carrier frequency. This is a result of dispersion in the fiber. Without dispersion noise amplification is independent of frequency and equal to the value at $f = 0$. Thus we conclude that dispersion has positive effect on system performance by attenuating the noise. Another observation in Figure 4.3 is that noise amplification at the carrier frequencies increases as the number of channels increase.

4.5.3 Carriers Modulated with a Single Pulse

In this case, we assume that the bit pattern for all the channels is set to $[0, \cdots, 0, 1, 0, \cdots, 0]$. In Figure 4.5 the input output spectrum is shown. The noise amplification before the channel select filter is shown in Figure 4.6. The non-stationary behavior of the noise after the channel select filter can be observed in Figure 4.7.

4.5.4 Carriers Modulated with a Random Pulse

This is the most general case for modulated carriers. Figure 4.8 shows noise amplification for both modulated and un-modulated carriers in a 5 channel WDM system. If we look closer to Figure 4.8, we observe that the power of the noise for modulated and unmodulated carrier case is approximately the same. However, if we consider the channel that centered around $f = 0$, we see that power of the noise in high frequencies is higher for modulated carrier case compared to unmodulated carrier case. As a consequence of this, we can infer that the correlation between noise samples is higher for unmodulated carrier case compared to modulated carrier case.

After the channel select filter, the noise amplification in time domain for modulated carrier case is shown in Figure 4.9. Due to non-constant power of noise, it is observed from Figure 4.9 that noise is non-stationary after the channel select filter. The covariance matrix for this case is shown in Figure 4.10.

In this chapter, we analyzed the noise in a WDM system with modulated carrier case. We have given numerical computation methodologies for the solution of NLSE equation and COVODE equation that models the noise covariance matrix propagation along the fiber. Also we developed frequency decomposed formulation of covariance matrix propagation and supplied solution methodology. Finally, the simulation results for different system parameters have been given.

In the next chapter we will analyze the noise effect on the system performance for a WDM system with modulated carriers by computing system's BER.

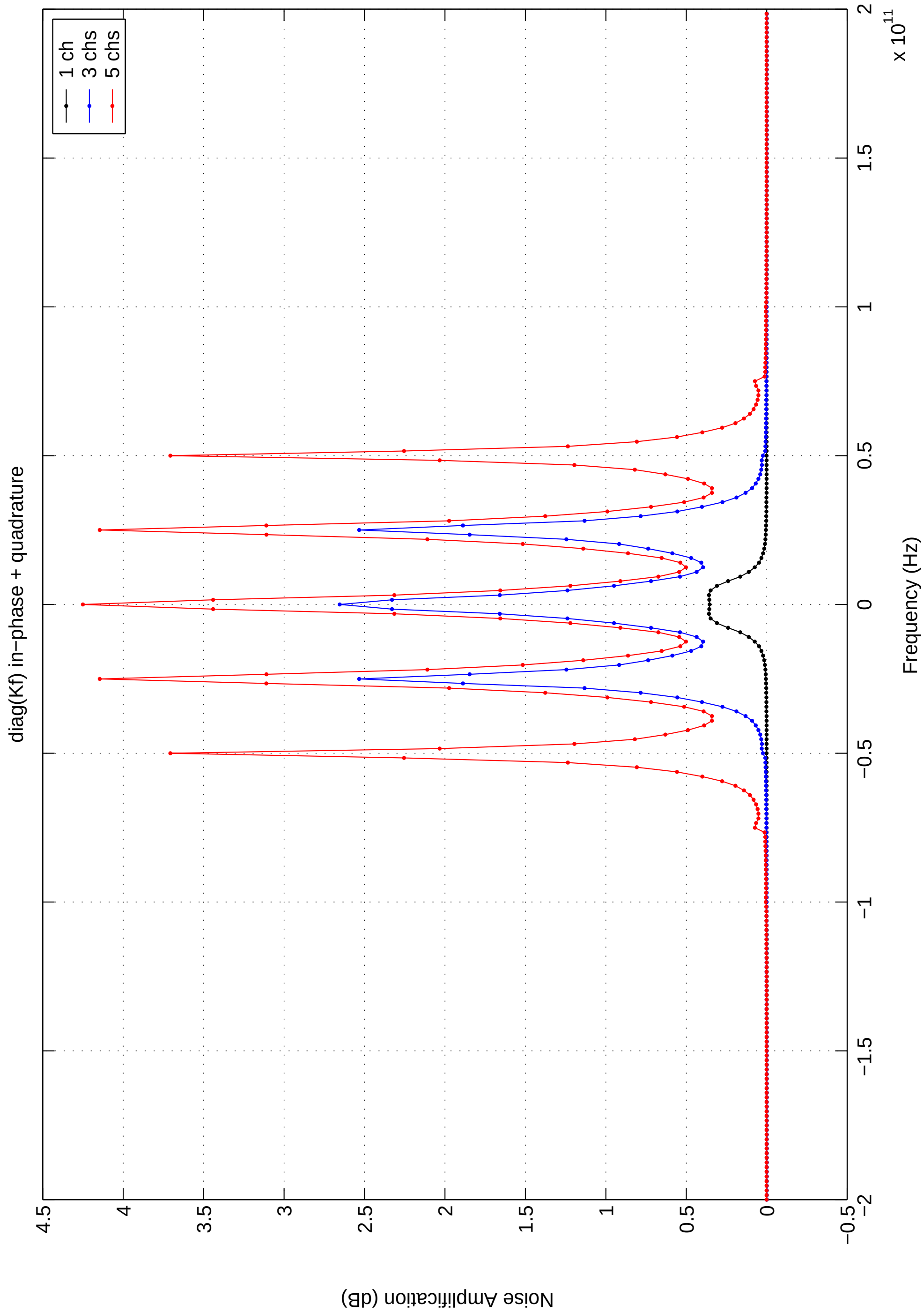

Figure 4.3: Unmodulated Carriers, diag($\mathbf{K}_f(z = L)$): in-phase + quadrature
System parameters: # of channels: 1-3-5, Channel spacing: 25 GHz,
Symbol rate: 12.5 Gs/sec, Launch Power: 10 mW, α *= 0.25 dB/km ,* β_2 *= -21.6 ps*^{2}*/km,*
β_3 *= 0.128 ps*^{3}*/km,* γ *= 1.2 1/(W·km),* L *: 80 km*

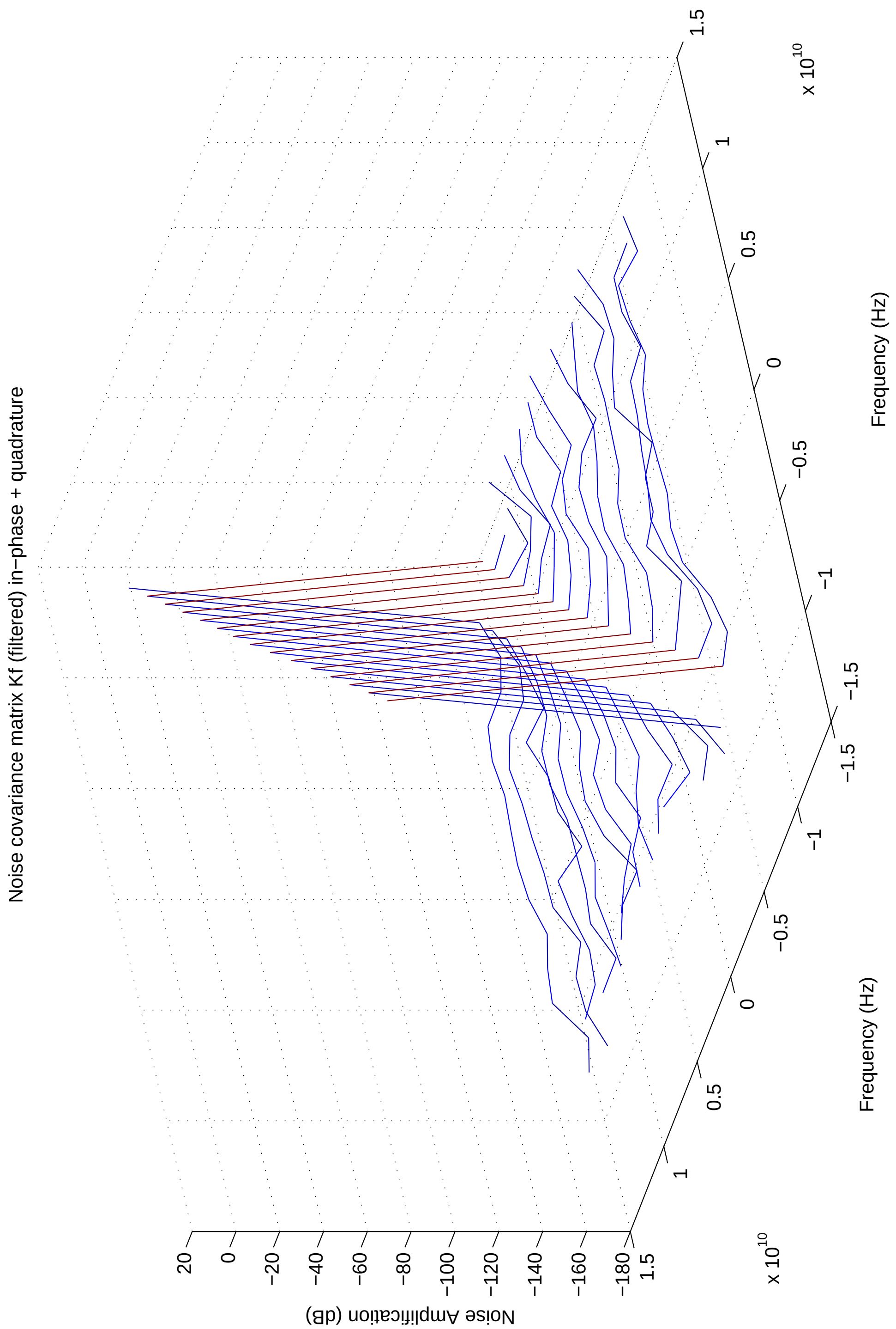

Figure 4.4: Unmodulated Carriers (filtered), $\mathbf{K}_f(z = L)$
System parameters: # of channels: 5, Channel spacing: 25 GHz,
Symbol rate: 12.5 Gs/sec, Launch Power: 10 mW, α = *0.25 dB/km ,* β_2 = *-21.6* ps^2/km*,*
β_3 = *0.128* ps^3/km*,* γ = *1.2 1/(W·km),* L : *80 km*

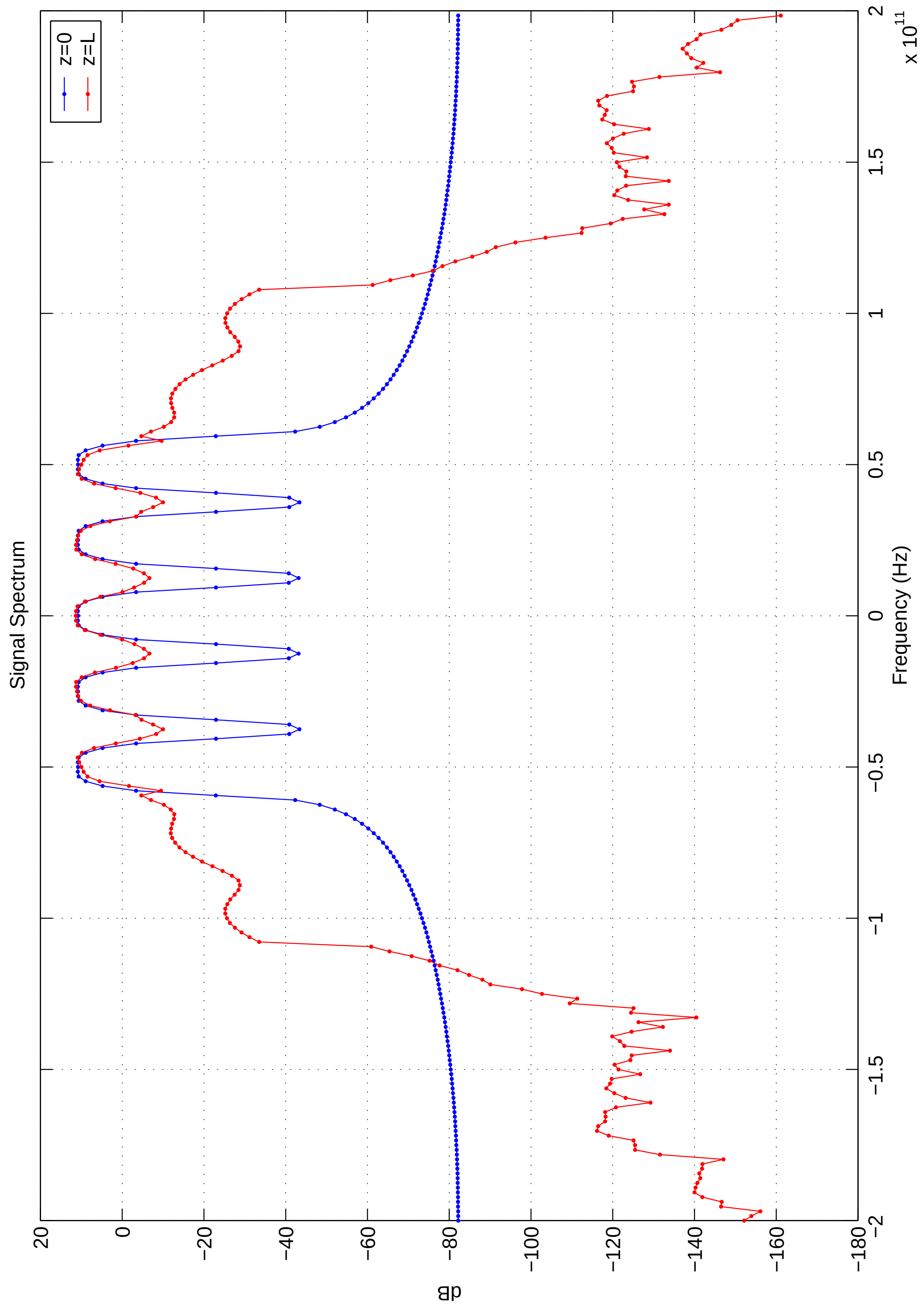

Figure 4.5: Modulated Carriers, single pulse, signal spectrum
System parameters: # of channels: 5, Channel spacing: 25 GHz,
Symbol rate: 12.5 Gs/sec, Launch Power: 10 mW, α = *0.25 dB/km* , β_2 = *-21.6 ps*^{2}*/km,*
β_3 = *0.128 ps*^{3}*/km,* γ = *1.2 1/(W·km),* L : *80 km*

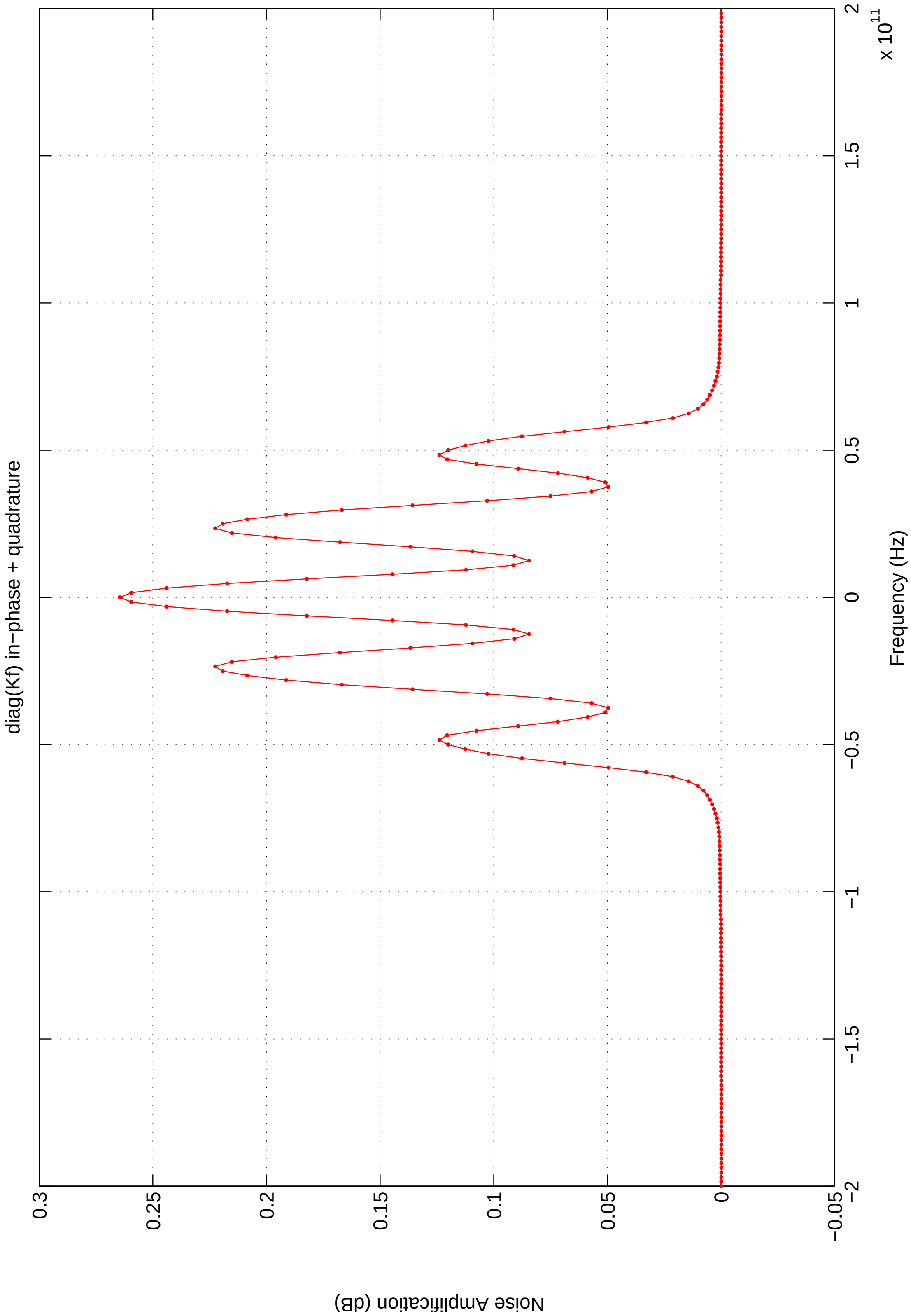

Figure 4.6: Modulated Carriers, single pulse, diag($\mathbf{K}_f(z = L)$): in-phase + quadrature
System parameters: # of channels: 5, Channel spacing: 25 GHz,
Symbol rate: 12.5 Gs/sec, Launch Power: 10 mW, α = *0.25 dB/km ,* β_2 = *-21.6 ps*^{2}*/km,*
β_3 = *0.128 ps*^{3}*/km,* γ = *1.2 1/(W·km), L : 80 km*

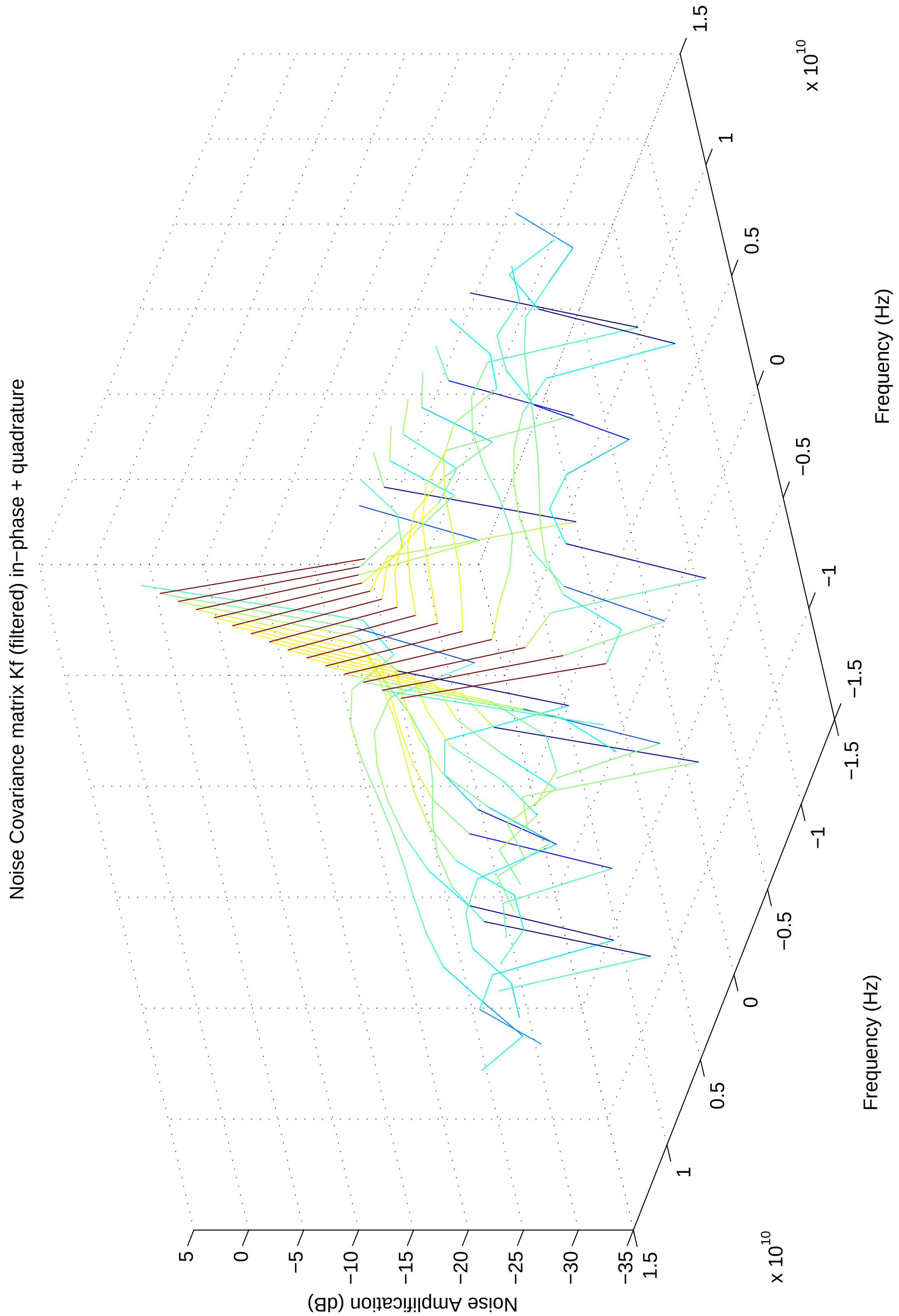

Figure 4.7: Modulated Carriers, single pulse, $\mathbf{K}_f(z = L)$ (filtered)
System parameters: # of channels: 5, Channel spacing: 25 GHz,
Symbol rate: 12.5 Gs/sec, Launch Power: 10 mW, α *= 0.25 dB/km ,* β_2 *= -21.6 ps*^{2}*/km,*
β_3 *= 0.128 ps*^{3}*/km,* γ *= 1.2 1/(W·km), L : 80 km*

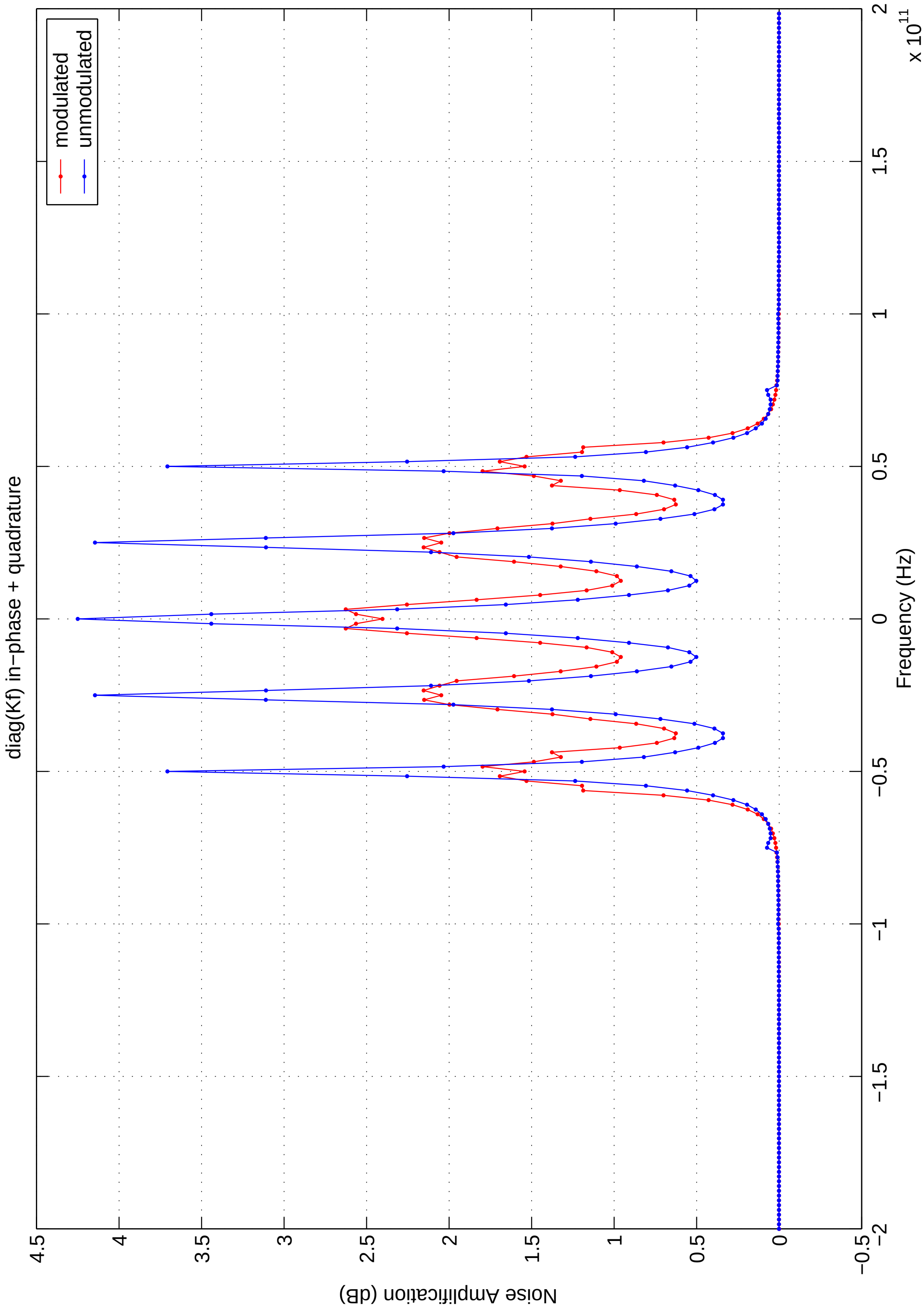

Figure 4.8: Comparison between unmodulated and modulated carriers, diag($\mathbf{K}_f(z = L)$): in-phase + quadrature
System parameters: # of channels: 5, Channel spacing: 25 GHz,
Symbol rate: 12.5 Gs/sec, Launch Power: 10 mW, α = *0.25 dB/km ,* β_2 = *-21.6 ps*^{2}*/km,* β_3 = *0.128 ps*^{3}*/km,* γ = *1.2 1/(W·km), L : 80 km*

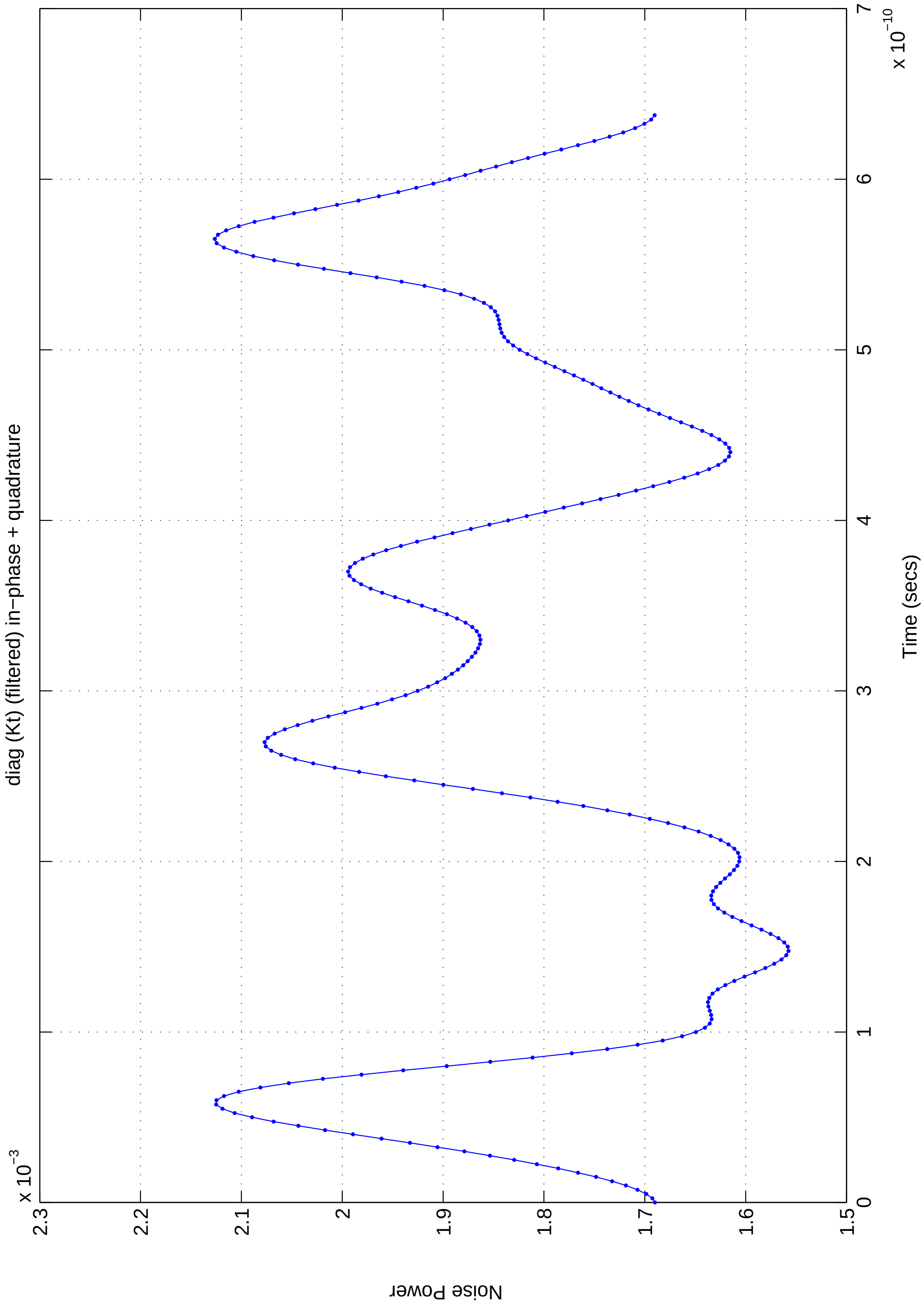

Figure 4.9: Modulated Carriers, random pulse stream, diag($\mathbf{K}_t(z = L)$)
System parameters: # of channels: 5, Channel spacing: 25 GHz,
Symbol rate: 12.5 Gs/sec, Launch Power: 10 mW, α *= 0.25 dB/km ,* β_2 *= -21.6* ps^2/km*,*
β_3 *= 0.128* ps^3/km*,* γ *= 1.2 1/(W·km), L : 80 km*

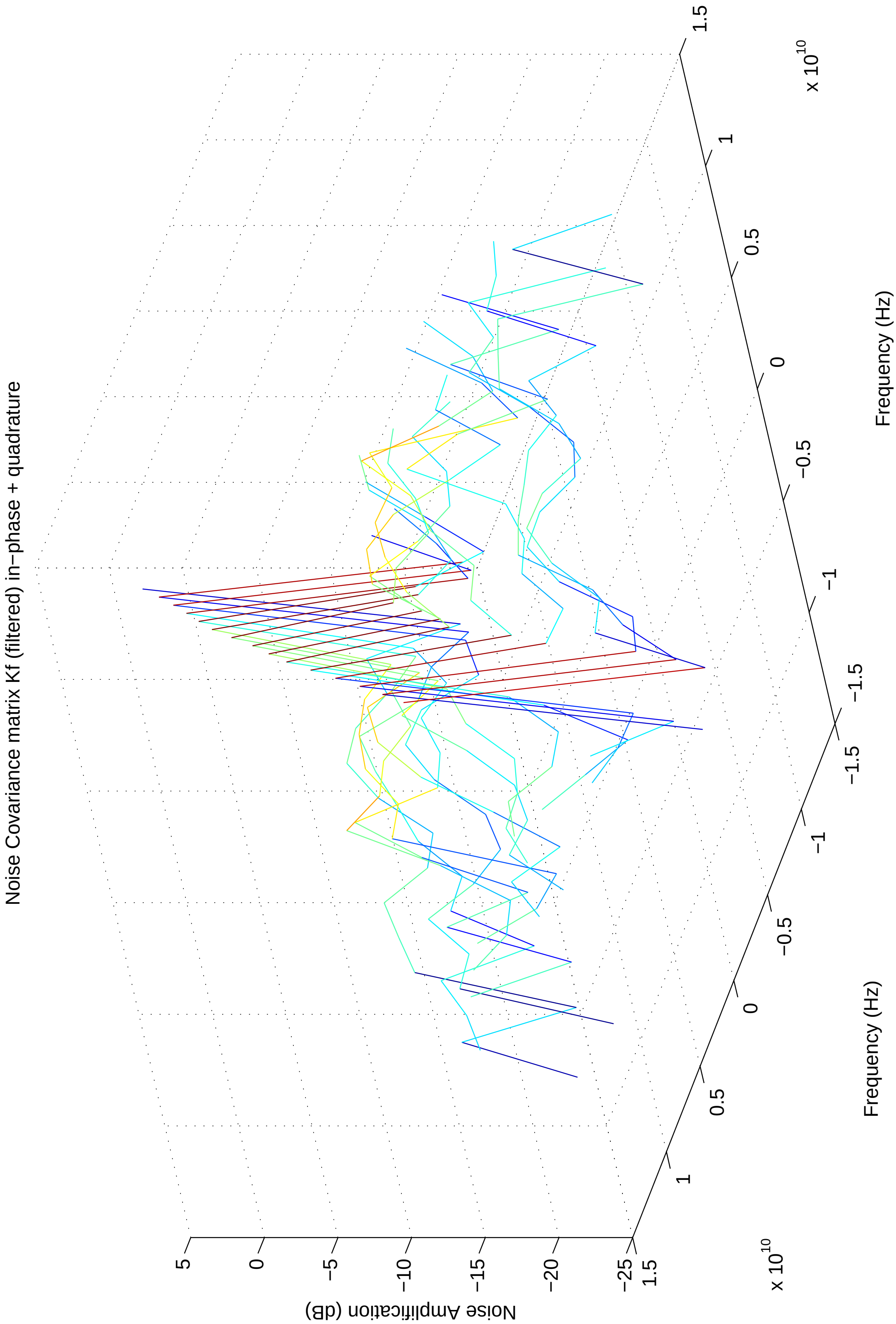

Figure 4.10: Modulated Carriers, random pulse stream, $\mathbf{K}_f(z = L)$ (filtered)
System parameters: # of channels: 5, Channel spacing: 25 GHz,
Symbol rate: 12.5 Gs/sec, Launch Power: 10 mW, α *= 0.25 dB/km ,* β_2 *= -21.6* ps^2/km*,*
β_3 *= 0.128* ps^3/km*,* γ *= 1.2 1/(W·km), L : 80 km*

Chapter 5

MODULATED CARRIER CASE BER CALCULATION

In chapter 4 we have developed mathematical formulations for noise propagation along the fiber for a single span OFCS. In this chapter we will supply noise propagation methodology for a multi-span WDM system and provide BER computation methodology for modulated carrier case.

5.1 BER Performance Evaluation Methodology

In this section we will provide BER evaluation methodology of an OFCS where the carriers are modulated. We will first supply the basic setup for data transmission and recovery. Then we will concentrate on covariance matrix propagation.

The transmitter models for BPSK and QPSK modulation schemes are shown in figures 5.1 and 5.1 respectively. In our case the pulse shaping function $p(t)$ is raised cosine pulse with roll-off factor taken to be 0.6. Note that the QPSK modulation is implemented such that the average power of the signal for both BPSK and QPSK modulation schemes after the transmitter is equal.

The determination of the symbol sequences at the receiver will be done by using differential detection which is done by comparing the phase differences between the subsequent signal samples to assign the symbol values. In our simulation we will use the constellation diagrams shown in figures 5.1 and 5.1 for BPSK and QPSK modulation schema respectively.

Likewise un-modulated carrier case we will evaluate the BER performance of the channel

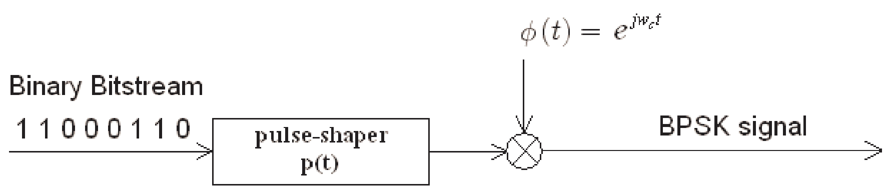

Figure 5.1: Conceptual transmitter structure for BPSK

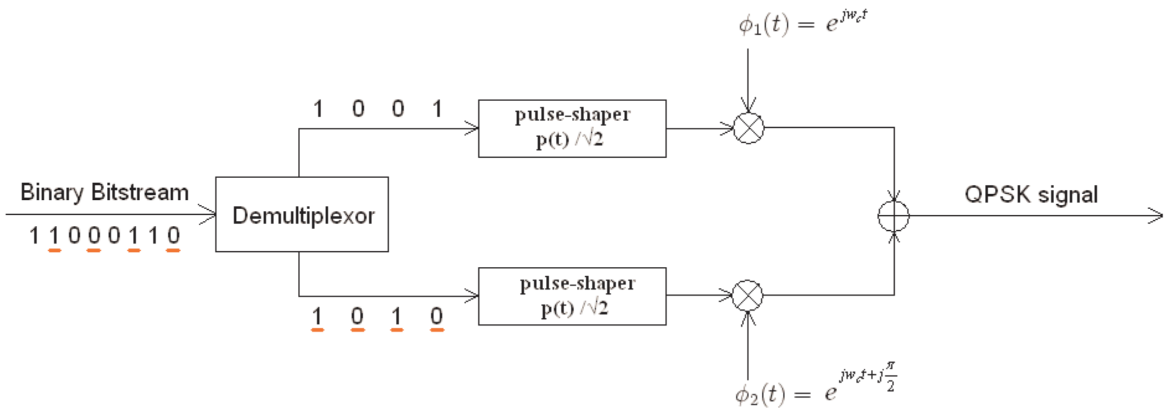

Figure 5.2: Conceptual transmitter structure for QPSK

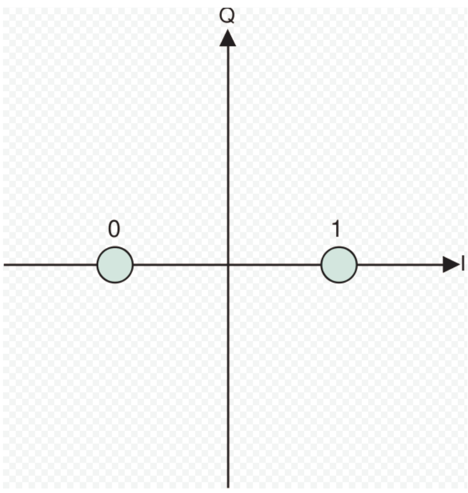

Figure 5.3: Constellation diagram for BPSK

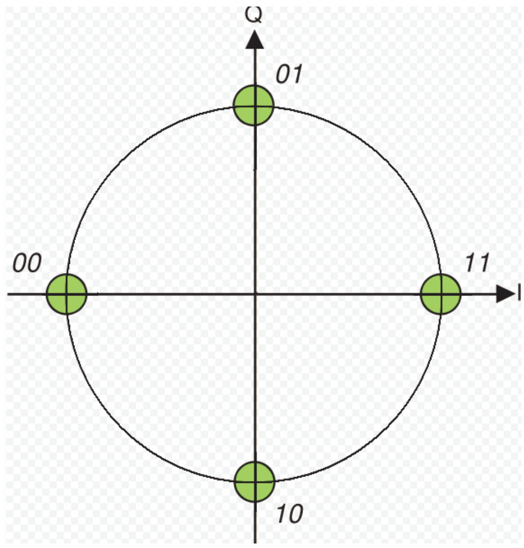

Figure 5.4: Constellation diagram for QPSK

that sits in the middle of the WDM spectrum. It is assumed that noise added by OAs is white Gaussian and has uncorrelated in-phase and quadrature components. Because a Gaussian process stays Gaussian in a linear system, we will assume that the noise impinging on the receiver is Gaussian as a result of linearization done in section 4.2.

A Gaussian process can be completely characterized by the first and second order statistical properties, i.e. mean and the correlation. In our case we will assume that noise impinging on the receiver is zero-mean Gaussian. In the un-modulated carrier case we have obtained the noise covariance matrix from the inverse Fourier transform of the noise power spectral density function. However, for the modulated carrier case, we have directly obtained a mathematical equation that describes the propagation of noise covariance matrix through the fiber as depicted by COVODE equation. Thus the solution of COVODE equation gives the required second order statistical properties of the noise.

In the analysis we will follow the following methodology in the evaluation of system BER value

- Find the complex noise covariance matrix, in frequency domain, $\mathbf{CF}(z)$ before filtering. We will apply dispersion compensation along the fiber. In our analysis we will assume that 95 % of dispersion is compensated at the OAs and the remaining dispersion is compensated at the receiver.

- Apply filtering, by using brick-wall filter, both on the large desired signal, $A(z,t)$, and the noise covariance matrix $\mathbf{CF}(z)$

- Compute the noise covariance matrix in time domain $\mathbf{CT}(z)$ by using the filtered $\mathbf{CF}(z)$ matrix

- Create a new noise covariance matrix, $\mathbf{CT_r}(z)$, such that it contains the covariances of noise samples seen by the receiver. Because for modulated carriers noise is unstationary, sampling time with sampling period plays very critical role for noise analysis. In our analysis we will assume that sampling is started from $t = 0$ and sampling period T_s is taken as $12.5GHz$. The $\mathbf{CT_r}(z)$ matrix will be created by considering these values.

- In time domain create large number of noise samples whose covariance matrix is $\mathbf{CT_r}(z)$ and add the created noise samples to the sampled output signal $A(z,t)$

- Compare the input and output bit sequence and count the number of errors

Let first define the matrices stated in the above procedure. We can represent the complex valued noise function, $a_c(z,t)$, as

$$a_c(z,t) = \mathbf{a}_r(z,t) + j\mathbf{a}_i(z,t) \tag{5.1}$$

where $\mathbf{a}_r(z,t)$ and $\mathbf{a}_i(z,t)$ are the in-phase and quadrature components of noise and $j = \sqrt{-1}$. The time dependency stated in equation 5.1 can be eliminated by using discretization as done in section 4.1

$$\mathbf{a_c(z)} \;=\; \begin{bmatrix} a(z,t_1) & a(z,t_2) & \cdots & a(z,t_{N_t}) \end{bmatrix}^{\dagger} \tag{5.2}$$

where $\mathbf{a_c(z)}$ is complex-valued vector function of z, † denotes matrix transpose operation and N_t is the total number of discrete time points taken between $[0, T_p)$, where T_p is the period of the signal envelope.

Because we discretizise the time and assumed that the input to the system is periodic we will use FFT operation to go back and forth between time domain and frequency domain.

Note that FFT operation actually corresponds to a matrix multiplication. Assuming that the FFT operation is denoted by $\mathfrak{F}$ matrix, in chapter 4 we defined the noise covariance matrix in frequency domain as

$$\begin{aligned}
\mathbf{K_f}(z) &= \mathrm{E}\left\{ \begin{bmatrix} \mathfrak{F}\mathbf{a}_r(z) \\ \mathfrak{F}\mathbf{a}_i(z) \end{bmatrix} \begin{bmatrix} (\mathfrak{F}\mathbf{a}_r(z))^* & (\mathfrak{F}\mathbf{a}_i(z))^* \end{bmatrix} \right\} \\
&= \begin{bmatrix} \mathfrak{F}\mathrm{E}[\mathbf{a}_r(z)\mathbf{a}_r(z)^\dagger]\mathfrak{F}^* & \mathfrak{F}\mathrm{E}[\mathbf{a}_r(z)\mathbf{a}_i(z)^\dagger]\mathfrak{F}^* \\ \mathfrak{F}\mathrm{E}[\mathbf{a}_i(z)\mathbf{a}_r(z)^\dagger]\mathfrak{F}^* & \mathfrak{F}\mathrm{E}[\mathbf{a}_i(z)\mathbf{a}_i(z)^\dagger]\mathfrak{F}^* \end{bmatrix} \\
&= \begin{bmatrix} \mathbf{K_f}^{rr}(z) & \mathbf{K_f}^{ri}(z) \\ \mathbf{K_f}^{ir}(z) & \mathbf{K_f}^{ii}(z) \end{bmatrix}
\end{aligned} \tag{5.3}$$

where $\mathbf{K_f}(z)$ denotes covariance matrix in frequency domain, $\mathbf{K_f^{rr}}(z)$, $\mathbf{K_f^{ri}}(z)$, $\mathbf{K_f^{ir}}(z)$ and $\mathbf{K_f^{ii}}(z)$ denotes the covariance matrices for noise in-phase component to the noise in-phase component, noise in-phase component to the noise quadrature component, noise quadrature component to the noise in-phase component and noise quadrature component to the noise quadrature component in frequency domain respectively, E is the expectation operator, $\mathfrak{F}$ is the FFT matrix, * denotes the complex conjugate transpose operation and † denotes matrix transpose operation.

We will use the following definition for the $\mathbf{CF}(z)$ matrix

$$\begin{aligned}
\mathbf{CF}(z) &= \mathrm{E}\left\{(\mathfrak{F}\mathbf{a_c}(z))(\mathfrak{F}\mathbf{a_c}(z))^*\right\} \\
&= \mathrm{E}\left\{(\mathfrak{F}\mathbf{a_r}(z) + j\mathfrak{F}\mathbf{a_i}(\mathbf{z}))((\mathfrak{F}\mathbf{a_r}(z))^* - j(\mathfrak{F}\mathbf{a_i}(z))^*\right\} \\
&= \mathfrak{F}\mathrm{E}[\mathbf{a_r}(z)\mathbf{a_r}(z)^\dagger]\mathfrak{F}^* - j\mathfrak{F}\mathrm{E}[\mathbf{a_r}(z)\mathbf{a_i}(z)^\dagger]\mathfrak{F}^* + j\mathfrak{F}\mathrm{E}[\mathbf{a_i}(z)\mathbf{a_r}(z)^\dagger]\mathfrak{F}^* + \mathfrak{F}\mathrm{E}[\mathbf{a_i}(z)\mathbf{a_i}(z)^\dagger]\mathfrak{F}^*
\end{aligned} \tag{5.4}$$

where E is the expectation operator, $\mathfrak{F}$ is the FFT matrix, * denotes the complex conjugate transpose operation and † denotes matrix transpose operation. By using the matrix definitions in equation 5.3, $\mathbf{CF}(z)$ matrix can be written as

$$\mathbf{CF}(z) = \mathbf{K_f^{rr}}(z) - j\mathbf{K_f^{ri}}(z) + j\mathbf{K_f^{ir}}(z) + \mathbf{K_f^{ii}}(z) \tag{5.5}$$

Dispersion compensation will be applied as follows:

- We will first obtain the dispersion matrix, that characterizes the dispersion along the fiber span, by using the solution of the NLSE equation, stated in 2.1,by ignoring attenuation, α, and non-linearity, γ.
- At the end of the fiber we will reverse the effect of dispersion by multiplying the signal envelope and the noise, which will affect the covariance matrix, with the inverse dispersion matrix.

If we rewrite the NLSE equation by setting $\alpha = 0$ and $\gamma = 0$ we obtain:

$$\frac{\partial A(z,t)}{\partial z} = -j\frac{1}{2}\beta_2\frac{\partial^2 A(z,t)}{\partial t^2} + \frac{1}{6}\beta_3\frac{\partial^3 A(z,t)}{\partial t^3} \tag{5.6}$$

where $A(z,t)$ is the signal envelope and β_2 and β_3 are dispersion parameters. Note that 5.21 is a linear partial differential equation and can be solved analytically. The solution can be found in frequency domain rather than in time domain as follows

$$\begin{aligned} \mathcal{F}\left\{\frac{\partial A(z,t)}{\partial z}\right\} &= \mathcal{F}\left\{-j\frac{1}{2}\beta_2\frac{\partial^2 A(z,t)}{\partial t^2} + \frac{1}{6}\beta_3\frac{\partial^3 A(z,t)}{\partial t^3}\right\} \\ \Longrightarrow \frac{\partial A(z,w)}{\partial z} &= \frac{1}{2}jw^2\beta_2 A(z,w) - \frac{1}{6}jw^3\beta_3 A(z,w) \\ \Longrightarrow \frac{\partial A(z,w)}{\partial z} &= \left\{\frac{1}{2}jw^2\beta_2 - \frac{1}{6}jw^3\beta_3\right\} A(z,w) \\ \Longrightarrow A(z,w) = \exp &\left(\left\{\frac{1}{2}jw^2\beta_2 - \frac{1}{6}jw^3\beta_3\right\} z\right) A(z=0,w) \end{aligned} \tag{5.7}$$

where $\mathcal{F}$ denotes Fourier transform and w represents the Fourier frequency. Note that we did not use any discretization in the solution of 5.7. By applying discretization, with respect to time as done in chapter 4, we will eliminate the time dependency of the signal. Also we will be able to use FFT operation for the Fourier transform. Let assume that the input envelope, which is complex valued, is discretizied as

$$\mathbf{A}(\mathbf{z}) = \begin{bmatrix} A(z,t_1) & A(z,t_2) & \cdots & a(A,t_{N_t}) \end{bmatrix}^{\dagger} \tag{5.8}$$

where † denotes matrix transpose operation and N_t is the total number of discrete time points. Then the discrete Fourier transform of $\mathbf{A}(z)$ becomes:

$$\begin{aligned}\mathcal{A}(z) &= \mathfrak{F}\left\{\begin{bmatrix} A(z,t_1) & A(z,t_2) & \cdots & A(z,t_{N_t})\end{bmatrix}^{\dagger}\right\} \\ &= \begin{bmatrix} A(z,w_1) & A(z,w_2) & \cdots & A(z,w_{N_t})\end{bmatrix}^{\dagger}\end{aligned} \tag{5.9}$$

where $\mathfrak{F}$ is the FFT matrix, † denotes matrix transpose operation and w_i, $i\ \epsilon\{1, 2, \cdots, N_t\}$, denotes the discrete Fourier frequencies. By using 5.9 we can rewrite the equation in the solution of 5.7

$$\frac{\partial A(z,w)}{\partial z} = \left\{\frac{1}{2}jw^2\beta_2 - \frac{1}{6}jw^3\beta_3\right\} A(z,w) \tag{5.10}$$

as

$$\frac{\partial}{\partial z}\begin{pmatrix} A(z,w_1) \\ A(z,w_2) \\ \vdots \\ A(z,w_{N_t}) \end{pmatrix} = \begin{pmatrix} \frac{1}{2}jw_1^2\beta_2 - \frac{1}{6}jw_1^3\beta_3 & 0 & \cdots & 0 \\ 0 & \frac{1}{2}jw_2^2\beta_2 - \frac{1}{6}jw_2^3\beta_3 & \cdots & 0 \\ \vdots & \vdots & \ddots & \vdots \\ 0 & 0 & \cdots & \frac{1}{2}jw_{N_t}^2\beta_2 - \frac{1}{6}jw_{N_t}^3\beta_3 \end{pmatrix}\begin{pmatrix} A(z,w_1) \\ A(z,w_2) \\ \vdots \\ A(z,w_{N_t}) \end{pmatrix} \tag{5.11}$$

We can rewrite 5.11 as

$$\dot{\mathcal{X}}(z) = \mathcal{D}\mathcal{X}(z) \tag{5.12}$$

where $^{\cdot}$ denotes $\frac{\partial}{\partial z}$ and

$$\mathcal{X}(z) = \begin{pmatrix} A(z,w_1) \\ A(z,w_2) \\ \vdots \\ A(z,w_{N_t}) \end{pmatrix}$$

and (5.13)

$$\mathcal{D} = \begin{pmatrix} \frac{1}{2}jw_1^2\beta_2 - \frac{1}{6}jw_1^3\beta_3 & 0 & \cdots & 0 \\ 0 & \frac{1}{2}jw_2^2\beta_2 - \frac{1}{6}jw_2^3\beta_3 & \cdots & 0 \\ \vdots & \vdots & \ddots & \vdots \\ 0 & 0 & \cdots & \frac{1}{2}jw_{N_t}^2\beta_2 - \frac{1}{6}jw_{N_t}^3\beta_3 \end{pmatrix}$$

The solution of 5.12 is

$$\mathcal{X}(z) = \exp(\mathcal{D}z)\mathcal{X}(z=0) \tag{5.14}$$

5.14 states the solution of NLSE equation by just taking the dispersion into account. Thus the $\exp(\mathcal{D}z)$ matrix denotes the effect of dispersion on the system. At the end of the fiber we will use the inverse of the $\exp(\mathcal{D}z)$ matrix, which is the $\exp(-\mathcal{D}z)$ matrix [6], to eliminate the dispersion effect. Note that we found the solution in frequency domain. Thus, in order to apply dispersion compensation we have to go frequency domain from time domain.

Because the $\mathcal{D}$ matrix is diagonal, thus $-\mathcal{D}z$, the $\exp(-\mathcal{D}z)$ matrix is simply the diagonal matrix where the diagonal elements are the exponentials of the diagonal elements of the $-\mathcal{D}z$ matrix. That is

$$\exp(-\mathcal{D}z) = \begin{pmatrix} \exp(-\frac{1}{2}jw_1^2\beta_2 + \frac{1}{6}jw_1^3\beta_3) & 0 & \cdots & 0 \\ 0 & \exp(-\frac{1}{2}jw_2^2\beta_2 + \frac{1}{6}jw_2^3\beta_3) & \cdots & 0 \\ \vdots & \vdots & \ddots & \vdots \\ 0 & 0 & \cdots & \exp(-\frac{1}{2}jw_{N_t}^2\beta_2 + \frac{1}{6}jw_{N_t}^3\beta_3) \end{pmatrix} \tag{5.15}$$

The complex conjugate of the dispersion compensation matrix, $\exp(-\mathcal{D}z)^*$, is

$$\begin{aligned}\exp(-\mathcal{D}z)^* &= \begin{pmatrix} \exp(\frac{1}{2}jw_1^2\beta_2 - \frac{1}{6}jw_1^3\beta_3) & 0 & \cdots & 0 \\ 0 & \exp(\frac{1}{2}jw_2^2\beta_2 - \frac{1}{6}jw_2^3\beta_3) & \cdots & 0 \\ \vdots & \vdots & \ddots & \vdots \\ 0 & 0 & \cdots & \exp(\frac{1}{2}jw_{N_t}^2\beta_2 - \frac{1}{6}jw_{N_t}^3\beta_3) \end{pmatrix} \\ &= \exp(\mathcal{D}z)\end{aligned} \tag{5.16}$$

where * denotes complex conjugate operation. In the derivation of 5.16 we used the identity $\exp(jw)^* = \exp(-jw)$. From 5.16 we observe that the conjugate of dispersion compensation matrix, $\exp(-\mathcal{D}z)^*$, is simply $\exp(\mathcal{D}z)$. We will use this property in the computation of dispersion compensated noise covariance matrix.

For a single-span WDM system, we will apply the following operations on the discretized envelope signal, $\mathbf{A}(\mathbf{z})$, to eliminate dispersion

- first go to frequency domain by using FFT matrix

- multiply by $\exp(-\mathcal{D}z)$ for dispersion elimination

- go to time domain by using inverse FFT matrix

By following the above steps we find the dispersion eliminated envelope signal as

$$\mathbf{A_{dc}(z)} = \mathfrak{F}^{-\mathbf{1}}[\exp(-\mathcal{D}z)\mathfrak{F}\{\mathbf{A(z)}\}] \tag{5.17}$$

where $\mathbf{A_{dc}(z)}$ is the dispersion compensated envelope signal and $\mathfrak{F}$ denotes FFT matrix and $\mathfrak{F}^{-\mathbf{1}}$ denotes inverse FFT matrix.

For the noise signal we will apply the same steps stated above. However, because we are mainly interested in noise characteristics rather than the noise itself, we will find the dispersion compensated noise covariance matrix and use it for further computations. Assuming that there is only one span in the fiber link, the noise covariance matrix after the dispersion compensation becomes

$$\begin{aligned}
\mathbf{K_f^{dc}}(z) &= \mathrm{E}\left\{\begin{bmatrix}\exp(-\mathcal{D}z)\mathfrak{F}\mathbf{a}_r(z)\\ \exp(-\mathcal{D}z)\mathfrak{F}\mathbf{a}_i(z)\end{bmatrix}\begin{bmatrix}(\exp(-\mathcal{D}z)\mathfrak{F}\mathbf{a}_r(z))^* & (\exp(-\mathcal{D}z)\mathfrak{F}\mathbf{a}_i(z))^*\end{bmatrix}\right\}\\
&= \begin{bmatrix}\exp(-\mathcal{D}z) & \mathcal{Z}\\ \mathcal{Z} & \exp(-\mathcal{D}z)\end{bmatrix}\underbrace{\begin{bmatrix}\mathfrak{F}\mathrm{E}[\mathbf{a}_r(z)\mathbf{a}_r(z)^\dagger]\mathfrak{F}^* & \mathfrak{F}\mathrm{E}[\mathbf{a}_r(z)\mathbf{a}_i(z)^\dagger]\mathfrak{F}^*\\ \mathfrak{F}\mathrm{E}[\mathbf{a}_i(z)\mathbf{a}_r(z)^\dagger]\mathfrak{F}^* & \mathfrak{F}\mathrm{E}[\mathbf{a}_i(z)\mathbf{a}_i(z)^\dagger]\mathfrak{F}^*\end{bmatrix}}_{\mathbf{K_f}(z)}\begin{bmatrix}\exp(\mathcal{D}z) & \mathcal{Z}\\ \mathcal{Z} & \exp(\mathcal{D}z)\end{bmatrix}\\
&= \begin{bmatrix}\exp(-\mathcal{D}z) & \mathcal{Z}\\ \mathcal{Z} & \exp(-\mathcal{D}z)\end{bmatrix}\mathbf{K_f}(z)\begin{bmatrix}\exp(\mathcal{D}z) & \mathcal{Z}\\ \mathcal{Z} & \exp(-\mathcal{D}z)\end{bmatrix}
\end{aligned} \tag{5.18}$$

where E is the statistical expectation operator, $\mathcal{Z}$ is the zero matrix with size equal to $\mathcal{D}$ matrix and $\mathbf{K_f^{dc}}(z)$ and $\mathbf{K_f}(z)$ are frequency domain noise covariance matrices after and before dispersion compensation respectively. In the derivation of 5.18 we used the identity $\exp(-\mathcal{D}z)^* = \exp(\mathcal{D}z)$ which is derived before. Note that because the dispersion compensation matrices are diagonal and $\exp(-\mathcal{D}z)^* = \exp(\mathcal{D}z)$, the multiplication of the noise covariance matrix with dispersion compensation matrices from left and right, as depicted by 5.18, has no effect on the power characteristics of the noise.

For a single span WDM system, dispersion compensation is straightforward and the process is stated above. For multi-span WDM link we have to propagate the large desired signal, $A(z,t)$ and the noise covariance, $\mathbf{K}(z)$, along the fiber and apply dispersion compensation at each OA. We will now present covariance matrix propagation methodology along the fiber.

To compute the noise covariance matrix at the end of the fiber link we will apply the following algorithm

- Set initial time domain noise covariance matrix to zero matrix: $\mathbf{K_{tp}(z)} \longleftarrow 0$
- For each span
  - Add OAs noise covariance matrix, $\mathbf{I}$, to the noise covariance matrix obtained from the previous span, $\mathbf{K_{tp}}(z)$.That is $\mathbf{K_{tn}(z)} \longleftarrow \mathbf{K_{tp}}(z) + \mathbf{I}$, where $\mathbf{I}$ denotes identity matrix.
  - Solve the COVODE equation with initial condition $\mathbf{K_{tn}}(z)$ to obtain $\mathbf{K_{tn}}(z+L)$, noise covariance matrix at the end of the span.
  - Compute frequency domain covariance matrix $\mathbf{K_{fn}}(z+L)$ from $\mathbf{K_{tn}}(z+L)$
  - Apply dispersion compensation on $\mathbf{K_{fn}}(z+L)$ to obtain $\mathbf{K^{dc}_{fn}}(z+L)$, dispersion compensated noise covariance matrix
  - Apply amplification on $\mathbf{K^{dc}_{fn}}(z+L)$ and obtain $\mathbf{K^{dca}_{fn}}(z+L)$, attenuation eliminated covariance matrix
  - Compute time domain covariance matrix $\mathbf{K^{dca}_{tn}}(z+L)$ from $\mathbf{K^{dca}_{fn}}(z+L)$
  - Update the previous $\mathbf{K^{p}_{t}}(z)$ matrix as $\mathbf{K^{p}_{t}}(z) \longleftarrow \mathbf{K^{dca}_{tn}}(z+L)$
- Apply dispersion compensation to the noise covariance matrix - Receiver

In the above algorithm we explicitly assume that

- The noise added by different OAs are uncorrelated.
- The noise added by each OA has un-correlated in-phase and quadrature components. This is characterized by adding identity, $\mathbf{I}$, matrix that is added at each OA.

Also in the algorithm we split out the dispersion compensation into to parts

- Dispersion compensation at the amplifier site will eliminate the 95% dispersion along the span
- Dispersion compensation at the receiver site will eliminate the total remaining dispersion along the fiber link.

We found the effect of dispersion on the system by solving the NLSE equation by setting α and γ parameters to zero and supplied the solution in vector form by 5.14 and stated that the $\exp(\mathcal{D}z)$ matrix, where $\mathcal{D}$ is given by 5.13, denotes dispersion effect on the system. For a single span fiber link we applied the dispersion compensation as shown by 5.18. For multi-span fiber link we will apply the same methodology shown by 5.18 with a slight change. Dispersion compensation at the amplifier site will be applied as

$$\mathbf{K}_{\mathbf{f}}^{\mathbf{dc}}(z=L) = \begin{bmatrix} \exp(-\mathcal{D}z) & \mathcal{Z} \\ \mathcal{Z} & \exp(-\mathcal{D}z) \end{bmatrix}_{z=0.95\cdot L} \mathbf{K}_{\mathbf{f}}(z=L) \begin{bmatrix} \exp(\mathcal{D}z) & \mathcal{Z} \\ \mathcal{Z} & \exp(\mathcal{D}z) \end{bmatrix}_{z=0.95\cdot L} \tag{5.19}$$

where L is the span length and $\mathbf{K}_{\mathbf{f}}^{\mathbf{dc}}(z=L)$ and $\mathbf{K}_{\mathbf{f}}(z=L)$ are the frequency domain covariance matrices after and before dispersion compensation respectively and $\mathcal{Z}$ is the zero matrix whit size equal to size of $\exp(\mathcal{D}z)$ matrix.

At the receiver site, assuming that the accumulated noise covariance matrix in frequency domain is $\mathbf{K}_{\mathbf{f}}(z)|_{z=N\cdot L}$, we will apply dispersion compensation as

$$\mathbf{K}_{\mathbf{f}}^{\mathbf{dc}}(z=N\cdot L) = \begin{bmatrix} \exp(-\mathcal{D}z) & \mathcal{Z} \\ \mathcal{Z} & \exp(-\mathcal{D}z) \end{bmatrix}_{z=0.05\cdot N\cdot L} \mathbf{K}_{\mathbf{f}}(z=N\cdot L) \begin{bmatrix} \exp(\mathcal{D}z) & \mathcal{Z} \\ \mathcal{Z} & \exp(\mathcal{D}z) \end{bmatrix}_{z=0.05\cdot N\cdot L} \tag{5.20}$$

where N is the number of spans, L is the span length and $\mathbf{K}_{\mathbf{f}}^{\mathbf{dc}}(z=N\cdot L)$ and $\mathbf{K}_{\mathbf{f}}(z=N\cdot L)$ are the frequency domain covariance matrices after and before dispersion compensation respectively and $\mathcal{Z}$ is the zero matrix whit size equal to size of $\exp(\mathcal{D}z)$ matrix.

To eliminate the attenuation effect we will first find the attenuation effect on the system and apply the same methodology as done for dispersion compensation. We will find the attenuation effect on the system by solving the NLSE equation by just taking the α parameter and setting β_2, β_3, and γ to zero. That is

$$\begin{aligned}&\frac{\partial A(z,t)}{\partial z} = -\alpha A(z,t)\\&\Rightarrow A(z,t) = \exp(-\alpha z)A(z=0,t)\end{aligned} \tag{5.21}$$

where $A(z,t)$ denotes large desired signal and α is the attenuation constant. To eliminate the attenuation we will multiply the large desired signal and the noise with $\exp(\alpha z)|_{z=L}$ at the end of each span. After the amplification noise covariance matrix becomes

$$\begin{aligned}\mathbf{K}_{\mathbf{f}}^{\mathbf{amp}}(z) &= \mathrm{E}\left\{\begin{bmatrix}\mathfrak{F}\exp(\alpha z)\mathbf{a}_r(z)\\ \mathfrak{F}\exp(\alpha z)\mathbf{a}_i(z)\end{bmatrix}\begin{bmatrix}(\mathfrak{F}\exp(\alpha z)\mathbf{a}_r(z))^* & (\mathfrak{F}\exp(\alpha z)\mathbf{a}_i(z))^*\end{bmatrix}\right\}\\ &= \exp(\alpha z)\underbrace{\begin{bmatrix}\mathfrak{F}\mathrm{E}[\mathbf{a}_r(z)\mathbf{a}_r(z)^\dagger]\mathfrak{F}^* & \mathfrak{F}\mathrm{E}[\mathbf{a}_r(z)\mathbf{a}_i(z)^\dagger]\mathfrak{F}^*\\ \mathfrak{F}\mathrm{E}[\mathbf{a}_i(z)\mathbf{a}_r(z)^\dagger]\mathfrak{F}^* & \mathfrak{F}\mathrm{E}[\mathbf{a}_i(z)\mathbf{a}_i(z)^\dagger]\mathfrak{F}^*\end{bmatrix}}_{\mathbf{K}_{\mathbf{f}}(z)}\exp(\alpha z)\\ &= \exp(2\alpha z)\mathbf{K}_{\mathbf{f}}(z)\end{aligned} \tag{5.22}$$

where $\mathbf{K}_{\mathbf{f}}^{\mathbf{amp}}(z)$ and $\mathbf{K}_{\mathbf{f}}(z)$ are the frequency domain covariance matrices after and before amplification respectively.

The algorithm for the large desired signal, $A(z,t)$, propagation is as follows

- Initialize $A(z=0,t)$
- For each span
  - Solve the NLSE equation with initial condition $A(z=0,t)$ to find $A(z=L,t)$
  - Apply dispersion compensation on $A(z=L,t)$ - Amplifier
  - Apply amplification on $A(z=L,t)$
  - Set $A(z=0,t) \Leftarrow A(z=L,t)$
- Apply dispersion compensation on $A(z=0,t)$ - Receiver

For single-span WDM system we supplied the dispersion compensation equation in 5.17. For multi-span WDM system we will use the same equation with slight change. At the amplifier site we will apply 95 % dispersion compensation and eliminate the remaining dispersion at the receiver site. Application of dispersion compensation at the amplifier site results in

$$\mathbf{A}^{\mathbf{dc}}(z = L) = \mathfrak{F}^{-1}[\exp(-\mathcal{D}z)|_{z=0.95 \cdot L}\mathfrak{F}\{\mathbf{A}(z = L)\}] \tag{5.23}$$

where $\mathbf{A}^{\mathbf{dc}}(z = L)$ is the dispersion compensated large desired signal at the end of the span, L denotes the span length, $\mathfrak{F}$ denotes the FFT matrix and $^{-1}$ denotes matrix inverse. Assuming that the large desired signal at the receiver is $\mathbf{A}(z)|_{z=N \cdot L}$, dispersion compensation at the receiver will be applied as

$$\mathbf{A}^{\mathbf{dc}}(z = N \cdot L) = \mathfrak{F}^{-1}[\exp(-\mathcal{D}z)|_{z=0.05 \cdot N \cdot L}\mathfrak{F}\mathbf{A}(z = N \cdot L)] \tag{5.24}$$

where $\mathbf{A}^{\mathbf{dc}}(z = N \cdot L)$ is the dispersion compensated large desired signal, L denotes the span length, N denotes the span number, $\mathfrak{F}$ denotes the FFT matrix and $^{-1}$ denotes matrix inverse.

To obtain the desired channel's signal envelope, we will apply filtering at the receiver site. If we denote the matrix χ for filtering operation, the noise covariance matrix after filtering becomes

$$\begin{aligned}
\mathbf{K}_{\mathbf{f}}^{\mathbf{f}}(z) &= \mathrm{E}\left\{ \begin{bmatrix} \chi\mathfrak{F}\mathbf{a}_r(z) \\ \chi\mathfrak{F}\mathbf{a}_i(z) \end{bmatrix} \begin{bmatrix} (\chi\mathfrak{F}\mathbf{a}_r(z))^* & (\chi\mathfrak{F}\mathbf{a}_i(z))^* \end{bmatrix} \right\} \\
&= \begin{bmatrix} \chi & \mathcal{Z} \\ \mathcal{Z} & \chi \end{bmatrix} \underbrace{\begin{bmatrix} \mathfrak{F}\mathrm{E}[\mathbf{a}_r(z)\mathbf{a}_r(z)^\dagger]\mathfrak{F}^* & \mathfrak{F}\mathrm{E}[\mathbf{a}_r(z)\mathbf{a}_i(z)^\dagger]\mathfrak{F}^* \\ \mathfrak{F}\mathrm{E}[\mathbf{a}_i(z)\mathbf{a}_r(z)^\dagger]\mathfrak{F}^* & \mathfrak{F}\mathrm{E}[\mathbf{a}_i(z)\mathbf{a}_i(z)^\dagger]\mathfrak{F}^* \end{bmatrix}}_{\mathbf{K}_{\mathbf{f}}(z)} \begin{bmatrix} \chi & \mathcal{Z} \\ \mathcal{Z} & \chi \end{bmatrix} \\
&= \begin{bmatrix} \chi & \mathcal{Z} \\ \mathcal{Z} & \chi \end{bmatrix} \mathbf{K}_{\mathbf{f}}(z) \begin{bmatrix} \chi & \mathcal{Z} \\ \mathcal{Z} & \chi \end{bmatrix}
\end{aligned} \tag{5.25}$$

where E is the statistical expectation operator, and $\mathbf{K}_{\mathbf{f}}^{\mathbf{f}}(z)$ and $\mathbf{K}_{\mathbf{f}}(z)$ are the frequency domain covariance matrices after and before filtering respectively. Note that all the variables in 5.25 are in frequency domain. We will use brick-wall filter in our simulations.

In the propagation of covariance matrix and in order to generate noise samples we have to find the noise covariances in time domain. We will use the following formula, which is given in chapter 4, to go back and forth between time and frequency domain covariance matrices:

$$\begin{aligned}\mathbf{K_f}(z) &= \mathrm{E}\left\{\begin{bmatrix}\mathfrak{F}\mathbf{a}_r(z)\\ \mathfrak{F}\mathbf{a}_i(z)\end{bmatrix}\begin{bmatrix}(\mathfrak{F}\mathbf{a}_r(z))^* & (\mathfrak{F}\mathbf{a}_i(z))^*\end{bmatrix}\right\}\\ &= \begin{bmatrix}\mathfrak{F} & 0\\ 0 & \mathfrak{F}\end{bmatrix}\underbrace{\begin{bmatrix}\mathrm{E}[\mathbf{a}_r(z)\mathbf{a}_r(z)^\dagger] & \mathrm{E}[\mathbf{a}_r(z)\mathbf{a}_i(z)^\dagger]\\ \mathrm{E}[\mathbf{a}_i(z)\mathbf{a}_r(z)^\dagger] & \mathrm{E}[\mathbf{a}_i(z)\mathbf{a}_i(z)^\dagger]\end{bmatrix}}_{\mathbf{K_t}(z)}\begin{bmatrix}\mathfrak{F}^* & 0\\ 0 & \mathfrak{F}^*\end{bmatrix}\end{aligned} \tag{5.26}$$

where $\mathbf{K_f}(z)$ and $\mathbf{K_t}(z)$ denotes frequency and time domain covariance matrices and $\mathfrak{F}$ denotes FFT matrix. Equation 5.26 gives a formula to compute the frequency domain covariance matrix by using the time domain covariance matrix. Also by using inverse Fourier transform (inverse FFT) we will use the equation 5.26 to compute the time domain covariance matrix from the frequency domain covariance matrix.

5.2 Noise Generation

Let assume that $\mathbf{K_t^{dcaf}}(z = N \cdot L)$ denotes the dispersion compensated, amplified and filtered noise covariance matrix in time domain. To generate noise samples we will compute the $\mathbf{CT}(z = N \cdot L)$, block noise covariance matrix, from $\mathbf{K_t^{dcaf}}(z = N \cdot L)$. Note that $\mathbf{CT}(z = N \cdot L)$ contains the covariances of all noise samples observed between $[0, T_p)$, where T_p is the signal period. In order to create sample noise values, we need to extract the covariances of noise samples that are seen by the receiver. For modulated carrier case, noise after the filtering is non-stationary as depicted in figure 4.10. Thus the sampling instance, with sampling period, plays a critical role in noise generation. In our analysis we will create the sampled noise covariance matrix with respect to time, $t = 0$ and take the symbol rate to be 12.5 Gs/sec. For the un-modulated carrier case, noise after the filtering is stationary as observed from the figure 4.4 implying that covariances of noise samples depends only on the sampling period not sampling instance.

We can create the sampled noise covariance matrix by extracting the covariances from $\mathbf{CT}(z = N \cdot L)$ matrix. Let define $\mathbf{CT_r}$ as the sampled noise covariance matrix. Note that

$\mathbf{CT_r}$ is complex valued and hermitian. Also note that while $\mathbf{CT}(z = N \cdot L)$, is 256×256, the sampled covariance matrix, $\mathbf{CT_r}$, is 8×8.

We will use $\mathbf{CT_r}$ to create correlated noise samples. We will assume that the noise impinging on the receiver is zero-mean Gaussian process. Let define the complex noise vector, n, impinging on the receiver as

$$\mathbf{n} = \mathbf{n_r} + j\mathbf{n_i} \tag{5.27}$$

where $\mathbf{n_r}$ and $\mathbf{n_i}$ are un-correlated zero-mean Gaussian noise vectors and $j = \sqrt{-1}$. To correlate noise samples let multiply the noise vector $\mathbf{n}$, by the matrix Q such that $\mathrm{E}[(Qn)(Qn)^*] = \mathbf{CT_r}$. We can find the Q matrix as follows

$$\begin{aligned}
\mathbf{CT_r} &= \mathrm{E}[(Q\mathbf{n})(Q\mathbf{n})^*] \\
&= \mathrm{E}[(Q(\mathbf{n_r} + j\mathbf{n_i}))(Q(\mathbf{n_r} + j\mathbf{n_i}))^*] \\
&= \mathrm{E}[Q(\mathbf{n_r}\mathbf{n_r}^* - j\mathbf{n_r}\mathbf{n_i}^* + j\mathbf{n_i}\mathbf{n_r}^* + \mathbf{n_i}\mathbf{n_i}^*)Q^*] \\
&= Q(\underbrace{\mathrm{E}[\mathbf{n_r}\mathbf{n_r}^*]}_{\text{Identity Matrix}} - j\underbrace{\mathrm{E}[\mathbf{n_r}\mathbf{n_i}^*]}_{\text{Zero Matrix}} + + j\underbrace{\mathrm{E}[\mathbf{n_i}\mathbf{n_r}^*]}_{\text{Zero Matrix}} + \underbrace{\mathrm{E}[\mathbf{n_i}\mathbf{n_i}^*]}_{\text{Identity Matrix}})Q^* \\
&= 2QQ^*
\end{aligned} \tag{5.28}$$

where E denotes statistical expectation operator.

To find the Q matrix such that $\mathbf{CT_r} = 2QQ^*$ we will use the SVD theorem. SVD theorem states that any complex valued matrix M, can be decomposed into three matrices U, Λ and V such that [26]

$$M = U\Lambda V^* \tag{5.29}$$

where U and V are unitary matrices, Λ is a diagonal matrix with positive entries and * denotes complex conjugate transpose operation. For Hermitian matrices $U = V$.

By using SVD we can find we can find such U, Λ and V matrices so that $\mathbf{CT_r} = U\Lambda V^*$. If we set the Q matrix to $Q = U\sqrt{\frac{\Lambda}{2}}V^*$ we ensure that $\mathbf{CT_r} = 2QQ^*$ holds. That is

$$
\begin{aligned}
&Q = U\sqrt{\frac{\Lambda}{2}}V^* \\
&\Rightarrow QQ^* = (U\sqrt{\frac{\Lambda}{2}}V^*)(U\sqrt{\frac{\Lambda}{2}}V^*)^* \\
&= U\sqrt{\frac{\Lambda}{2}} \underbrace{V^*V}_{textIdentityMatrix} \sqrt{\frac{\Lambda}{2}}U^* \\
&= U\Lambda U^* = U\Lambda V^* \\
&= \mathbf{CT_r}
\end{aligned} \tag{5.30}
$$

To compute the system BER value we will create large number of random noise vectors, multiply the created noise vectors by the Q matrix to correlate them, add the correlated noise vectors to the sampled large signal $A(z,t)$ vector, determine the symbol sequence at the receiver, compare the symbol sequence with the symbol sequence transmitted, count the number of symbol errors and divide the number of symbol errors to the total number of symbols used in the simulation to find the system's SER. Note that while the BER value for DBPSK modulation scheme is same as the SER value, for DQPSK modulation scheme because there are 2 bits for each symbol, BER value is half of the SER value.

5.3 Simulation Results

In this section we will provide the simulation results that show system BER value for different system settings. For simulations we will use a 5-channel system and use 8 logarithmically equally spaced power levels between 0.1 mW and 10 mW. In the analysis we will set the noise power such that when there is no Kerr non-linearity and the power of the carriers are set to 1 mW, the system's BER value will be 10^{-4}. In the simulation we will use 10^7 symbol blocks, each containing 8 symbols, for noise samples. However, note that because the modulation is differential there are actually 7 symbols for each symbol block.

Because the the computational complexity of solving COVODE equation as described in chapter 4 is so high, for our analysis we will supply the results for just 2 special cases:

- *No noise amp*: BER is evaluated by ignoring Kerr non-linearity in the system. For this case $\mathbf{CT_r}$ matrix becomes diagonal since there is no correlation among noise samples.

Also note that in this case BER equals to 10^{-4} when the launched power per channel is 1 mW.

- *Noise amp with no disp*: In this case, dispersion is ignored but Kerr non-linearity is taken into account. Note that dispersion compensation has no significance since there is no dispersion in the system for this case. For this case, the noise covariance matrix before channel select filter becomes diagonal, meaning that there is no correlations between noise samples. However, correlations within noise samples, i.e. in-phase and quadrature noise components for the same noise sample, do exist. After the channel select filter, for the selected channel the time domain noise covariance matrix becomes a full matrix indicating the existence of correlations between noise samples.

Because the solution of COVODE equation and required NLSE equation take much time, for the simulations provided in this section we used

- Split-Step method for the solution of $NLSE$ equation [25]
- Forward-Euler in the integration of z dependent part of the COVODE equation
- Trapezoid rule in the integration of $\frac{\partial}{\partial t}$ dependent part of the COVODE equation

We compared the results of the COVODE equation that are obtained by the above method and the method that is supplied in chapter 4 and found the results matches each other.

Before supplying simulation results, let we summarize the steps that we will follow for noise sample generation and error counting:

- First find the accumulated noise covariance matrix, in frequency domain, $\mathbf{K_f}(z = N{\cdot}L)$ before filtering. Please note that, each OA compensate 95 % of dispersion and at the receiver the remaining dispersion is compensated. Also each OA amplifies both the large desired signal,$A(z,t)$ and the noise. Thus the $\mathbf{K_f}(z = N \cdot L)$ matrix is actually amplified - dispersion compensated noise covariance matrix.
- Compute the filtered noise covariance matrix $\mathbf{K_f^f}(z = N \cdot L)$ as described by 5.25

- Compute the filtered noise covariance matrix, $\mathbf{K_t^f}(z = N \cdot L)$, in time domain by using 5.26
- Compute $\mathbf{CT}(z = N \cdot L)$ by using $\mathbf{K_t^f}(z = N \cdot L)$
- Create a new covariance matrix, $\mathbf{CT_r}$, from $\mathbf{CT}(z = N \cdot L)$. Note that $\mathbf{CT_r}$ contains the covariances of the noise samples that are seen by the receiver
- Generate large number of correlated noise vectors by using $\mathbf{CT_r}$ as described in previous section
- Add the noise vectors to the large desired signal, which is also dispersion compensated and filtered, and count the errors by comparing the input and output bit pattern

5.3.1 Noise Amplification

In this section we will concentrate on the noise amplification of the channel that sits in the middle of the WDM spectrum, where the channel carriers are assumed to be unmodulated.

Figure 5.3.1 shows the noise amplifications that are obtained by using the transfer function methodology , which is discussed in chapter 3, and covariance matrix methodology, which is discussed in chapter 4.The graph shows the noise amplification of the middle channel where the total number of channels are taken to be 1, 3 and 5 and signal power is taken as $10mW$ per channel.

Note that as it is stated in chapter 3, because for unmodulated case noise is stationary we have computed the noise spectral properties for each channel individually and directly obtained the noise amplification for each channel. However, in the covariance matrix methodology case we have propagated the noise covariance matrix that contains the covariances of the noise samples around whole WDM spectrum. Thus in order to find the noise amplification one has to do filtering at the end of the fiber. In Figure 1 we plotted the noise amplification of the middle channel that is filtered out, by using brick-wall filter, at the end of the fiber.

From figure 5.3.1 we observe that

- For 1 channel system the results are exactly same

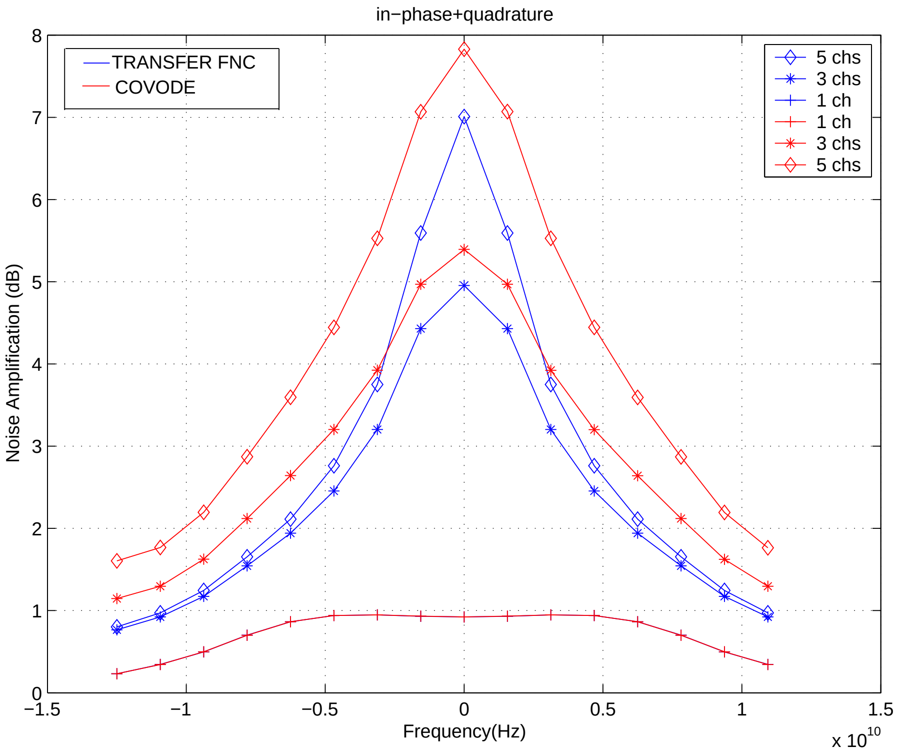

Figure 5.5: *System parameters: # of channels: 1, 3, and 5, Channel spacing: 25 GHz, Symbol rate: 12.5 Gs/sec, Launch Power: 10 mW,* α *= 0.25 dB/km ,* β_2 *= -21.6 ps*^{2}*/km,* β_3 *= 0.128 ps*^{3}*/km,* γ *= 2 1/(W·km), L : 80 km, # of spans: 1*

- For 3 and 5 channel system, noise amplification that is obtained by the solution of COVODE equation is higher than the noise amplification that is obtained by the transfer methodology case.

The main reason for the difference is the inclusion of side channels in the solution of COVODE equation. In the transfer function methodology we explicitly assumed that noise around each channel is stationary, which allowed us to compute the spectral properties of the noise to compute separately for each channel, and applied the filtering in the beginning of the solution. However, in the solution of COVODE equation we took the noise around whole WDM spectrum and propagated the noise spectral properties in that way. Thus noise amplification shown in figure 5.3.1

- obtained by transfer function methodology : shows the noise amplification for just taking the middle channel

- obtained by the solution of COVODE equation : shows the noise amplification by also taking care of the side channels of the middle channel

The inclusion of the side channels increases the noise power at the center frequency interval [-12.5 GHz 12.5GHz], thus it is reasonable to obtain a higher value compared to just taking the channel itself. In addition, we expect the difference between noise amplifications, that are obtained by transfer function and covariance matrix propagation methodology, to increase as more channels are added to the system. However the increase will not be so much as more and more channels are added to the system. This is because as more channels added to the system the effect of the further channels on the center channel becomes negligible.

5.3.2 BER Comparison

In the previous section we supplied the noise amplifications that are obtained by both transfer function methodology and covariance matrix propagation methodology. In this section we will supply BER results that are obtained by using covariances of noise samples obtained by the solution of COVODE equation.

Figure 5.6 shows the BER results, for DBPSK and DQPSK modulation schema, that are obtained by using the methodology discussed in chapter 3 and by using the solution of the

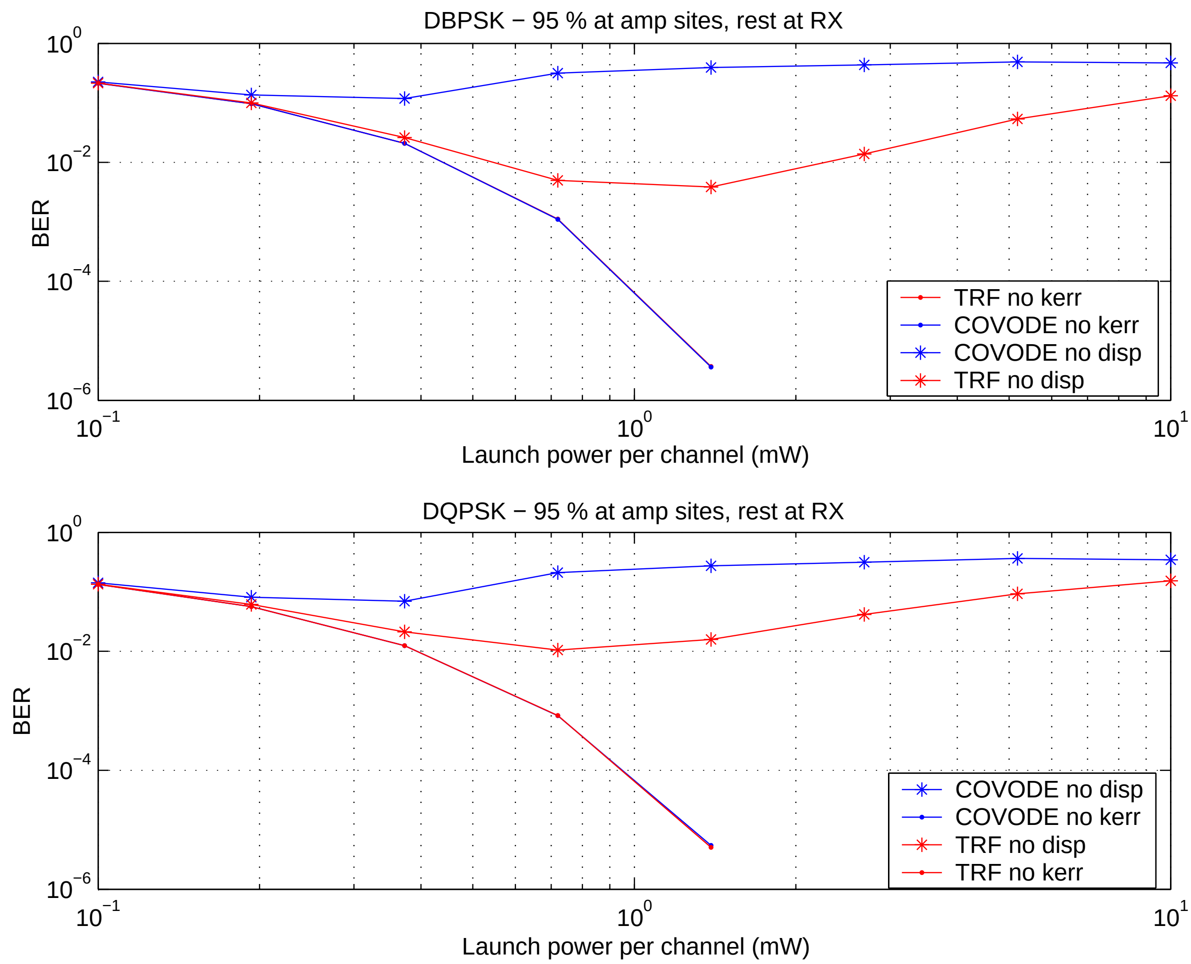

Figure 5.6: (95% dispersion compensation at the OAs , rest at the receiver) *System parameters: # of channels: 5, Channel spacing: 25 GHz, Symbol rate: 12.5 Gs/sec, Launch Power: 0.1-10 mW,* α = *0.25 dB/km ,* β_2 = *-21.6* ps^2*/km,* β_3 = *0.128* ps^3*/km,* γ = *2 1/(W·km), L : 80 km, # of spans: 8*

COVODE equation and methodology discussed in this chapter. As stated in the beginning of the section we will supply the simulation results for just two special cases: *No noise amp* and *Noise amp with no disp*. The results obtained in this section shows the BER of the channel that sits in the middle.

We also made simulations for modulated carriers. The signal(s) -for the middle channel- that is/are used in DBPSK and DQPSK simulation is/are shown in figures 5.3.2, 5.3.2 and 5.3.2.

Simulation results for the modulated carrier case is much like the plots given in figure 5.6.

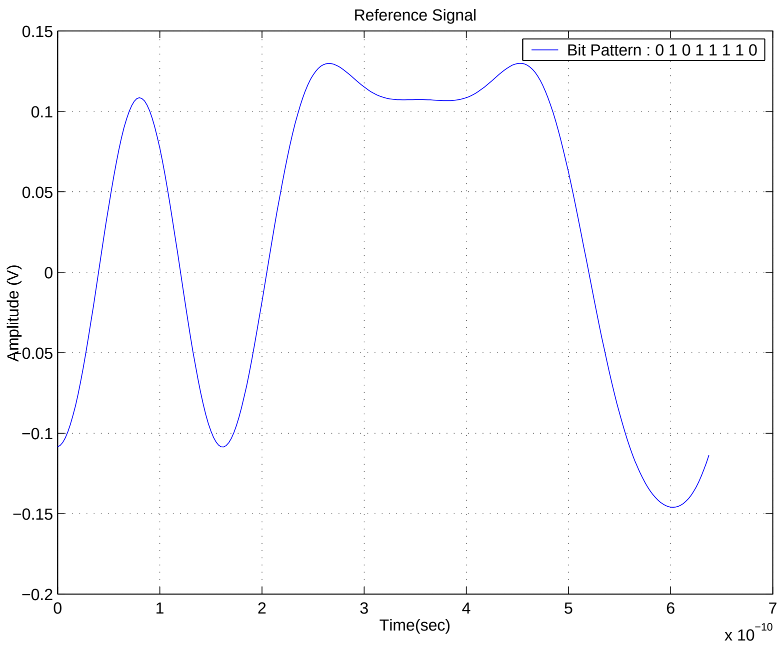

Figure 5.7: DBPSK Input Signal

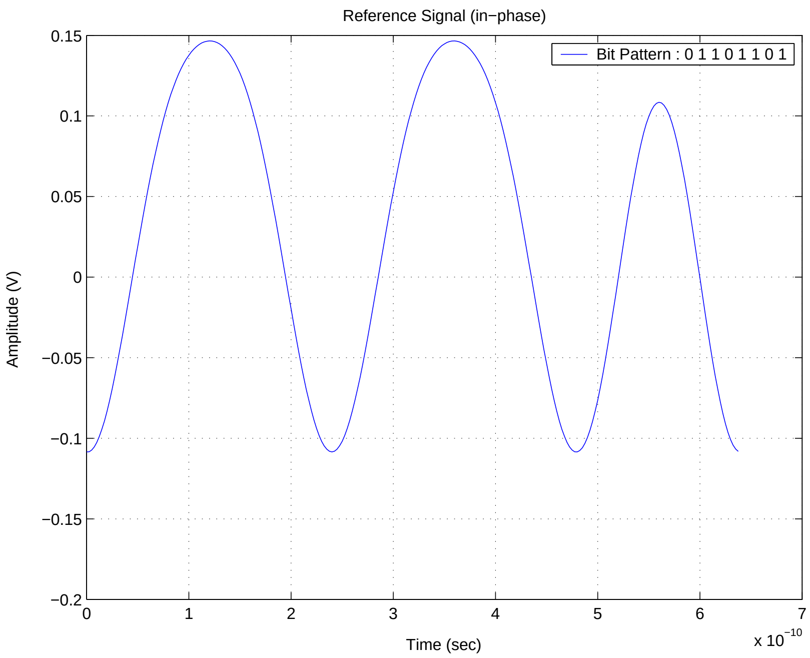

Figure 5.8: DQPSK Input Signal - In-Phase

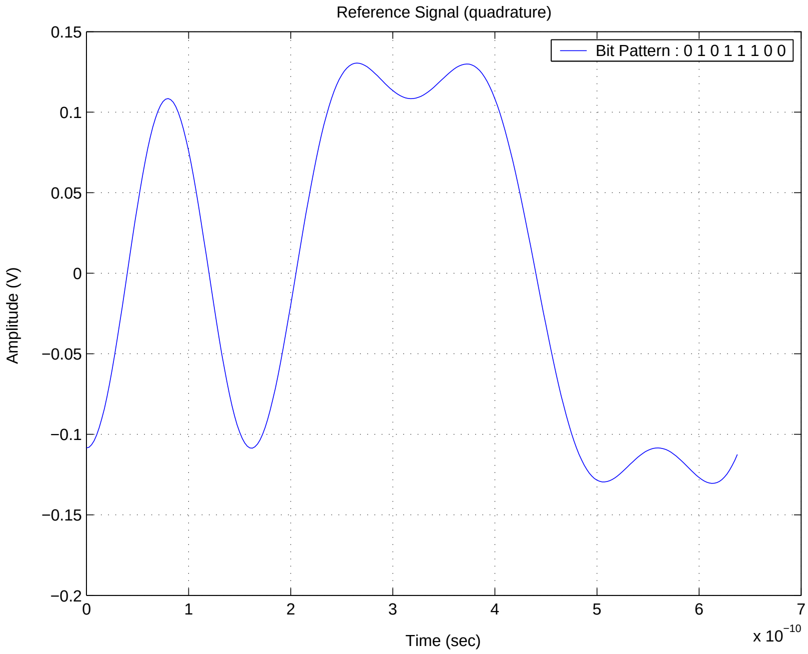

Figure 5.9: DQPSK Input Signal - Quadrature

This is because we made the simulations just for taking either dispersion or non-linearity into account. The plot is given by 5.10.

From figure 5.6 we observe that for *No noise amp* case all plots show the same behavior. For *Noise amp with no disp* case the results which are obtained by using the COVODE equation with transfer function approach have slightly higher BER values compared to BER values obtained by transfer function methodology. One of the reasons for this difference is the BER computation methodology. In transfer function methodology, described in 3, we created noise covariance matrix just for two consecutive noise samples and used it for BER evaluation. However in the methodology that we presented in this chapter, we computed the covariance of all noise samples that are seen by the receiver and used the computed covariance matrix in BER computation.Another reason for the difference is the numerical solution of NLSE equation. In the transfer function methodology we assume the signal impinging on the receiver is restored to its original power level. However, in the covariance matrix case, we are propagating the large desired signal by numerically solving the $NLSE$ equation and applying filtering at the receiver site which changes the signal envelope.

In this chapter we supplied a methodology to find out the system's BER value for

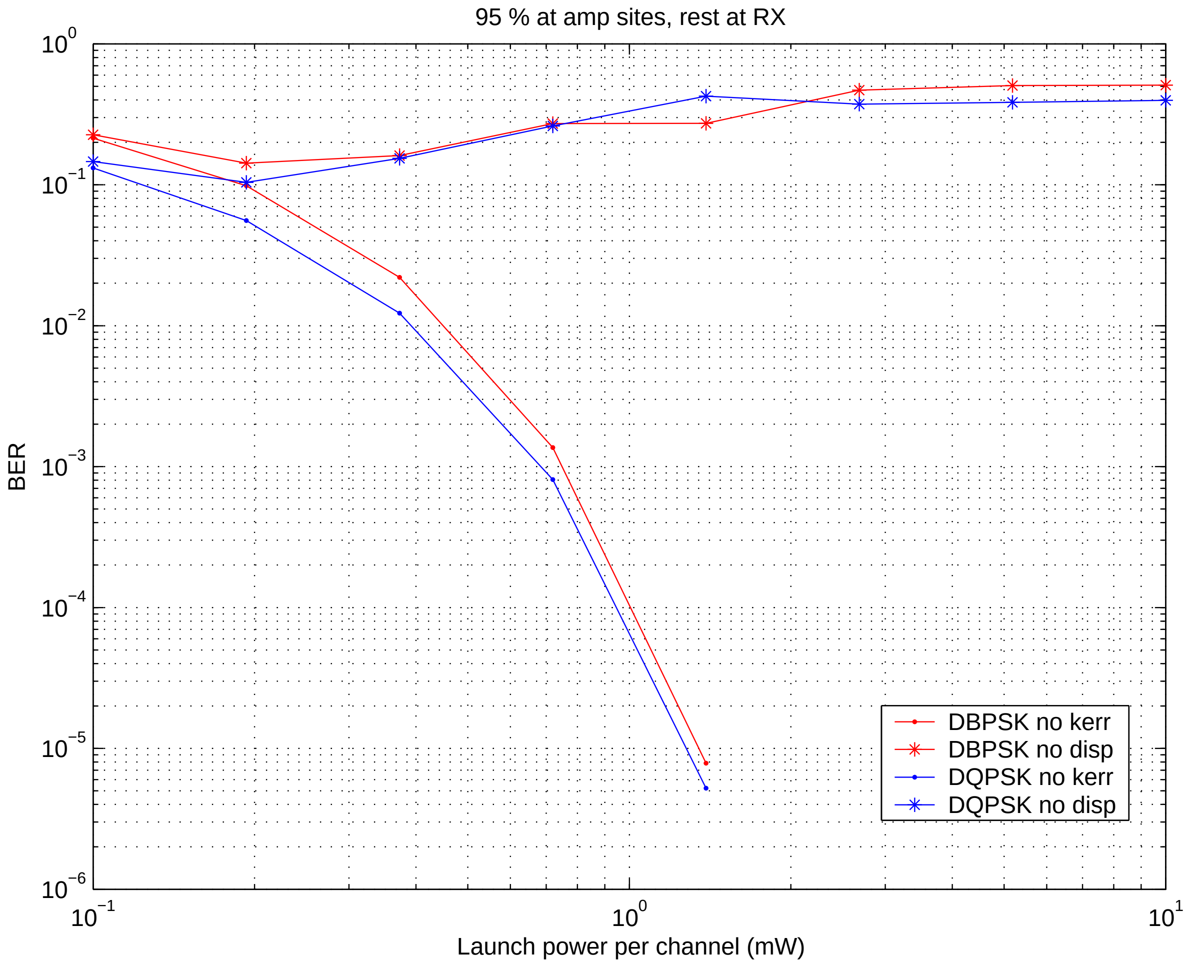

Figure 5.10: (95% dispersion compensation at the OAs , rest at the receiver) *System parameters: # of channels: 5, Channel spacing: 25 GHz, Symbol rate: 12.5 Gs/sec, Launch Power: 0.1-10 mW,* α = *0.25 dB/km ,* β_2 = *-21.6* ps^2/km*,* β_3 = *0.128* ps^3/km*,* γ = *2 1/(W·km), L : 80 km, # of spans: 8*

a WDM fiber optical system where the carriers are modulated. We supplied covariance matrix propagation within fiber spans, noise generation mechanism and BER evaluation methodology by using the covariances obtained from the solution of COVODE equation. We also supplied simulation results for two special system settings - *No noise amp with* and *Noise amp with no disp* and showed that for these two special cases two different system analysis methods - transfer function methodology described in chapter 3 and covariance matrix propagation described in chapter 4 - give the similar results.

Chapter 6

CONCLUSION

6.1 Summary

Optical fiber communication systems plays a critical role in today's communication systems. Their usage is not limited to telecommunications but include industry, medical and military application as well.

In this thesis we analyzed the noise effect on system performance of WDM optical fiber communication systems. We first gave a general information about OFCSs and problems associated with optical fibers: the affects of attenuation, dispersion and Kerr non-linearity have been discussed on optical signal in chapter 1.

In chapter 2 we supplied the NLSE equation that governs the complex signal envelope in a single mode fiber. We also supplied a general overview of noise analysis mechanism implemented in the thesis.

We focused on un-modulated optical carrier case in chapter 3 where we have used the transfer function methodology in noise analysis: we first computed, both analytically and numerically, inter and intra transfer function matrices among channels and used the computed transfer function matrices in the computation of noise spectral densities at the end of the fiber. We have supplied various plots that shows intra and inter transfer functions and noise spectral densities for various system settings. At the end of chapter 3 we supplied simulation results that show WDM system BER performance for DBPSK and DQPSK modulation schemes. From the simulations we observed that the existence of dispersion greatly increases the system performance. We also observed that the inclusion of correlations among noise samples increases the system performance further.

We treated the modulated optical carrier case in chapter 4, where we gave the numerical formulation of noise covariance matrix, numerical solution of NLSE equation and numerical solution of COVODE equation that describes the noise covariance matrix propagation along the fiber. We also developed formulation of noise propagation in frequency domain and supplied solution methodology. We have also supplied simulation results that show noise amplification for one fiber span for different system settings.

In chapter 5, which is the main contribution of the thesis, we gave BER computation methodology for modulated carrier case. We supplied methodology for noise covariance matrix propagation within fiber spans, obtaining noise covariance matrix at the receiver and noise generation for system BER analysis. Due to complexity of the solution of COVODE equation we supplied simulation results for just to special case where we ignore either dispersion or non-linearity. For these two special cases we observed that both transfer function and covariance matrix propagation methodologies gave similar results.

6.2 Future Work

The computational cost of the solution of COVODE equation or the solution of frequency decomposed formulation of covariance matrix propagation is very high. Thus the propagation of the covariance matrices within fiber spans take very much time and make modulated carrier case analysis difficult. This difficulty can be solved by computing the time dependent transfer functions, that transfers the input covariance matrix to the covariance matrix at the output of the fiber span. In this case computation of the transfer function matrices for one fiber span becomes sufficient to propagate the covariance matrix within fiber spans. The formulation and implementation of transfer function matrices is part of future work.

Due to complexity of the solution of COVODE equation, for modulated carrier case we supplied simulation results for two special cases that are obtained by ignoring either dispersion or non-linearity. A detailed analysis in parallel with transfer function matrix computation is also part of future work.

BIBLIOGRAPHY

[1] Govind P. Agrawal. *Fiber-Optic Communication Systems.* Wiley-Interscience, June 15, 2002.

[2] S.T. Hung. A.S. Hodel. Solution and applications of the lyapunov equation for control systems. *IEEE Transactions on Industrial Electronics*, 39 (3):194–202, 1992.

[3] Carena A. Curri V. Gaudino R. Poggiolini P. Benedetto S. Bosco, G. Suppression of spurious tones induced by the split-step method infiber systems simulation. *Photonics Technology Letters, IEEE*, 12:489 – 491, May 2000.

[4] Alan W. Bush. *Perturbation Methods for Engineers and Scientists.* CRC, 1992.

[5] Steven C. Chapra. *Applied Numerical Methods with MATLAB for Engineers and Scientists.* McGraw-Hill, June 25, 2004.

[6] Carmen Chicone. *Ordinary Differential Equations with Applications.* Springer, 2006.

[7] A. Demir and A. Sangiovanni-Vincentelli. *Analysis and Simulation of Noise in Nonlinear Electronic Circuits and Systems.* Kluwer Academic Publishers, 1998.

[8] Alper Demir. Non-monte carlo formulations and computational techniques for the stochastic non-linear schrdinger equation. *Computational Physics*, 201(1):148 – 171, 2004.

[9] Alper Demir. Nonlinear phase noise in optical-fiber-communication systems. *Lightwave Technology*, 25(8):2002–2032, Aug. 2007.

[10] Gerhard Wanner E. Hairer, S. P. Norsett. *Solving Ordinary Differential Equations I: Nonstiff Problems.* Springer-Verlag, December 15, 1986.

[11] Bengt Fornberg and Tobin A. Driscoll. A fast spectral algorithm for nonlinear wave equations with linear dispersion. *Journal of Computational Physics*, 155:456–467, 1999.

[12] C.W. Gardiner. *Handbook of Stochastic Methods for Physics, Chemistry and the Natural Sciences*. Springer-Verlag, 1983.

[13] James Gerhart. *Mastering Math for The Building Trades*. McGraw-Hill, 2000.

[14] J. P. Gordon and L. F. Mollenauer. Phase noise in photonic communications systems using linear amplifiers. *Opt. Lett.*, 15:1351–, 1990.

[15] Keang-Po Ho. *Phase-Modulated Optical Communication Systems*. Springer, July 1, 2005.

[16] John H. Hubbard and Beverly H. West. *Differential Equations: A Dynamical Systems Approach*. Springer, March 30, 1995.

[17] Oliver Ibe. *Fundamentals of Applied Probability and Random Processes*. Academic Press, October 19, 2005.

[18] Aly-Khan Kassam and Lloyd N. Trefethen. Fourth-order time stepping for stiff pdes. *SIAM J. Sci. Comput.*, 26:1214–1233, 2005.

[19] Andy Martin, Kevin Brown, Paul Rigby, and Simon Riley. *Pure Mathematics*. Trans-Atlantic Publications, July 1999.

[20] Robert Morrow. *Wireless Network Coexistence*. McGraw-Hill Professional, August 1, 2004.

[21] Djafar K. Mynbaev and Lowell L. Scheiner. *Fiber-Optic Communications Technology*. Prentice Hall, October 23, 2000.

[22] S.O. Pillai. *Solid State Physics*. New Age International (P) Ltd, 2005.

[23] G.W. Stewart R.H. Bartels. Solution of the equation ax + xb = c. *Comm. ACM*, 15:820–826, 1972.

[24] Chraplyvy A.R. Forghieri F. Gnauck A.H. Derosier R.M. Tkach, R.W. Four-photon mixing and high-speed wdm systems. *Journal of Lightwave Technology*, 13:841 – 849, May 1995.

[25] Lloyd N. Trefethen. *Spectral Methods in MATLAB*. SIAM: Society for Industrial and Applied Mathematics, February 15, 2001.

[26] Lloyd N. Trefethen and David Bau III. *Numerical Linear Algebra*. SIAM: Society for Industrial and Applied Mathematics, 1997.

[27] Steven J. Ruuth Uri M. Ascher and Brian T. R. Wetton. Implicit-explicit methods for time-dependent partial differential equations. *SIAM Journal on Numerical Analysis*, 32:797–823, Jun., 1995.

VITA

Mehmet Akgül was born in Konya, Turkey on May 17,1982. He received his B.Sc. degree in Electrical and Electronics Engineering from Boğaziçi University,Istanbul, in 2005. From August 2005 to August 2007, he worked as a teaching and research assistant in Koc University, Turkey. Since March 2008, he has been working as an application consultant at KoçSistem, Istanbul, Turkey.